

MECHANISM OF AFLATOXIN-INDUCED MUTAGENESIS

By

Ying-Chih Lin

A DISSERTATION

Presented to the Cell, Developmental & Cancer Biology Program

and the Oregon Health & Science University

School of Medicine

In partial fulfillment of

the requirements for the degree of

Doctor of Philosophy

February 2015

School of Medicine

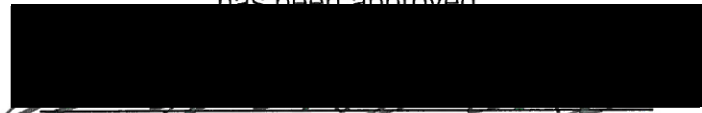
Oregon Health & Science University

CERTIFICATE OF APPROVAL

This is to certify that the Ph.D. dissertation of

Ying-Chih Lin

has been approved



R. Stephen Lloyd



Maureen Hoatlin



Amanda McCullough



Fred Robinson



Michael Cohen

TABLE OF CONTENTS

LIST OF TABLES AND SCHEMES	iv
LIST OF FIGURES	v
LIST OF ABBREVIATIONS	vii
ACKNOWLEDGEMENTS	ix
ABSTRACT	xi
CHAPTER 1: Introduction	1
Global Health Issue: Hepatocellular Carcinoma	2
Environmental Risk of Aflatoxins	3
Experimental Carcinogenesis of Aflatoxin B ₁	5
Metabolism of Aflatoxin B ₁	6
Genotoxicity of Aflatoxin B ₁	11
DNA Repair of Aflatoxin B ₁ -DNA Adducts	14
Nucleotide excision repair	14
Base excision repair	18
Mutagenesis induced by Aflatoxin B ₁	20
<i>TP53</i> gene mutation	22
Mutagenic precursor	30
Research Objectives	31

CHAPTER 2: Molecular basis of aflatoxin-induced mutagenesis	
– role of the aflatoxin B ₁ -formamidopyrimidine adduct	32
Preface	33
Introduction	34
Materials and Methods	36
Results	41
Discussion	53
CHAPTER 3: Error-prone replication bypass of the primary	
aflatoxin B ₁ DNA adduct, AFB ₁ -N7-Gua	60
Preface	61
Introduction	62
Materials and Methods	65
Results	68
Discussion	80
CHAPTER 4: The critical role of mammalian pol ζ in response	
to aflatoxin B ₁ exposure	86
Preface	87
Introduction	88
Materials and Methods	91
Results	93

Discussion	96
CHAPTER 5: Removal of aflatoxin B1-formamidopyrimidine adducts by human DNA glycosylase Nei endonuclease VIII-like 1 (hNEIL1)	100
Preface	101
Introduction	102
Materials and Methods	104
Results	106
Discussion	111
CHAPTER 6: Summary and Conclusion	114
CHAPTER 7: Future Directions	117
Reference	121

LIST OF TABLES AND SCHEMES

Table 1. Mammalian DNA polymerases.	24
Table 2. Mutation spectrum generated from replication bypass of AFB ₁ -FAPY adducts in COS-7 cells.	43
Table 3. Mutation spectrum and frequency following replication past AFB ₁ -N7-Gua adducts in COS-7 cells.	70
Table 4. Rate constants determined at 37°C under single turnover conditions for cleavage of AFB ₁ -FAPY in complementary duplex and bubble DNAs.	110
Scheme 1. Minimal kinetic scheme used for the analysis of the glycosylase/lyase activity of hNEIL1.	107

LIST OF FIGURES

Figure 1. Structures of aflatoxins.	5
Figure 2. The major metabolism of AFB ₁ and formation of DNA adducts.	7
Figure 3. Replication blockage of pol δ by AFB ₁ -FAPY.	44
Figure 4. Nucleotide insertion opposite AFB ₁ -FAPY by pol δ .	45
Figure 5. Replication bypass of AFB ₁ -FAPY by yeast pol ζ .	47
Figure 6. Replication bypass of AFB ₁ -FAPY by human pol κ .	50
Figure 7. Replication bypass of AFB ₁ -FAPY by human pol η catalytic core.	51
Figure 8. Resumption of replication by pol δ downstream of AFB ₁ -FAPY.	53
Figure 9. Proposed model of TLS past AFB ₁ -FAPY.	57
Figure 10. Replication bypass of AFB ₁ -N7-Gua by pol δ .	72
Figure 11. Single nucleotide insertion opposite AFB ₁ -N7-Gua by pol δ -Exo.	74
Figure 12. Single-nucleotide incorporations and primer extensions opposite AFB ₁ -N7-Gua by yeast pol ζ_4 and human pol κ , η and ι .	76
Figure 13. Primer extensions past AFB ₁ -N7-Gua catalyzed by yeast pol ζ_4 and human pol κ , η and ι .	77
Figure 14. Resumption of replication by pol δ downstream of AFB ₁ -N7-Gua.	80

Figure 15. Proposed model of TLS past AFB ₁ -N7-Gua.	83
Figure 16. Disruption of pol ζ confers hypersensitivity to AFB ₁ .	94
Figure 17. <i>Rev3L</i> deletion changes cell cycle distribution following AFB ₁ exposure.	96
Figure 18. DNA sequences used in glycosylase assays.	105
Figure 19. Minimal kinetic scheme used for the analysis of the glycosylase/lyase activity of hNEIL1.	109
Figure 20. Single turnover analysis for removal of AFB ₁ -FAPY in bubble-structured DNA by hNEIL1.	110

LIST OF ABBREVIATIONS

AFB₁: Aflatoxin B₁
AFB₁-FAPY: AFB₁-formamidopyrimidine
AFB₁-N7-Gua: 8,9-dihydro-8-(N7-guanyl)-9-hydroxyafatoxin B₁
AP: Abasic site
APE1: AP endonuclease 1
BER: Base excision repair
BSA: Bovine serum albumin
CPD: Cyclobutane pyrimidine dimer
CTG: CellTiter-Glo luminescent cell viability assay
CYP450: Cytochrome P450
DBD: DNA-binding core domain
DMSO: Dimethyl sulfoxide
DN: Dominant negative
Dpo4: DNA polymerase IV
5'-dRP: 5' deoxyribose-5-phosphate
DSB: Double-strand break
E. coli: *Escherichia coli*
FapyA: 4,6-diamino-5-formamidopyrimidine
FapyG: 2,6-diamino-4-hydroxy-5-formamidopyrimidine
FBS: Fetal bovine serum
Fpg: Formamidopyrimidine DNA glycosylase
GGR: Global genome repair
Gh: Guanidinohydantoin
GOF: Gain of function
GSH: Glutathione
GST: Glutathione S-transferase
GSTM1: Glutathione S-transferase mu 1
HBV: Hepatitis B virus
HCC: Hepatocellular carcinoma
HCV: Hepatitis C virus
hNEIL1: Human DNA glycosylase Nei endonuclease VIII-like 1
HR: Homologous recombination
hTERT-HME1: hTERT-immortalized human mammary epithelial cells
IARC: International Agency for Research on Cancer
ICL: Interstrand cross-link
IPTG: Isopropyl-β-D-thiogalactopyranoside
KD: Knockdown
KI: Knock-in
KO: Knockout
LOF: Loss of function
MEC: Mammary epithelial cells
MEF: Mouse embryonic fibroblast

NADPH: Nicotinamide adenine dinucleotide 2'-phosphate reduced tetrasodium salt hydrate
ND: Nondamaged
NER: Nucleotide excision repair
NMR: Nuclear magnetic resonance
OH: 3'-hydroxyl
5-OHC: 5-hydroxycytosine
5-OHU: 5-hydroxyuracil
OR: Odds ratio
8-oxoG: 7,8-dihydro-8-oxoguanine
PI: Propidium iodide
Pol: DNA polymerase
Ppb: parts per billion
Rb: Retinoblastoma
Sp: Spiroimidodihydantoin
Ss: Single-stranded
SSB: Single strand break
SV40: Simian virus 40
TAg: T antigen
TCR: Transcription-coupled repair
Tg: Thymine glycol
TLS: Translesion synthesis
T_m: Melting temperature
XP: Xeroderma pigmentosum
XPA: The xeroderma pigmentosum group A protein
WT: Wild-type

ACKNOWLEDGEMENTS

It is hard to believe that there is an end to this long tunnel, but here I am--seeing the light! I have been very fortunate to have many people travel along by my side through this journey; your support made this dissertation possible.

I would first like to thank my mentor, Dr. Stephen Lloyd, for your guidance and patience with me through these years. You have trained me to be an independent researcher by giving me freedom to figure things out on my own, and created a collegiate environment where all ideas are welcome for discussion. More importantly, you always reminded me of big picture perspectives when I was buckled down by technical details and doubted my own ability. Your optimistic attitude is infectious; I always feel so much more energetic and motivated after having a discussion with you. It is a true honor to be your student.

I would like to extend my thanks to Dr. Irina Minko for her technical guidance and numerous stimulating discussions for my project.

This project would not have been possible without our collaborators, Drs. Michael Stone, Peter Burgers, and Richard Wood for providing me essential reagents and cell lines.

Thanks to my thesis committee, Drs. Maureen Hoatlin, Amanda McCullough, Fred Robinson for your inputs to help make progress of my project.

Many thanks go to Dr. Marcus Calkins for his generous help and support during the preparation and revision of my qualifying exam proposal.

Special thanks to my dear friends, Drs. Serah Choi and Jason White, for your encouragement and support to pursue a graduate degree. I really enjoyed my time spent with you guys at the University of Pittsburgh.

To my family in Taiwan, there are simply not enough words to describe how much I appreciate your unconditional love and support to see me through this graduate school work, reminding me of what is important in life. You are the motivation that kept me going when times were hard. I also want to thank my Aunt Lillian for her support and care. Meeting with you and Uncle Jeff on weekends always delighted my day.

I also want to give my thanks to my in-laws, Shelley and Dorne Yeager. You provide a perfect getaway for Torin and I when we need it.

Last but not the least, I want to thank my dear husband for his unwavering love and faith in us. Although it certainly was hard on us to get both our training simultaneously in two different states, we managed to stay strong and support each other. Thank you very much for being there whenever I need you, I certainly could not have come this far without you.

ABSTRACT

Hepatocellular carcinoma (HCC) is a serious global public health issue. With 782,000 new cases diagnosed in 2012, HCC is the second leading cause of death related to cancer worldwide. The majority of HCC cases occur in developing countries in Southeast Asia, Sub-Saharan Africa and China. Hepatitis B virus (HBV) infection and aflatoxin exposure are the two main factors contributing to HCC in these high incidence regions. While HBV vaccination provides an effective way to lower the risk of HCC, there are an estimated 5 billion people at risk of chronic exposure to aflatoxins through contaminated food. To develop effective treatment, early diagnosis, and intervention strategies, a better understanding of the mechanisms by which aflatoxins induce HCC is paramount.

Aflatoxin B₁ (AFB₁) is the most potent hepatocarcinogen among the aflatoxins. The first chapter of this dissertation provides a review of the mechanism of action of AFB₁ in hepatocarcinogenesis, with a focus on the differential susceptibilities between species and individuals, and highlights unanswered questions that await further investigation.

Upon exposure to AFB₁, DNA damage and mutations have been observed. Genetic alterations are considered to be the initial step of tumor development, but how AFB₁-induced DNA lesions result in mutations remains unclear. To address this question, the aim of the second and third chapters of this dissertation is to determine the mutagenic potential of the primary and secondary AFB₁-DNA adducts in primate cells. The biochemical function of a subset of eukaryotic translesion synthesis (TLS) DNA polymerases, whose DNA damage tolerance mechanism carries a risk of

mutagenesis, is also explored with regard to replication bypass of AFB₁-DNA adducts. To extend these studies, the aim of chapter four of the dissertation is to narrowly focus on elucidating the biological role of pol ζ in response to AFB₁.

Cells have evolved a variety of DNA repair pathways to prevent mutation and genome instability. One key observation regarding AFB₁-induced genotoxicity is that the secondary AFB₁-DNA adducts appear to accumulate in mammalian cells for several days after a single dose of AFB₁ exposure, raising the question of how these adducts are repaired in mammalian cells. In this regard, the aim of chapter five of this dissertation is to evaluate the catalytic efficiency of human DNA glycosylase Nei endonuclease VIII-like 1 (hNEIL1) in excision of the secondary AFB₁-DNA adducts in order to determine the involvement of base excision repair (BER) for combating AFB₁-induced genotoxicity.

Overall, the results presented in this dissertation advance our state of knowledge about the mechanism of AFB₁-induced mutagenesis in mammalian cells through the function of TLS pol ζ, and how BER may modulate the genotoxic and mutagenic outcomes.

CHAPTER 1

INTRODUCTION

Global Health Issue: Hepatocellular Carcinoma

Primary liver cancer poses an international public health concern as the second leading cause of cancer-related deaths worldwide, with >700,000 estimated cases per year. This mortality is virtually identical to its annual incidence throughout the world, highlighting the need for development of effective treatments and early diagnostic tools¹. Hepatocellular carcinoma (HCC) represents the major histological subtype among liver cancers.

Nearly all HCC cases are preceded with chronic liver injury that is attributable to some environmental and dietary risk factors, since hepatocarcinogenesis rarely derives from healthy livers. The global distribution of HCC incidence reflects the geographical variations of the prevalence of certain major risk factors. Most HCCs occur in developing countries, especially in Eastern Asia and Africa, where chronic hepatitis B virus (HBV) infection and chronic dietary exposure to aflatoxins are endemic, with exceptions in Japan and Egypt where the dominant risk factor is hepatitis C virus (HCV) infection^{2,3}. However, the incidence of HCC in western countries has been noted to be markedly increasing. The prevalence of HCV infection, alcoholic- and non-alcoholic steatohepatitis, obesity and diabetes may be related risk factors³⁻⁶. Other etiologies for HCC incidence include certain rare genetic disorders such as hemochromatosis and α -1 antitrypsin deficiency⁶. Currently, more than 240 million people are estimated to have chronic HBV infection, 347 million people with diabetes, and 5 billion people are at risk of aflatoxin exposure in the world^{7,8}. Therefore, it is of great interest to understand the mechanisms of action of

diverse etiological factors in developing HCC, in order to implement optimal intervention and surveillance strategies for those at risk. This dissertation project focuses on elucidation of aflatoxin B₁ (AFB₁)-induced mutagenesis in mammalian cells as an early step of hepatocarcinogenesis.

Environmental Risk of Aflatoxins

Aflatoxins were first identified in the 1960's as causative agents for an epidemic initially in Britain, called "Turkey X" disease, in which numerous young turkeys, ducklings and chicks died because of ingestion of fungal-contaminated feeds originating from South America. The culprit mold was recognized to be *Aspergillus flavus*, therefore the name of the toxins was designated as such (*A. flavus* toxin). The discovery, toxicology, and molecular epidemiology of aflatoxins, and interventions for reducing aflatoxin exposure have been extensively reviewed^{9,10}. Only information relevant for the understanding of the significance of this project is included in the sections below.

In addition to *Aspergillus flavus*, another fungus that generates aflatoxin is *Aspergillus parasiticus*, and it is also commonly found as a contamination in a variety of foods such as peanuts, corn, tree nuts and rice for both human and animal consumption^{9,10}. Contamination can occur at any stage of food production when conditions are suitable for fungal growth and production of the toxin. Important factors contributing to the generation of the toxins include humidity, temperature, genotypes of the crops, damage of the crops in the field due to drought, heavy rainfall or an infestation of insects or inadequate drying during

post-harvest storage. Thus, developing countries in areas of Southeast Asia and Sub-Saharan Africa are particularly at high risk of aflatoxin exposure due to the optimal climates for fungal growth, the lack of effective infrastructure for food processing and regulation, and insufficient food supply and diversity in people's diet. For example, during the 1980s in the People's Republic of China, the contamination of aflatoxins in foods was reported to range between 23-500 parts per billion (ppb), and dietary aflatoxin intake by people residing in regions of high HCC incidence was 4-221 $\mu\text{g}/\text{day}$ ^{11,12}. The U.S. Food and Drug Administration sets 20 ppb as the action level for aflatoxins in foods for human consumption.

Outbreaks of acute aflatoxicosis due to ingestion of aflatoxin-contaminated foodstuffs in humans have been reported in several regions in developing countries including India, Malaysia and Kenya⁹. One of the most severe episodes occurred in Kenya 2004, causing 317 cases and 125 deaths¹³. The exposure to aflatoxins was estimated to be 50 mg/day in this incidence⁹. Liver is the primary target organ of aflatoxicosis with clinical symptoms involving abdominal pain, vomiting, pulmonary edema, and fatty liver with necrosis. On the other hand, chronic exposure to low doses of aflatoxins has been shown to be associated with the incidence of HCC in humans based on several epidemiological studies, and comprehensive reviews of those data are available^{9,14-16}. It is estimated that about 5-28% of all new HCC cases worldwide could be attributable to aflatoxin exposure¹⁴. Moreover, aflatoxins have been implicated in the acceleration of the development of HCC by about 20 years in the background of HBV infection. This early onset HCC has been observed in Qidong, China¹⁷.

Experimental Carcinogenesis of Aflatoxin B₁

In many earlier reports, aflatoxin-contaminated meal has been shown to induce tumor formation in various animal species¹⁸. It was recognized that aflatoxins consist of four structurally-related chemicals, namely B₁, B₂, G₁, and G₂, based on their blue or greenish yellow fluorescence under ultraviolet light (Figure 1). Among them, AFB₁ is the most potent hepatocarcinogen, while AFB₂ and AFG₂ are relatively nontoxic, because these compounds lack the double bond in the terminal furan ring to form an epoxide^{19,20}.

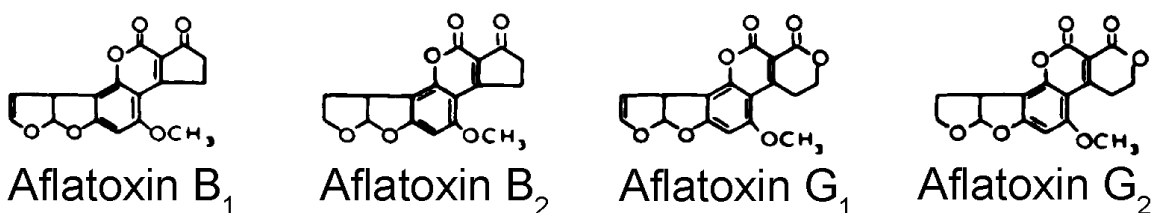


Figure 1. Structures of aflatoxins (Adapted from¹⁹).

Carcinogenic studies using different animal models revealed species variations in the susceptibility to AFB₁-induced HCC. The duck, rat and rainbow trout represent among the most sensitive species to the toxic and hepatocarcinogenic effects of AFB₁ in contrast to the relatively resistant species such as mice. However, new-born mice appear to be more responsive to its carcinogenicity^{18,21-24}. Explanations for the interspecies differences in susceptibility to AFB₁ have been provided by studies of the metabolism of AFB₁, which is critical for exerting its biological activity (discussed below). Nonhuman primates, primarily Rhesus monkeys, are also susceptible to AFB₁-induced

HCC^{25,26}, pancreatic carcinoma, gall bladder carcinoma and osteogenic sarcoma^{27,28}, highlighting the potential risk of developing cancers in humans following AFB₁ exposure. Based on sufficient data from human epidemiological and experimental animal studies, aflatoxin B₁ (AFB₁) and mixed aflatoxins were classified as Group I carcinogens in humans by the International Agency for Research on Cancer (IARC) in 1994²⁹.

Metabolism of Aflatoxin B₁

AFB₁ alone is not carcinogenic. The necessity of metabolic activation of AFB₁ by microsomal enzymes in order to bind macromolecules and exert its biological effect was first demonstrated by R. Colin Garner and colleagues in the 1970s^{30,31}. Since then, enormous efforts have been undertaken to identify and characterize the metabolites and enzymes involved in the metabolism of AFB₁ that may contribute to the interspecies and inter-individual risk to the adverse effects of AFB₁. The major Phase I hepatic metabolisms of AFB₁ include the CYP450-mediated epoxidation, hydroxylation, O-demethylation and ketoreduction. Studies of these metabolic pathways have been reviewed³².

Hepatic microsomal CYP450-mediated oxidation generates multiple metabolites, containing the highly toxic AFB₁-8,9-epoxide and AFM₁, and relatively nontoxic AFQ₁, the latter two are the hydroxylated products^{32,33} (Figure 2). AFM₁ can be found in milk and milk products when lactating animals ingest contaminated feed. Dietary AFM₁ is about one-third and one-tenth as carcinogenic as the parent compound AFB₁ in trout³⁴ and rats³⁵, respectively.

There are no reports on the isolation of AFB₁-8,9-epoxide from biological samples due to its highly reactive nature. However, studies of the adducted macromolecules and the successful synthesis of AFB₁-8,9-epoxide *in vitro*³⁶ have caused it to be considered the ultimate carcinogenic form of AFB₁. In addition to the direct interaction with DNA (discussed below), the epoxide can undergo hydrolysis to AFB₁-8,9-dihydrodiol (Figure 2), followed by rearrangement to a dialdehyde that is capable of binding to protein lysine groups via Schiff base formation. This reaction is evidenced by AFB₁-albumin adducts found in human and rat blood samples as biomarkers of exposure^{37,38}. Potentially, this adds to the underlying mechanisms leading to the toxic effect of AFB₁.

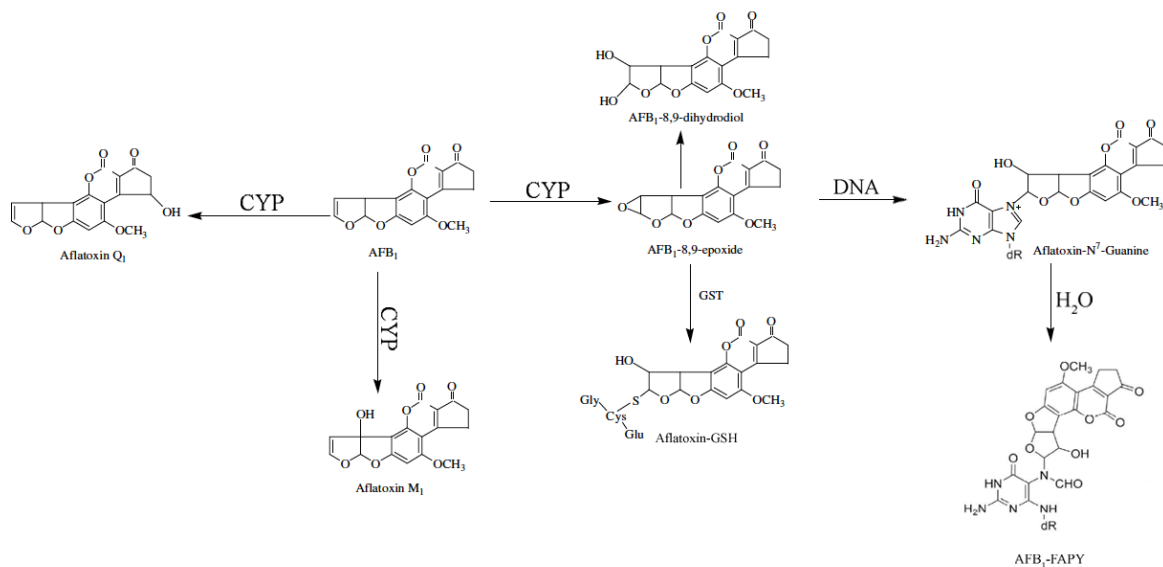


Figure 2. The major metabolism of AFB₁ and formation of DNA adducts (Adapted from^{33,39})

Substantial variations in the composition of metabolites upon AFB₁ activation exist among different species. Human and monkey hepatic microsomes primarily convert AFB₁ to AFQ₁ with small amounts of AFB₁-8,9-epoxide and AFM₁. This is in contrast to the observation in rats and mice, in which the AFB₁-8,9-epoxide is the predominant metabolite. Moreover, mouse liver microsomes demonstrated higher activity for epoxide formation compared to those derived from rat⁴⁰.

Multiple forms of CYP450 enzymes with the capacity to activate AFB₁ have been reported. Depending on the animal species and organs examined, different isoforms may be involved^{33,41}. Human CYP3A4 was suggested to be the dominant enzyme for AFB₁ activation in a wide range of concentrations⁴²⁻⁴⁴. However, another line of evidence indicated that both human CYP1A2 and CYP3A4 were capable of catalyzing formation of the epoxide, and depending on the level of exposure, one may be more relevant than the other. In cases of low-level dietary exposure, CYP1A2 appeared to have higher affinity for AFB₁; however, the biological importance of this observation needs to be carefully considered giving that CYP1A2 expression level might be relatively low. Therefore, when exposed to high concentration of AFB₁, the more abundant CYP3A4 may be responsible for the conversion to AFB₁-8,9-epoxide⁴⁵⁻⁴⁸.

Conjugation of AFB₁-8,9-epoxide with reduced glutathione (GSH) that is catalyzed by glutathione S-transferase (GST) (Figure 2) represents a critical Phase II detoxification pathway that determines the interspecies sensitivity to the carcinogenic effect of AFB₁ among rodents⁴⁹⁻⁵². Both mice and hamsters were

found to be more resistant to AFB₁-induced hepatocarcinogenesis with less AFB₁-DNA adduct formation than rat^{18,52-54}. Although mouse and hamster microsomal CYP450 oxygenases have a higher activity for AFB₁-8,9-epoxide conversion than the microsome preparation from rat, the liver cytosolic fraction of mouse and hamster also appeared to generate more detoxifying AFB₁-GSH conjugates compared to rat^{51,52,55,56}. The extent of protection against AFB₁-DNA binding by GSH conjugation to the AFB₁ intermediate in hamster and mouse is more drastic than that detected in rat, offering an explanation for the final lower yield of AFB₁-DNA adducts in the resistant species^{50-52,56,57}. The GST with high specific activity towards AFB₁-8,9-epoxide conferring resistance to mouse has been identified to be the constitutively expressed alpha class GST isozyme (mYc)⁵⁸⁻⁶⁰. In contrast, the rat homologue (Yc₂) is expressed at a very low baseline level, but it can be induced by antioxidants such as ethoxyquin to provide resistance through its relatively higher AFB₁-8,9-epoxide conjugation activity compared to other constitutively expressed α -class GSTs⁶¹⁻⁶³. In summary, Phase I metabolism in mice activates AFB₁ to a greater extent compared to rats. However, a particularly efficient GSH conjugation mediated by GST mYc confers resistance to mice, whereas uninduced rats without an effective Phase II detoxification pathway represent species with high sensitivity to AFB₁ hepatocarcinogenesis.

As opposed to rodents, human α -class GSTs presented little catalytic activity for AFB₁-8,9-epoxide, but rather, the μ -class glutathione S-transferase mu 1 (GSTM1) demonstrated significant capability for AFB₁-GSH formation.

However, its efficiency is about three orders of magnitude lower than that of rat Yc₂^{63,64}. A genetic polymorphism involving a null allele of *GSTM1* has been reported in the human population that exhibited loss of *GSTM1* enzymatic activity^{65,66}. Studies of *GSTM1* in detoxification of AFB₁ revealed that reduced or null activity of *GSTM1* correlated well with increased AFB₁-DNA adduct formation *in vitro*⁶⁷, suggesting potential protection against AFB₁ by *GSTM1* in humans. However, epidemiological analyses of the association between *GSTM1* genotype and the presence of AFB₁ adducts and aflatoxin-related HCC produced mixed results. Some data support the idea that *GSTM1* null allele may increase HCC risk upon exposure to AFB₁⁶⁸⁻⁷¹, while others observed little link between aflatoxin-associated HCC risk and the polymorphic genotype⁷²⁻⁷⁴. In addition, interaction between chronic HBV infection, aflatoxin exposure and genetic susceptibility of *GSTM1* null allele to HCC development has been suggested⁷⁰. Nevertheless, polymorphisms in *GSTM1* genotype, particularly in ethnic Chinese populations, is considered to be an independent risk factor for HCC⁷⁵⁻⁷⁷. In summary, while it is evident that differential capacities for detoxification of AFB₁ among rodents may account for the species sensitivities to AFB₁-induced hepatocarcinogenesis, the existence of genetic susceptibility in AFB₁-metabolizing enzymes for HCC development with aflatoxin etiology in humans remains unclear.

Genotoxicity of Aflatoxin B₁

Metabolic oxidation of the unsaturated bond at the positions of 8 and 9 on the terminal furan ring of AFB₁ by cytochrome P450 (CYP450) generates the highly reactive intermediate AFB₁-8,9-epoxide (Figure 2)^{36,41}, that covalently binds to the nucleophilic atoms in nucleic acids or proteins. The site of nucleophilic attack in DNA at the N7 atom of deoxyguanosine results in the formation of the DNA adduct 8,9-dihydro-8-(N7-guanyl)-9-hydroxyaflatoxin B₁ (AFB₁-N7-Gua)⁷⁸⁻⁸¹(Figure 2). This AFB₁-DNA adduct is chemically unstable due to the positive charge on the imidazole ring. Therefore, spontaneous depurination, in addition to removal by a DNA repair mechanism (discussed later), may occur to release AFB₁-N7-Gua, which can be detected in the urine and used as a biomarker for exposure in molecular epidemiological studies^{82,83}. The half-life of AFB₁-N7-Gua is considered short, about 8 h, compared with 3 weeks for the AFB₁-albumin adducts⁹.

Based on molecular dosimetry studies of AFB₁-N7-Gua in animal models and human epidemiological data, the AFB₁-N7-Gua adduct is considered to be a biologically effective measure for exposure and cancer risk. A linear correlation between dose and the concentration of AFB₁-N7-Gua in rat and rainbow trout liver DNA, and human urine samples has been reported^{12,84-87}. This linearity can be further translated into the dose-risk relationship in rat and rainbow trout⁸⁸. Results from a prospective cohort study conducted in Shanghai, China indicated that individuals with AFB₁-N7-Gua adduct formation had a 9.1-fold increase in relative risk of developing HCC, while others with both AFB₁-N7-Gua and HBV

infection had a 60-fold increase when compared to control. Overall, these data demonstrated that AFB₁-N7-Gua adduct plays a predictive role in the hepatic cancer risk assessment^{89,90}. Thus, elucidating the mechanisms that modulate AFB₁-N7-Gua formation is particularly important for understanding the interspecies variations in the susceptibility to AFB₁-induced hepatocarcinogenesis and cancer risk assessment at the individual level in humans. Specifically, metabolic activation of AFB₁, detoxification of AFB₁-8,9-epoxide, and DNA repair of AFB₁-N7-Gua are the cellular processes that have been studied extensively.

In addition to depurination, AFB₁-N7-Gua can be rearranged to the imidazole ring-open form, AFB₁-formamidopyrimidine (AFB₁-FAPY)⁹¹⁻⁹³(Figure 2). It has been shown that about 20% of the initial AFB₁-N7-Gua converted to AFB₁-FAPY in rat liver DNA 24 hr after administration of a single dose of AFB₁⁹⁴.

Structural studies using nuclear magnetic resonance (NMR) methodologies have revealed that the AFB₁ moiety of both AFB₁-N7-Gua and AFB₁-FAPY intercalates above the 5' face of the modified base in duplex oligodeoxynucleotides, leading to interstrand stacking interactions with adjacent base pairs as the AFB₁ moiety spans across the helix⁹⁵⁻⁹⁸. Consequently, the oligodeoxynucleotides were thermodynamically stabilized upon the intercalated AFB₁ modification as reflected by increased melting temperature (T_m), which is a unique feature compared to other types of DNA damage except cross-linking agents^{97,99}. Intriguingly, the stability induced by these adducts can be quite different. The cationic lesion typically causes an increase of 2-5°C in T_m ⁹⁹,

whereas the stabilization of an oligodeoxynucleotide duplex was increased 15°C when the AFB₁-FAPY adduct was positioned in 5'-d(CTAT^{FAPY}GATTCA)-3'•5'-d(TGAATCATAG)-3' oligodeoxynucleotide⁹⁷. There were two factors predicted to contribute to this very substantial stabilization: 1) imidazole ring opening of AFB₁-FAPY allows better parallel intercalation within the DNA base pairs to enhance stacking interaction with minimal helical bending, 2) hydrogen bonding between the formyl group of the pyrimidine and the 3' neighboring base A⁶N6H in this sequence context⁹⁷.

It has been observed via NMR that AFB₁-N7-Gua and AFB₁-FAPY adducts induced differential helix bending in the refined structures of AFB₁-modified duplex. In contrast to the FAPY lesion, which caused no bending⁹⁷, the cationic AFB₁ adduct was found to bend the DNA helical axis about 20° at the phosphodiester backbone 5' to the adduct site, especially in the modified strand of 5'-d(ACATC^{AFB}GATCT)-3'•5'-d(AGATCGATGT)-3'⁹⁸. Interestingly, no DNA bending was observed in another duplex sequence, d(TAT^{AFB}GCATA)₂, which allowed two AFB₁ to intercalate symmetrically resulting in equal and opposite bends at each of the two adjacent intercalation sites and caused a net effect of cancellation of the bending⁹⁶. As will be described below, despite similarities in the 5' intercalation of AFB₁ moiety, the FAPY adducts induce less distortion in the DNA helix than the cationic lesions, leading to inefficient recognition and removal by nucleotide excision repair (NER) in mammalian cells, as reflected by the prolonged detection of AFB₁-FAPY in the genome.

DNA Repair of Aflatoxin B₁-DNA Adducts

DNA repair is an evolutionarily conserved mechanism for cells to minimize cell death, mutations, replication errors, and genomic instability by correcting DNA damage induced both endogenously and exogenously. The importance of functioning DNA repair activity has been exemplified in Xeroderma pigmentosum (XP) patients who have an autosomal recessive genetic defect in which nucleotide excision repair (NER) enzymes are mutated, leading to a reduction in or elimination of NER. Due to the deficiency in removal of UV-induced DNA lesions by NER, the majority of XP patients are sensitive to sun exposure and predisposed to skin cancer through accumulation of mutations and other chromosomal changes^{100,101}. Another example of defective DNA repair function associated with increased cancer risk is *BRCA1* gene mutations, which result in altered protein function in several cancer types including breast and ovarian cancers in women. As a tumor suppressor gene, *BRCA1* encodes a protein involved in the DNA damage response pathway to enable homologous recombination for accurate DNA double-strand break repair to maintain genome integrity and suppress tumor formation^{102,103}. Given the importance of DNA repair in the prevention of cancer development, it is of particular interest to understand how AFB₁-induced DNA damage is repaired and to what degree the repair mechanism modulates the adverse effects of AFB₁.

Nucleotide excision repair

In the case of removal of bulky AFB₁-DNA adducts, the NER pathway has been

the main focus of investigations because it is primarily responsible for the repair of bulky and helix-distorting DNA damage such as UV-induced 6-4 photoproducts and polycyclic aromatic hydrocarbons such as benzo[a]pyrene from smoking¹⁰⁰. There are two subpathways of NER: global genome repair (GGR) and transcription-coupled repair (TCR). TCR is responsible for removal of lesions that block RNA polymerase on the transcribed strand of active genes, while GGR removes DNA damage from the untranscribed strand and heterochromatin in the genome. Damage recognition of GGR and TCR is conducted by different protein factors, while subsequent steps are believed to be identical between these two subpathways. The XP group A protein (XPA) is involved in damage verification downstream of the recognition step in mammalian NER^{100,101}. Interestingly, *XPA*-deficient mice appeared to be more susceptible to AFB₁-induced liver cancer¹⁰⁴, suggesting that NER plays a role in repair of DNA damage caused by AFB₁ to minimize its carcinogenic outcome.

Studies in *Escherichia coli* (*E. coli*) containing plasmids adducted with either AFB₁-N7-Gua or AFB₁-FAPY revealed that both lesions can be repaired by basal level NER without SOS induction¹⁰⁵. SOS response is an inducible DNA repair network for bacterial survival when an increase in DNA damage occurs¹⁰⁶. In addition, purified bacterial NER proteins, UvrABC endonucleases, demonstrated similar efficiencies in binding and cleavage of both adducts *in vitro*¹⁰⁷.

Interestingly, AFB₁-FAPY appeared to be more persistent in mammalian cells. Within 24 hr following a single dose exposure to AFB₁, AFB₁-FAPY

accumulated and became the predominant lesions in cultured human normal fibroblasts and rat liver DNA. Moreover, no significant decrease was observed in the amount of AFB₁-FAPY in the next 24-48 hr period studied, suggesting that if enzymatic removal of AFB₁-FAPY exists in mammalian cells, it would be a slow process^{94,108}. On the other hand, the half-life of AFB₁-N7-Gua has been noted to be 7.5 hr in rat liver DNA⁹⁴, which can be attributed to the combined effects of non-enzymatic depurination and conversion of AFB₁-FAPY and enzymatic removal by NER. The *in vitro* rate of depurination and AFB₁-FAPY conversion is pH-dependent. AFB₁-FAPY formation is favored under slightly basic conditions, while acidic environments stabilize AFB₁-N7-Gua⁸².

The role of NER in AFB₁-DNA adduct removal is supported by the observation of rapid accumulation of AFB₁-N7-Gua and AFB₁-FAPY in cultured human XPA skin fibroblasts in comparison to normal human fibroblasts¹⁰⁸. However, as it is evident that AFB₁-N7-Gua may be repaired by NER, the increase of AFB₁-FAPY in XPA cells could be explained alternatively as the result of slower loss of AFB₁-N7-Gua, allowing for more AFB₁-FAPY conversion. The concept of the cationic adduct repaired by NER was further corroborated by *in vitro* assays, in which rat and mouse liver nuclear extracts exhibited incision and repair synthesis on plasmids adducted with AFB₁-N7-Gua¹⁰⁹. Moreover, increased repair activity towards AFB₁-N7-Gua was observed in mouse liver extracts pretreated with AFB₁ *in vivo*^{109,110}. In contrast, large variations in FAPY removal by mouse liver extracts have been reported¹⁰⁹, and AFB₁ pretreatment resulted in no change of AFB₁-FAPY adduct repair by mouse liver extracts^{109,110}.

Interestingly, when different mouse strains and AFB₁ dosing protocols were used, the opposite trend was reported with respect to which types of adducts were repaired more efficiently, the cationic or FAPY lesions of AFB₁^{109,110}. It was noted that mouse liver extract appeared to have higher repair activity than that derived from rat for AFB₁-DNA adduct, suggesting an underlying mechanism for the differential inter-species susceptibility to AFB₁-induced carcinogenesis¹⁰⁹.

In recent years, human epidemiological studies indicated that polymorphisms in XPC and XPD genes are associated with increased AFB₁-related HCC risk in Chinese populations residing in Guangxi, a high AFB₁ exposure area in China^{111,112}. Particularly, the adjusted odds ratio (OR) of homozygous XPC codon 939 Gln alleles for HCC was 1.81, and it became 22.33 and 18.38 for individuals who also had long (>48 years) and high level of AFB₁ exposure according to the AFB₁-DNA adduct level (≥ 2.01 $\mu\text{mol/mol}$ of DNA), respectively¹¹². Similarly, the XPD polymorphism Lys751Gln in homozygotes was associated with an increased risk of HCC (adjusted OR was 2.47). Individuals with the genotype and long AFB₁ exposure were at an even higher risk for HCC (adjusted OR = 470.25) compared to those with homozygous Lys alleles (adjusted OR = 149.12). XPC performs damage detection as the first step in GGR, while XPD is a helicase in the transcription factor TFIIH complex to unwind DNA downstream of damage recognition in NER^{100,101}. Taken together, to further our current body of knowledge on the protective role of NER against AFB₁, investigations using *in vitro* assays to compare the repair capacity for AFB₁-DNA adducts, particularly the persistent FAPY lesions, by liver nuclear extracts

derived from normal and NER-deficient human (or mouse) may be necessary. It would be of interest to test whether NER activity can be induced in cultured human hepatocytes in response to AFB₁ treatment, thereby increasing removal of the cationic and FAPY lesions of AFB₁ in the *in vitro* assay.

Base excision repair

Base excision repair is the mechanism responsible for removal of the majority of endogenous DNA damages that are small, non-helix-distorting base lesions from the genome. Common substrates for BER include non-bulky DNA bases modified by oxidation, deamination or alkylation. The first step of BER is catalyzed by a lesion-specific DNA glycosylase that can cleave the N-glycosidic bond of the base and leave an abasic site (AP) in the DNA if the enzyme only has a monofunctional glycosylase activity. Then, the AP endonuclease 1 (APE1) cleaves the phosphodiester backbone immediately 5' to the AP site, generating a 3'-hydroxyl (OH) and 5'-deoxyribose-5-phosphate (5'-dRP), that can be removed by the lyase activity of DNA polymerase β (pol β). On the other hand, bifunctional DNA glycosylases possess both glycosylase activity and lyase activity, allowing them to incise the DNA backbone immediately 3' to the AP site via β - or δ -elimination reaction to produce a single strand break with a 3'-phospho α , β -unsaturated aldehyde or 3'-phosphate group. Subsequent end processing would be carried out by APE1 or polynucleotide kinase 3'-phosphatase to give rise to proper 3'-OH and 5'-phosphate termini for downstream repair synthesis and sealing the nick by pol β and XRCC1-LIG3 α , respectively, as the short-patch

(single-nucleotide) pathway. Alternatively, BER may proceed via a long-patch, strand-replacement synthesis process that has been reviewed elsewhere^{113,114}.

Human epidemiological studies have shown that individuals with the polymorphism of XRCC1 Arg399Gln have a higher risk of detectable AFB₁-DNA adducts, p53 mutation in codon 249 and HCC incidence¹¹⁵⁻¹¹⁷. It is currently unclear how XRCC1 Arg399Gln polymorphism could allow higher levels of AFB₁-DNA adducts, since it functions downstream of lesion-specific DNA glycosylases in BER; potentially XRCC1 has yet to be identified functions.

The involvement of the BER pathway in protection against AFB₁ genotoxicity was examined with respect to a role of *E. coli* formamidopyrimidine DNA glycosylase (Fpg) in initiating repair at AFB₁-FAPY. However, conflicting data have been reported. An *in vitro* enzyme assay revealed that Fpg can excise AFB₁-FAPY from calf thymus DNA or rat liver DNA¹¹⁸, whereas bacterial *fpg* mutant cells repaired AFB₁-FAPY from plasmids at a comparable level relative to wild-type cells, suggesting that Fpg does not contribute to the removal of FAPY lesions *in vivo*¹⁰⁵. Fpg is a bifunctional glycosylase with substrate specificity favoring oxidized purines such as 7,8-dihydro-8-oxoguanine (8-oxoG) and 2,6-diamino-4-hydroxy-5-formamidopyrimidine (FapyG)¹¹⁹. While it remains unclear whether mammalian NER or BER can repair AFB₁-FAPY adducts, it was of interest to investigate the potential role of BER initiated by other DNA glycosylases such as human Nei Endonuclease VIII-like 1 (hNEIL1), since this enzyme has a wide range of substrates such as FapyG, 4,6-diamino-5-formamidopyrimidine (FapyA) and thymine glycol (Tg)¹²⁰⁻¹²².

Mutagenesis Induced by Aflatoxin B₁

Cancer is a genetic disorder in which accumulated genetic alterations lead to uncontrolled cell growth and proliferation. Among numerous observed genetic changes, the most common include point mutations, copy number variations, and chromosomal rearrangements. The etiology of many cancers and mutations is often unclear. Some environmental and chemical carcinogens are known mutagens, such as UV irradiation and aflatoxins, which cause DNA damage that subsequently results in a wide spectrum of mutations. Mutagenesis in tumor suppressor genes and oncogenes may confer growth advantages to allow oncogenic transformation.

It is thought that AFB₁-induced mutagenesis plays an important role in the initiation of HCC. Although both point mutations and chromosomal changes, such as base substitutions and loss of heterozygosity, have been reported upon exposure to AFB₁, point mutations will be the focus of this project. A variety of cellular and animal models have been developed to examine the mutagenicity of AFB₁. For example, studies in bacterial and human cells containing a shuttle vector as a mutation target revealed an increased mutation frequency with G:C to T:A transversion being the predominant mutation type following AFB₁ exposure compared to untreated control^{123,124}. Similarly, AFB₁ exposure to neonatal mice has been shown to elevate mutation frequencies in liver DNA, primarily G to T transversion followed by G:C to A:T transition, in the *gpt* and *cII* transgenes that had been previously integrated into the mouse genome¹²⁵⁻¹²⁷. These results are

consistent with the observation that the N7 of guanine residues is the major site of adduct formation by activated AFB₁⁷⁸⁻⁸¹.

Following the notion that cellular DNA repair pathways may modulate the genotoxicity and mutagenicity of AFB₁, it has been shown that NER deficiency not only increased mutation frequency, but also influenced the distribution of mutation hotspots within a gene¹²⁸. Differential sequence specificity of AFB₁-induced mutations was observed in human XPA and DNA repair-proficient cells, and tandem base substitutions were only found at GG sites in XPA cells. Interestingly, the authors did not find correlation between the mutation hotspots and the level of modification by AFB₁ using a DNA polymerase stop assay.

Different interspecies susceptibility to AFB₁ hepatocarcinogenesis was reflected by their response to the mutagenic effect of AFB₁. Analysis of the *lacI* mutant frequency in the lambda/*lacI* transgenic rodent models showed that AFB₁ increased liver mutation frequencies over background by ~20-fold in the transgenic rat, with a shift in mutational spectrum to predominantly G to T transversions. In contrast, no difference in mutation spectrum and frequency was detected in AFB₁-treated transgenic mouse liver compared to that under spontaneous condition¹²⁹, a result that is consistent with the robust detoxification of AFB₁ as discussed above. Taken together, the signature point mutation induced by AFB₁ is G to T transversion, whose frequency and hotspot location may be influenced by metabolism and DNA repair in different cellular contexts to confer various susceptibilities to the mutagenic and carcinogenic effects of AFB₁.

TP53 gene mutation

Results from epidemiological studies revealed a mutation hotspot at the third position of codon 249 in the *TP53* tumor suppressor gene with a G to T transversion (AGG ->AGT, *R249S*), leading to an amino acid substitution from arginine to serine in the p53 protein (p.R249S), in about half of the HCC samples examined from regions with high aflatoxin exposure and prevalence of HBV infection¹³⁰⁻¹³². This mutation hotspot is not commonly found in other types of cancer or in HCCs from other areas in the world with low or negligible AFB₁ exposure¹³³⁻¹³⁷. When HBV-associated HCC patients were stratified into two groups based on their risk of AFB₁ exposure, the *R249S* frequency was about 50% among the patients at high risk of exposure, in contrast with 0-8% of patients who were at low risk had *R249S*^{133,136}, suggesting a strong association between the incidence of *R249S* and aflatoxin exposure. Moreover, the frequencies of *R249S* in normal liver tissue from HCC patients residing in Qidong, China, and Thailand were found to coincide with the level of AFB₁ exposure¹³⁸. Qidong and Thailand were considered to have high and low AFB₁ exposure, respectively. Interestingly, there was no correspondence of *R249S* between the normal liver and the HCC samples from the same patients, suggesting a causative role of AFB₁ for *TP53 R249S* mutation as an early event of HCC development. This mutation may increase the probability of mutant cells to progress along the pathway of hepatocarcinogenesis, but additional factors are required for the complete transformation into liver cancer.

Experimentally, AFB₁ has been shown to form adducts at codon 249 and others in exon 7 of *TP53* gene^{139,140}. Consistently, *R249S* was preferentially induced by AFB₁ in human HCC cells HepG2 and non-tumorigenic SV40-immortalized human liver epithelial cells, accompanied by G to T and C to A transversions in adjacent codons at lower frequencies^{141,142}. Similarly, AFB₁-treated mouse embryonic fibroblasts (MEFs) harboring the *cII* transgene as a mutation reporter showed frequent G to T transversion in two codons that had identical sequence contexts to that of codon 249 of human *TP53*¹⁴³. These empirical results support the idea of AFB₁ as the etiological factor for *R249S* mutation in HCCs. However, no correlation between this mutation hotspot and the preference of adduct formation or delayed removal of adduct was found¹⁴⁰, suggesting other mechanisms may contribute to the highly mutable property of codon 249 of *TP53* by AFB₁ in cellular systems.

Point mutations may be generated during replication or repair synthesis. The replicative DNA polymerases (pol) δ and ϵ responsible for synthesizing the majority of the genome, exhibit extremely low error frequency at 10^{-6} ~ 10^{-7} due to their intrinsic high fidelity polymerizing and proofreading exonucleolytic activities¹⁴⁴. However, cells utilize translesion synthesis (TLS) polymerases to replicate past DNA lesions that block pol δ and ϵ to prevent replication fork stalling and potentially induce mutations, because these polymerases have flexible active site to accommodate abnormal base pairing with damaged bases and lack exonucleolytic activities. There are 15 DNA polymerases identified in mammalian cells (Table 1), and among them at least 5 DNA polymerases are

extensively studied for their TLS function, namely pol ζ , η , ι , κ and Rev1. It is of particular interest to identify DNA polymerase(s) that could synthesize past AFB₁-DNA adducts and to investigate the effect of sequence-context on the DNA polymerase(s) for the bypass reaction. This may advance our understanding of the intrinsic mutability of codon 249 in the *TP53* gene, as an explanation for the high mutation frequency of *R249S* in AFB₁-associated HCCs.

DNA polymerase	Catalytic subunit (gene, size of protein and protein domain structure* in humans)	Function	Family [‡]
Pol α	<i>POLA1</i> (166 kDa) 	DNA replication priming	B
Pol δ	<i>POLD1</i> (124 kDa) 	DNA replication, NER and MMR	B
Pol ϵ	<i>POLE</i> (262 kDa) 	DNA replication, NER and MMR	B
Pol γ	<i>POLG</i> (140 kDa) 	Mitochondrial DNA replication and repair	A
Pol β	<i>POLB</i> (38 kDa) 	BER and meiotic recombination	X
Pol λ	<i>POLL</i> (63 kDa) 	V(D)J recombination; possibly end joining and BER	X
Pol μ	<i>POLM</i> (55 kDa) 	V(D)J recombination; possibly end joining	X
TDT	<i>DNTT</i> (58 kDa) 	Immunoglobulin diversity at junctions of coding regions	X
Pol ζ	<i>REV3L</i> (353 kDa) 	TLS and mutagenesis	B
REV1	<i>REV1</i> (138 kDa) 	TLS and mutagenesis, anchor for several DNA polymerases	Y
Pol η	<i>POLH</i> (78 kDa) 	Bypass of UV radiation-induced DNA adducts, especially CPDs	Y
Pol ι	<i>POLI</i> (80 kDa) 	Backup enzyme for bypass of UV radiation-induced DNA adducts and BER	Y
Pol κ	<i>POLK</i> (99 kDa) 	Bypass of bulky adducts, backup enzyme for NER	Y
Pol θ	<i>POLQ</i> (290 kDa) 	Defence against ionizing radiation-induced DNA damage	A
Pol ν	<i>POLN</i> (100 kDa) 	ICL repair or testis-specific function?	A

Table 1. Mammalian DNA polymerases. BER, base excision repair; CPD, cyclobutane pyrimidine dimer; ICL, interstrand crosslink; MMR, mismatch repair; NER, nucleotide excision repair; Pol, polymerase; TDT, terminal deoxynucleotidyltransferase; TLS, translesion DNA synthesis; UV, ultraviolet. Blue, DNA polymerase domain; green, exonuclease domain; red, 5'-deoxyribose phosphate (dRP) lyase domain; yellow, BRCT domain; grey, helicase-like domain; red line, dRP lyase activity. *Most eukaryotic DNA polymerase proteins are named with Greek letters (for example, α , β and γ) and the genes are named with the corresponding roman letter. †In mammalian cells, these enzymes fall into four distinct families, designated A, B, X and Y, based on amino acid sequence relationships (Adapted from¹⁴⁵).

In response to DNA damage, p53 protein functions as a sequence-specific transcription factor by regulating the expression of target genes that are involved in a variety of cellular processes such as DNA repair, cell cycle arrest, senescence and apoptosis, to prevent subsequent genomic instability and tumorigenesis^{146,147}. It is therefore possible that *TP53 R249S* is selected during hepatocarcinogenesis, enabling the p.R249S mutant protein to confer growth advantages for clonal expansion of liver cells under repeated DNA damage induced by chronic exposure to AFB₁.

Several experimental systems have been developed to study the biological effects of p.R249S mutant protein with respect to loss of function (LOF), dominant negative (DN) effect and gain of function (GOF). It appears that when p.R249S mutant proteins were expressed ectopically in p53-null human cancer cells such as osteosarcoma SAOS-2, lung cancer H1299 and colorectal cancer HCT116 cells, it lost transactivation function, with an inability to inhibit cell growth or induce apoptosis compared to wild-type (WT) p53^{148,149}. Consistently, LOF in DNA-binding activity of endogenously expressed p.R249S was observed in both hepatocellular carcinoma Mahlavu and PLC/PRF/5 cells¹⁵⁰.

Considering that AFB₁-induced *TP53 R249S* mutation occurs at an early stage of hepatocarcinogenesis, it is important to understand the role of the mutant protein in a WT-p53 cellular background. When the p.R249S mutant protein was expressed in normal human mammary epithelial cells (MEC) 76N, it inhibited the transactivation activity of WT p53 and immortalized MEC strain 76N with detectable telomerase activity¹⁵¹. Interestingly, other p53 hotspot mutant

proteins, R248W and R273H, that also exhibited impaired transactivation activity only induced prolonged life span not immortalization, indicating that a specific DN effect or GOF of p.R249S was sufficient for immortalization of MECs. It would be of interest to determine whether *TP53 R249S*-induced immortalization is tissue-specific by using a similar approach in normal human hepatocytes. Later, Junk et al. examined the effect of p.R249S mutant/WT heterozygosity using a different cell model, hTERT-immortalized human mammary epithelial cells (hTERT-HME1), by stably expressing p.R249S via lentiviral delivery system in the presence of WT p53¹⁵². The authors found the DN effect of p.R249S on WT p53 with regard to gene expression and DNA binding at a genome-wide level, but no effect on cell proliferation, clonogenicity, anchorage-independent growth or cell cycle distribution; instead it increased the migratory and invasive potential of these cells with alterations in gene expression that were not detected in WT-expressing HME1, highlighting GOF of p.R249S. It would be helpful to test whether these effects of *TP53 R249S* will hold true in human hepatocytes. Taken together, these observations are especially pertinent to the notion that AFB₁-induced *TP53 R249S* mutation occurs at an early stage of hepatocarcinogenesis, providing some insights into how this hotspot mutation may contribute to the processes of immortalization and mobility, ultimately leading to tumorigenesis.

Several GOF characteristics of p.R249S have been reported in the literature. To understand GOF of the mutant protein, p53-null cancer cell lines are often utilized. In contrast to WT p53, the p.R249S mutant exhibited interaction with the paralogs of p53, p63 and p73, when they were co-expressed

in lung cancer H1299 cells^{153,154}. Moreover, Xu et al. demonstrated that prion-like aggregation may serve as a mechanism for the DN effect and GOF of p.R249S¹⁵⁵. The mutant protein can self-assemble and co-aggregate with WT p53, p63 and p73 to form molecules with molecular weight of 800 kDa or higher in human osteosarcoma SAOS-2 cells. This aggregation led to co-precipitation of the mutant protein and WT p53, p63 and p73 into inactive cellular inclusions. Recently, it has been shown that expression of p.R249S in the H1299 cells promotes multinucleation and centrosome abnormalities with mitotic defects¹⁵⁴, suggesting an outcome of genomic instability. It is currently unclear how these GOF of p.R249S may affect tumor initiation and progression; it is possible that the interaction with p63 and p73 may be associated with chemoresistance, migration, invasion and metastasis as shown by other tumor-derived p53 mutants^{147,156}. It is also conceivable that other GOFs of p.R249S have yet to be identified. Further investigations are warranted, especially in the context of hepatocarcinogenesis.

In addition to the work performed in human cells, there have been some interesting observations regarding the effect of p53 mutation using mouse cell models. Dumenco et al. showed that expression of a murine equivalent of human *TP53 R249S*, mR246S (CGA-> AGT), consisting of two base pair changes in codon 246, enhanced colony formation in murine hepatocytes AML12¹⁵⁷. These cells are continuously replicating, differentiated and nontumorigenic and contain WT p53. The authors noted that the growth advantage conferred by mR246S was distinct in murine hepatocytes because this phenotype was not observed in

murine NIH3T3 fibroblast cells. No effect of mR246S on anchorage-independent growth or tumor formation was observed in nude mice, indicating that although mR246S confers growth advantage, it is not sufficient to transform the AML12 cells. Further investigations by Lee and Sabapathy have shown that the DN effect of mR246S was apparent with respect to target gene expression, cell survival and cell cycle arrest in a knock-in (KI) mouse embryonic stem cell model, regardless of its differentiation state¹⁵⁸. Interestingly, the KI cells exhibited high tumorigenicity, similar to p53 null cells, in a carbon-tetrachloride-induced liver injury model, when compared to p53 WT or heterozygous ES cells. Recently, the same authors conducted a more detailed investigation of the DN effect and GOF of mR246S to tissues and organism level using a KI mouse strain that carries the *R246S* mutation. They concluded that the DN effect of mR246S is cell-type specific as an acute response mediated by p53, without long-term promotion for tumorigenesis, compared to p53 heterozygous control. No GOF of mR246S was identified in comparison to p53-null control¹⁵⁹. Specifically, they found that in contrast to bone marrow and primary MEFs, thymocytes, T and B cells and lymphoid organs from KI mice exhibited the DN effect on cell death after challenge with irradiation. Regardless of their sensitivity to irradiation, all of them demonstrated the DN effect on transactivation of p53-target genes. Intriguingly, the DN effect observed at the cellular level did not translate into the incidence of tumorigenesis with respect to lymphoma/thymoma/sarcoma with or without external challenges. The same tumorigenesis and transcriptome analyses were used for GOF studies. Overall, their findings emphasize the notion that the

specificities of cell, tissue and cancer types should be taken into consideration for any biological questions. To understand the role of *TP53 R249S* mutation in AFB₁-induced hepatocarcinogenesis, an experimental design that studies hepatocytes and liver cancer as the consequence of a chronic low dose AFB₁ challenge may be more appropriate to recapitulate how HCC occurs in humans.

Biophysical analyses of p53 have provided some insights into how the *R249S* mutation affects the protein structure and physicochemical properties that may consequently alter its cellular function. The amino acid R249 is located in the DNA-binding core domain (DBD) of p53¹⁶⁰, which is the most conserved region between species and confers DNA-binding specificity to the protein. The importance of p53 DBD is underscored by the fact that more than 95% of the oncogenic mutations occur in this region¹³⁷. Crystallographic studies have revealed that human p53 DBD folds into a large β -sandwich as a scaffold for a DNA-binding surface, that consists of two large loops (L2 and L3) for minor groove interaction and a loop-sheet-helix motif for contact with DNA major groove¹⁶⁰. Although R249 in L3 is not directly involved in DNA binding, it remains important for stabilizing the surrounding structure. NMR studies have shown that the p.R249S core domain has an overall conformation similar to that of WT p53, except for a local distortion in both L2 and L3 with more flexibility in the β -sandwich^{161,162}. In WT p53 DBD, R249 stabilizes L3 and L2 through formation of a salt bridge with Glu-171 in L2 and hydrogen bonds with Gly-245 and Met-246 in L3¹⁶⁰. Upon the replacement of serine, these interactions were disrupted and, as a result, the mutant p53 DBD was destabilized by about 2 kcal/mol and partially

unfolded, and showed loss of DNA binding activity¹⁶³. Moreover, mutant p.R249S core domain has been shown to denature at a faster rate at physiological temperatures compared to that of WT p53 due to the thermodynamic instability found in mutant protein¹⁶⁴. The destabilizing properties of p.R249S was further corroborated by the availability of four crystal structures of the mutated p53 DBD, including WT and three other mutant-type conformations¹⁴⁹. The difference between the three mutant conformations was in the region surrounding the mutation site. Results from both NMR and crystallographic studies indicated that p.R249S does not possess a denatured conformation, but is rather an ensemble of native and native-like conformations^{149,162}.

Investigations into the biological effect of *TP53 R249S* mutation provide a good example of how AFB₁ induces HCC from a mutagenic standpoint. As previously described, AFB₁ causes DNA damage that leads to G to T mutation. However, the pertinent question of how these DNA lesions can give rise to such point mutations is currently unclear.

Mutagenic precursor

Results derived from the majority of the mutagenesis studies described above represent the overall mutagenic outcome following AFB₁ exposure, although the DNA damage caused by AFB₁ is a mixture of AP, AFB₁-N7-Gua and AFB₁-FAPY adducts. Little information exists on the relative importance of the individual AFB₁-DNA adducts in the mutagenesis of G to T transversions. It has been shown that the cationic and FAPY lesions are mildly to moderately mutagenic

with mutation frequencies of 4% and 32%, respectively, in bacteria when replicated past a specific lesion site in a shuttle vector^{165,166}. As expected, G to T mutation was the predominant point mutation induced by both adducts. One pertinent question regarding AFB₁ carcinogenesis in animals and humans is which AFB₁-DNA adducts serve as the mutagenic precursor to the frequently observed G to T mutation in mammalian cells.

Research Objectives

The goal of this dissertation project is to investigate the mutagenic potential of the primary and secondary AFB₁-DNA adducts, AFB₁-N7-Gua and AFB₁-FAPY, respectively, in mammalian cells. We hypothesized that these two adducts are mutagenic in mammalian cells and TLS polymerases may play a role in replication past them in an error-prone manner when they block normal replicative polymerases as bulky adducts. Additionally, we also hypothesized that DNA repair mechanisms, particularly the BER pathway, may be involved in repair of AFB₁-FAPY via the action of DNA glycosylase NEIL1 that is capable of removing FAPY lesions, which share structural similarity to AFB₁-FAPY.

CHAPTER 2

Molecular basis of aflatoxin-induced mutagenesis – role of the aflatoxin B₁-formamidopyrimidine adduct

Ying-Chih Lin^{1,2}, Liang Li³, Alena V. Makarova⁴, Peter M. Burgers⁴, Michael P. Stone³, R. Stephen Lloyd^{1, 5} (2014) Molecular basis of aflatoxin-induced mutagenesis – role of the aflatoxin B₁-formamidopyrimidine adduct, *Carcinogenesis* 35, 1461-1468.

¹ Oregon Institute of Occupational Health Sciences and

² Cancer Biology Program, Oregon Health & Science University, Portland, OR 97239, USA

³ Department of Chemistry, Vanderbilt University, Nashville, TN 37235, USA

⁴ Department of Biochemistry and Molecular Biophysics, Washington University School of Medicine, St. Louis, MO 63110, USA

⁵ Department of Molecular and Medical Genetics, Oregon Health & Science University, Portland, OR 97239, USA

Preface

This work is published in *Carcinogenesis*.

The author conceived, designed and performed experiments, data analyses, and wrote the manuscript.

Liang Li and Michael P. Stone provided AFB₁-FAPY adducted oligodeoxynucleotides and contributed to the critical reading of the manuscript.

Alena V. Makarova and Peter M. Burgers provided yeast pol δ and pol δ -Exo, and contributed to the critical reading of the manuscript.

R. Stephen Lloyd contributed to the conception of the project, experimental design, the editing and critical reading of the manuscript, and provided funding and lab space for the execution of this work.

Adapted and modified with permission from

Ying-Chih Lin, Liang Li, Alena V. Makarova, Peter M. Burgers, Michael P. Stone, R. Stephen Lloyd (2014) Molecular basis of aflatoxin-induced mutagenesis – role of the aflatoxin B₁-formamidopyrimidine adduct, *Carcinogenesis*, 35, 1461-8.

Copyright (2014) Oxford University Press

Introduction

Chronic dietary exposure to AFB₁, through the consumption of food products contaminated with the fungi *Aspergillus flavus* and/or *Aspergillus parasiticus*, is a significant risk factor for the development of early onset HCC. HCC is the third leading cause of cancer death worldwide, with distinct geographical distributions, mainly in sub-Saharan Africa and Southeast Asia where concomitant risk factors frequently include both HBV infection and AFB₁ exposure^{9,16,167}.

The biological basis of AFB₁-related HCC has been ascribed in part to the genotoxic and mutagenic effects of AFB₁. Upon metabolic activation by cytochrome P450 enzymes⁴¹, AFB₁ is converted to the highly reactive intermediate AFB₁-8,9-epoxide³⁶, which can covalently bind to the N7 atom of deoxyguanosine in DNA to form the AFB₁-DNA adduct, AFB₁-N7-Gua⁷⁸⁻⁸¹. In addition to spontaneous depurination, under slightly basic and physiological conditions, the AFB₁-N7-Gua adduct rearranges to the open-ringed AFB₁-FAPY adduct. This lesion is the persistent AFB₁-DNA adduct in humans and animal models⁹¹⁻⁹⁴ (Figure 2). Mutational analyses using several *in vitro* and *in vivo* model systems have revealed that the predominant mutations induced by AFB₁ exposure are G to T transversions^{123,128,141,168-170}. Further, in more than half of the HCC patient samples that were obtained from geographic locations with known high AFB₁ exposures, DNA sequence analyses revealed a G to T mutation at the third position of codon 249 in the *p53* tumor suppressor gene^{130,131}. Mutagenesis studies in SOS-induced *E. coli*, which utilized site-specifically modified DNAs containing either the AFB₁-N7-Gua or AFB₁-FAPY

adducts in a shuttle vector, demonstrated that both AFB₁-N7-Gua and AFB₁-FAPY adducts were promutagenic with mutation frequencies of 4% and 32%, respectively, and that both types of lesions caused predominantly G to T transversions^{165,166}. Based on its persistence in animal tissues, it is of particular interest to determine the mutagenic property of AFB₁-FAPY adducts in primate cells.

When mammalian cells replicate DNA that contains residual DNA damage induced both endogenously and exogenously, the majority of these adducts block high fidelity replicative polymerases (i.e. pol δ and ϵ) and thus, cells utilize specialized DNA polymerases, known as translesion synthesis (TLS) polymerases to directly replicate past the damaged nucleotides. TLS polymerases not only possess flexible active sites to accommodate abnormal base alterations, but also lack proofreading exonuclease activities to remove potential misinsertions. As a result, the bypass of damaged nucleotides by TLS polymerases may lead to mutations. This process has been recognized to play a significant role in spontaneous and damage-induced point mutagenesis. The conservation of TLS polymerases across all three domains of life highlights their functional role in DNA damage tolerance and the maintenance of genome stability. Five eukaryotic TLS polymerases have been studied extensively, including pol ζ in the B family and members of the Y family: pol κ , η , ι and REV1^{145,171-174}. Depending on the types of DNA damage, each polymerase may have distinct and/or similar bypass abilities. The insertion opposite a lesion and extension from the inserted nucleotide can be carried out by a single TLS

polymerase alone, or through a concerted effort of different combinations of two TLS polymerases, followed by a reversion to normal replicative polymerase downstream of the damaged nucleotide^{172,175,176}. For example, pol η can bypass the UV-induced *cis-syn* T-T cyclobutane pyrimidine dimer (CPD) accurately and efficiently^{177,178}, but in the absence of pol η , replication bypass of CPDs has been suggested to be catalyzed by pol κ and/or ι in combination with pol ζ in an error-prone manner^{179,180}.

The molecular mechanism of AFB₁-induced mutagenesis has not been fully investigated. Banerjee *et al.* reported that the archaea *Sulfolobus solfataricus* DNA polymerase IV (Dpo4), a homolog of human pol κ , can bypass AFB₁-FAPY in an error-prone manner *in vitro*¹⁸¹. The goals of the current study were to investigate both the spectra and frequency of mutations generated following the replication of single-stranded (ss) DNAs containing a site-specific AFB₁-FAPY adduct in primate cells. By using a ss vector that prohibited any repair prior to TLS, it was possible to assess the replication fate of these adducts and infer the underlying mechanisms of replication bypass of AFB₁-FAPY adducts using *in vitro* replication assays.

Experimental procedures

Materials

COS-7 cells were purchased from the American Type Culture Collection. The pMS2 shuttle vector was a generous gift from Dr. Masaaki Moriya (State University of NY, Stony Brook, NY). Uracil DNA glycosylase, T4 DNA polymerase,

T4 polynucleotide kinase, T4 DNA ligase and *EcoRV* were obtained from New England BioLabs. [γ - ^{32}P]ATP was purchased from PerkinElmer Life Sciences. Bio-Spin columns were obtained from Bio-Rad. Amicon Ultra centrifugal filter devices were purchased from Millipore. Human pol κ , ι and yeast pol ζ were obtained from Enzymax, LLC. Human pol η catalytic cores were kindly provided by Dr. Robert Eoff (University of Arkansas). Wild type and the exonuclease-deficient form of *Saccharomyces cerevisiae* pol δ holoenzymes were purified as previously described¹⁸². Dulbecco's modified Eagle's medium, Opti-MEM (reduced serum medium), L-glutamine, antibiotic-antimycotic, and Lipofectin reagent for tissue culture and *E. coli* Max Efficiency DH5 α cells were purchased from Invitrogen. Phosphate-buffered saline and 100 mM dNTPs were purchased from GE Healthcare Life Sciences. All other general reagents and chemicals were purchased from Fisher and Sigma-Aldrich.

Oligodeoxynucleotides

A 12-mer oligodeoxynucleotide (5'-ATAATTXAATCC-3') containing an AFB₁-FAPY adduct (Figure 2) as designated by X was prepared as previously described¹⁸¹. Nondamaged (ND) oligodeoxynucleotides (12- and 46-mers) and primer DNAs were purchased from Integrated DNA Technologies, Inc.

Site-specific mutagenesis assay

Oligodeoxynucleotides (12-mers) containing a site-specific AFB₁-FAPY or ND dG were inserted into ss pMS2 shuttle vector, as previously described¹⁸³⁻¹⁸⁵. Briefly,

a 44-mer scaffold DNA was synthesized to be perfectly complementary to the linearized vector sequences following *EcoRV* cleavage of the spontaneously formed duplex hairpin, such that all positions of thymine were substituted with uracil nucleotides (5'-CUCGAGGGCCCCUGCAAGCGAUG**GGAUUCAAUUAAU**AUCGCUGGUACCGAGCUCGAAUUC-3'). The central 12 nucleotides (in bold) were complementary to the control and adducted DNAs to be inserted. The ss circular pMS2 DNA (15 pmol) was digested with *EcoRV*, followed by the addition of scaffold DNAs at equal molar concentrations to form the partially gapped duplex. The 12-mer (15 pmol) was then annealed into the gapped duplex, and ligation was carried out at 12°C for >48 hr. Scaffold and linear DNA fragments were eliminated by uracil DNA glycosylase and T4 DNA polymerase treatments in the absence of dNTPs.

Transfection of COS-7 cells, extraction of progeny DNA, *E. coli* transformation and differential hybridization analyses were carried out as previously described^{184,185} with minor modifications. Following isolation of the replicated DNAs, progeny plasmids were used to transform *E. coli* DH5 α according to the manufacturer's protocols (Invitrogen). Aliquots of bacterial cultures were grown in 96-well plates, lysed with 0.25 N NaOH and applied to a Hybond membrane using a vacuum manifold apparatus. The membranes were pH neutralized and washed, followed by the DNA being cross-linked to the membrane using a UV Stratalinker. To determine the mutation spectrum at the adducted site, differential hybridizations were conducted with a series of 5'-radiolabeled probes (5'-GATAT

AATTNAATCCATCGCTT-3', where N refers to G, T, A, or deletion) at 44°C overnight. A bridge oligodeoxynucleotide probe (5'-ATCCATCGCTTGCAAGGG-3') was synthesized to be complementary to the sequence at the junction of the vector and insert and it was used to confirm the proper insertion of the control or adducted 12-mers. The interpretation of the data from the differential DNA hybridization analyses were confirmed by direct DNA sequencing. DNAs that hybridized with the bridge probe, but not with any of the mutation or deletion probes, were further analyzed by DNA sequencing at the DNA Services Core at Oregon Health & Science University.

Construction of site-specifically modified linear templates for in vitro replication assays

Linear ss template DNAs (46-mers) containing a site-specific AFB₁-FAPY were generated according to a previously reported procedure¹⁸⁴ with the following modifications. Briefly, the 12-mer oligodeoxynucleotides (400 pmol) containing AFB₁-FAPY were centrally ligated between equal molar concentrations of a 16-mer (5'-ATTATGCAGCGATAGA-3') and an 18-mer (5'-ATCGCTGGTACCGACTCG-3') at the 5' and 3' end, respectively. These three DNAs were sequentially ordered by hybridization to a 42-mer scaffold DNA (5'-AGTCGGTACCAGCGATGGATTCAATTATTCTATCGCTGCATA-3'). The 5' end of an 18-mer was ³²P labeled for purposes of purification of the full-length product. Reactions were performed using 800 units of the T4 DNA ligase at 20°C overnight. The ligated products were separated from all other reactant DNAs by electrophoretic

separation through 10% acrylamide denaturing gels containing 8 M urea. DNAs that migrated at the correct size were cut from the gel and extracted using 0.5 M ammonium acetate/10 mM magnesium acetate buffer, desalted with water and concentrated by Amicon 3k centrifugal filter devices. The sequence of the ligation product 46-mer was: 5'-ATTATGCAGCGATAGAATAATTGAATCCATCGCT GGTACCGACTCG-3', where the underlined G is AFB₁-FAPY.

In vitro DNA replication assay

Oligodeoxynucleotide primers were synthesized to be complementary to several positions within the 46-mers such that the 3' end of each primer was designed to hybridize 10 or 1 nucleotide upstream from the lesion site (-10 and -1 primers, respectively), immediately opposite the adduct (0 primer) or 2, 3 or 5 nucleotides downstream of the lesion site (+2, +3 or +5 primers, respectively). Three additional variations of the 0 primer were also synthesized to contain a mismatched nucleotide (A, T, or G) at the 3' end (0-A, 0-T, 0-G primers, respectively). The sequences of each of these primers appear as figure insets. The primers were ³²P labeled and annealed to the 46-mer template at a 1:2 molar ratio in the presence of 40 mM NaCl, heated at 90°C for 2 min and cooled to room temperature. *In vitro* primer extension reactions were carried out using 5 nM primer-template complex in 25 mM Tris-HCl (pH 7.5), 8 mM MgCl₂, 10% glycerol, 100 µg/ml of bovine serum albumin, and 5 mM dithiothreitol at 37°C for 30 min unless otherwise specified in the figure legends. Concentrations of dNTP(s) and polymerases are given in the figure legends. The reactions were

terminated by the addition of an equal volume of a solution containing 95% (v/v) formamide, 20 mM EDTA, 0.02% (w/v) xylene cyanol, and 0.02% (w/v) bromophenol blue. Reaction products were resolved by electrophoresis through 15% acrylamide denaturing gels containing 8 M urea and visualized using a PhosphorImager screen.

Results

Mutagenic potential of AFB₁-FAPY adducts in primate cells

To evaluate the mutagenic potential of the AFB₁-FAPY adduct (Figure 2) in primate cells, site-specific mutagenesis assays were carried out by transfecting a ss shuttle vector that had been engineered to contain a site-specific AFB₁-FAPY adduct or control ND dG, into African green monkey kidney COS-7 cells. Since the input DNA was exclusively ss, DNA repair mechanisms were not operational until DNA replication bypass was complete. Following a 48 hr incubation to allow replication of the shuttle vector, the resultant progeny plasmids were extracted and transformed into DH5 α *E. coli* cells. Following selection for ampicillin resistance and growth of individual colonies, DNAs were extracted and analyzed for mutation spectra and frequencies by differential hybridization strategies. To assure that the control and adduct-containing 12-mer DNAs had been correctly inserted into the shuttle vector, progeny plasmid DNAs were hybridized with an oligodeoxynucleotide bridge probe, spanning both the 12-mer insert and the vector. Replicates of these DNAs were also hybridized with oligodeoxynucleotide probes that would only recognize the 12-mer sequences surrounding the

adducted site with perfect complementarity. Thus, using stringent differential hybridization conditions, a mutagenic spectrum could be inferred. To confirm the accuracy of the differential hybridization results, representative colonies were picked for DNA sequencing to verify the correct identification of the mutation by each sequence-specific probe. All plasmid DNAs that hybridized only with the bridge probe, indicating the presence of the adducted oligodeoxynucleotide insert, but not with any sequence-specific mutation probes, were subjected to DNA sequencing to determine the sequence of the progeny DNA.

Analyses of these data revealed that the mutation frequency was exceptionally high, in which 97% of the translesion bypass events for the AFB₁-FAPY adduct led to a mutagenic outcome (Table 1). No mutations were detected with the control ND sequence (Table 1). The mutation spectrum included single base substitutions and deletions. The predominant mutations that were introduced as a result of replicating past the AFB₁-FAPY adducts were G to T transversions, accounting for 86% of all mutations scored, followed by a much lower frequency of G to A transitions (~10%), even less frequent G to C transversions and deletions that accounted for < 3% of the total events observed. Overall, these data demonstrate that replication of DNAs containing an AFB₁-FAPY adduct in primate cells was highly mutagenic. The predominant G to T transversion strongly agrees with previously reported mutational analyses of HCC patient samples from regions known for high aflatoxin exposure^{130,131}.

DNA modification	Colonies scored	Mutated	Single base substitutions			Deletions	Other position substitution	Frequency of mutation (%)
			G to T	G to A	G to C			
ND	189	0	0	0	0	0	0	0
AFB ₁ -FAPY	203	197	170 (86.3%)	16 (8.1%)	5 (2.5%)	5 (2.5%)	1 (0.5%)	97

Table 2. Mutation spectrum generated from replication bypass of AFB₁-FAPY adducts in COS-7 cells.

AFB₁-FAPY blocks replicative pol δ

Since the mutagenesis data described above demonstrated that DNA polymerases in COS-7 cells could bypass the AFB₁-FAPY adduct, an investigation was initiated to identify which of the replicative or TLS DNA polymerases could be responsible for the cell-based mutagenesis. Although these are very large lesions that would be anticipated to block replicative DNA polymerases, yeast replicative DNA polymerase δ was analyzed for its capacity to catalyze replication past the biologically stable AFB₁-FAPY adduct. *In vitro* replication assays were designed to measure bypass under running (-10 primer) start conditions (Figure 3). Although pol δ efficiently extended the -10 primer on the ND template to full length products, the presence of the AFB₁-FAPY adduct blocked extension of the primer at one and two nucleotides prior to the lesion, even at the highest concentration of pol δ tested (Figure 3, compare lanes 3 and 6). Additionally, these data suggest that the efficiency of loading pol δ , even on

the -10 primer may be impeded due to the presence of the adduct, since overall primer utilization was significantly decreased (Figure 3, compare lanes 2 and 5). Furthermore, there was no detectable full-length bypass product of AFB₁-FAPY. These results demonstrated that AFB₁-FAPY represents a strong replication block to pol δ.

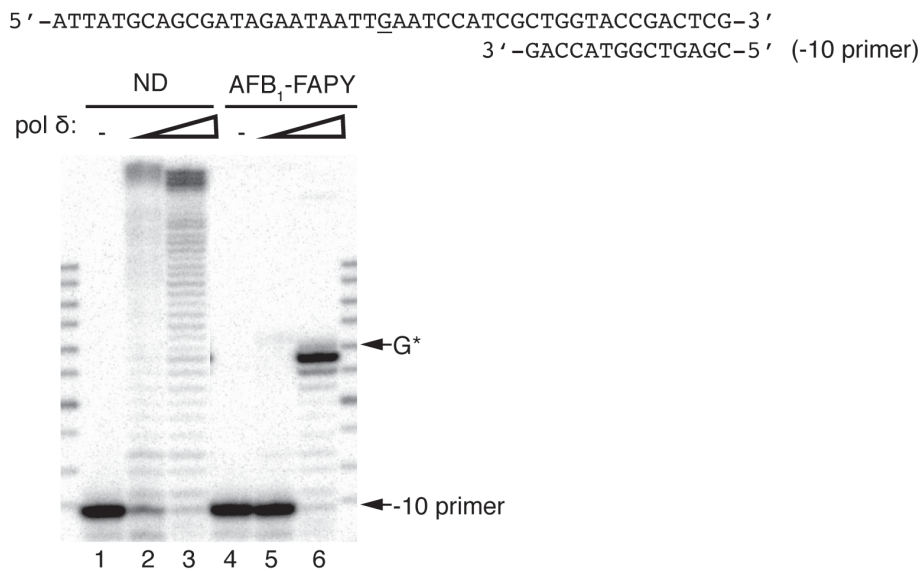


Figure 3. Replication blockage of pol δ by AFB₁-FAPY. -10 oligodeoxynucleotide primers were annealed to ND or AFB₁-FAPY-containing DNA templates. Primer extensions were catalyzed by 1 nM (lane 2, 5) or 50 nM (lane 3, 6) pol δ in the presence of 100 μM dNTPs. G*, adducted site.

Standing start single and combined dNTP reactions were also performed using a -1 primer. However, the exonucleolytic activity of pol δ dominated all polymerization reactions, with no nucleotide incorporation detected (Figure 4A-B). In addition, when an exonuclease-deficient form of pol δ (pol δ-Exo) was used, it poorly inserted all four dNTPs opposite the lesion and could extend from a

mispaired A opposite AFB₁-FAPY-dG (note the band at +2 site in lane 2 Figure 4C). Comparative analyses of differences in nucleotide incorporation between pol δ and pol δ-Exo revealed that the proofreading function of the exonuclease prevented miscoding and synthesis past AFB₁-FAPY by pol δ.

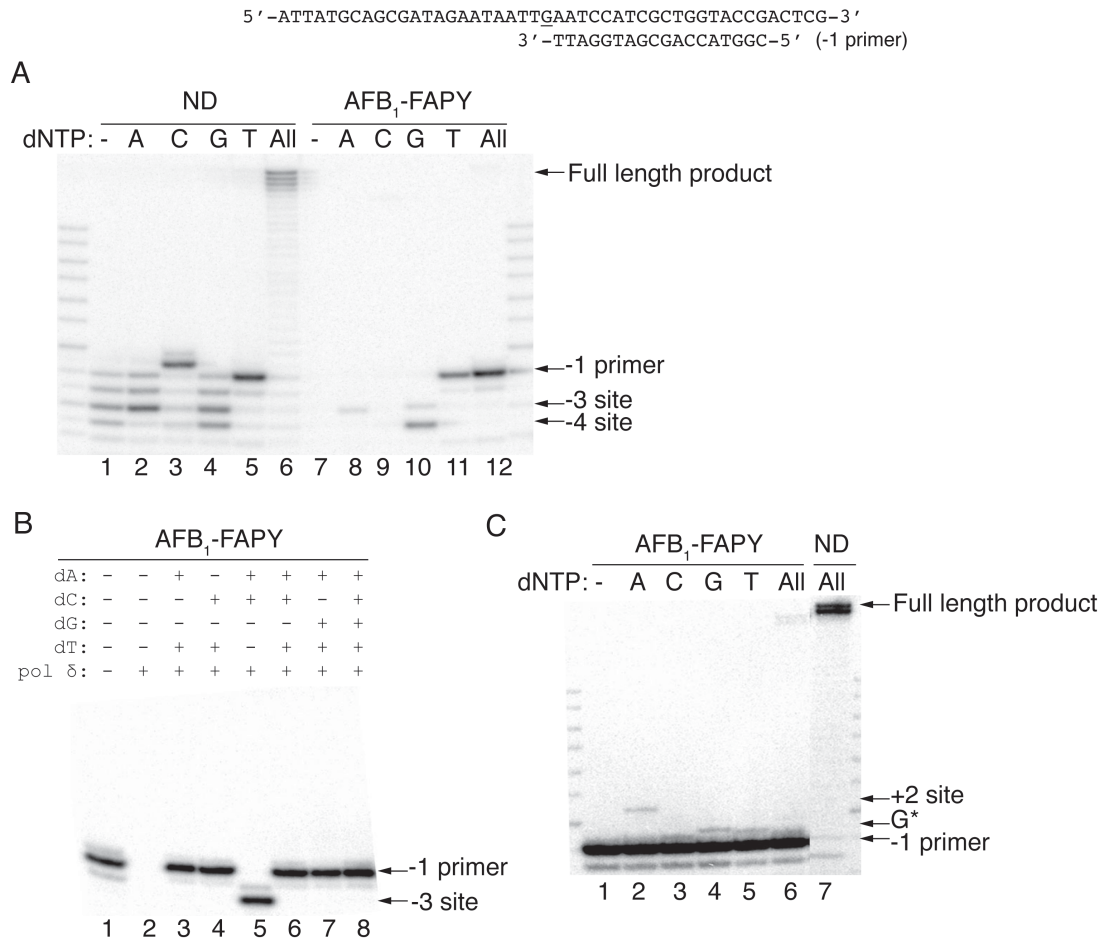


Figure 4. Nucleotide insertion opposite AFB₁-FAPY by pol δ. The -1 primers were annealed to ND or AFB₁-FAPY-containing DNA templates. (A) Single-nucleotide insertion and primer extensions were catalyzed by 1 (lane 1-6) or 50 nM (lane 7-12) pol δ in the presence of 100 μM individual or all dNTPs. (B) dNTP combination and primer extension reactions were conducted with 50 nM pol δ in the presence of combinations of 500 μM dNTPs. (C) Single-nucleotide

insertion opposite AFB₁-FAPY catalyzed by 20 nM pol δ -Exo in the presence of 100 μ M individual or all dNTPs. G* indicates the position of the adducted site.

Pol ζ -mediated replication bypass of AFB₁-FAPY leads to G to T mutation

Since pol δ (and by inference other replicative polymerases) could not bypass this lesion, investigations were designed to test the ability of DNA pol ζ to replicate past the AFB₁-FAPY adducts *in vitro*. As shown in Figure 5A, pol ζ preferentially inserted an A opposite the lesion, as evidenced by the extension product at the +2 site. This insertion of three nucleotides most likely represented an incorporation of dA opposite the adduct, followed by an additional synthesis of two nucleotides downstream (Figure 5A lane 8). Furthermore, a full-length bypass product was observed when all dNTPs were added, demonstrating that AFB₁-FAPY can be bypassed by pol ζ (Figure 5A lane 12). Analyses of single-nucleotide incorporation reactions with the ND template showed that as expected, pol ζ preferentially inserted a correct C, while A, G or T could also be utilized, albeit less efficiently (Figure 5A lanes 2-5).

Next, the hypothesis that pol ζ could preferentially extend beyond a misincorporated A opposite the AFB₁-FAPY lesion was tested (Figure 5B). Extension reactions were conducted using primers with different 3' end opposite the adducted nucleotide. Pol ζ preferentially extended the mispaired-A primer when annealed to the damaged template (Figure 5B lane 13). Using higher concentrations of pol ζ , it was possible to detect extension products off of all mispairs, but not from the nonmutagenic dC (data not shown). Under conditions

using the ND template, all primers were efficiently extended (Figure 5B lanes 5-8).

Thus, our results constitute the first biochemical evidence that pol ζ can catalyze replication bypass of AFB₁-FAPY adducts by preferentially misincorporating dA opposite the lesion and extending beyond the misinsertion. These data suggest that pol ζ could be the major DNA polymerase responsible for the predominant G to T mutation induced by AFB₁-FAPY *in vivo* (Table 1).

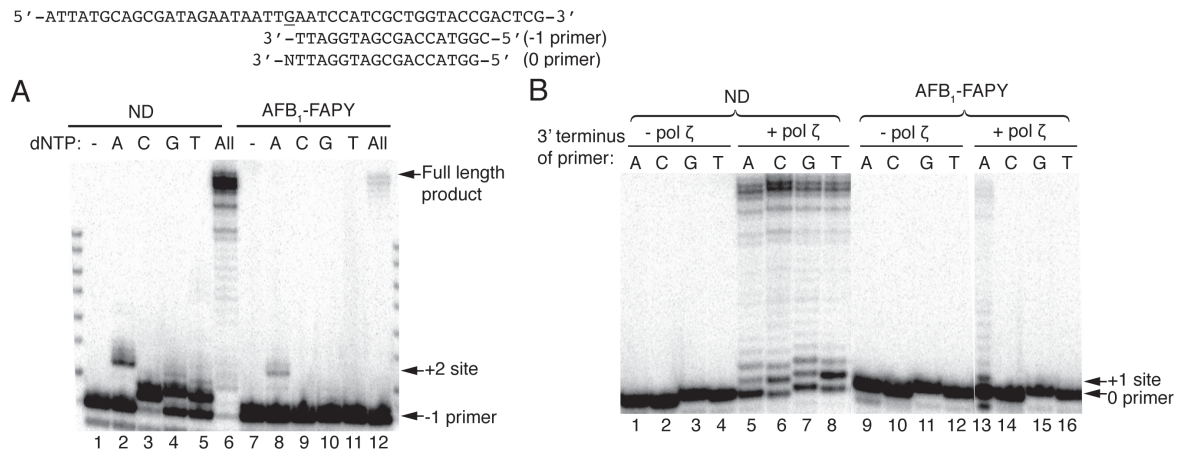


Figure 5. Replication bypass of AFB₁-FAPY by yeast pol ζ . The -1 or 0 oligodeoxynucleotide primers with different 3' end (where N represents either A, C, G or T) were annealed with ND or AFB₁-FAPY adducted DNA templates. (A) Single-nucleotide incorporations and primer extension reactions were catalyzed by 5 nM (ND) or 50 nM (AFB₁-FAPY) pol ζ in the presence of 100 μ M individual or all dNTPs. (B) Oligodeoxynucleotide primer extensions from the matched C or mismatched A, G, and T 3' terminus opposite ND or AFB₁-FAPY were catalyzed by 10 nM pol ζ in the presence of 100 μ M dNTPs.

Replication bypass of AFB₁-FAPY by human pol κ , η and ι

To test whether members of the Y-family TLS polymerases (pols κ , η , and ι) could also contribute to the observed mutagenesis (Table 1), the ability of these polymerases to catalyze replication bypass of the AFB₁-FAPY adduct was examined. While primer extensions were readily detected on a ND template for all polymerases (Figure 6 and 7), when either human pol κ (Figure 6A) or η (Figure 7A) encountered the AFB₁-FAPY adduct, replication was stalled following insertion opposite the lesion. Additionally, pol κ -catalyzed replication showed major pause sites one and two nucleotides prior to the lesion (Figure 6A lanes 5-6), while pol η also paused one nucleotide before and after the lesion (Figure 7A lanes 5-6). Similar to data shown for pol δ , both pol κ and η exhibited reduced loading and primer utilization on the adducted templates. Analyses of single-nucleotide incorporation reactions revealed that both pol κ and η could incorporate all dNTPs opposite AFB₁-FAPY, albeit inefficiently (Figure 6B lanes 8-12 and 7B lanes 8-12, respectively). Further extensions beyond the lesion to +2 and/or +3 sites were observed when either dATP alone or all dNTPs were present in the reaction, with both pol κ and η , generating minute amounts of full-length bypass products when all four dNTPs were included in the reaction. Pol κ appeared to incorporate all four dNTPs with equal efficiency, while pol η preferentially incorporated purines over pyrimidines. Since these data do not match the observed mutagenic spectra, we consider that pol ζ is the most likely candidate for catalyzing the cellular bypass reaction.

To further examine the possible mechanism by which pol κ and η might contribute to G to T mutagenesis, primer extensions were carried out using four 0

primers, that contained a matched or mismatched nucleotide at the 3' end opposite the lesion. It was hypothesized that preferential primer extension would occur from the mispaired A, thus accounting for the mutagenic outcome. Pol κ extended mismatched-A primers that had been annealed to the damaged template somewhat more efficiently than the corresponding mismatched-G or -T primers, while the correct C primer was not extended (Figure 6C). As anticipated, correctly matched-C primers that had been annealed to the ND template were efficiently utilized. In contrast, pol η more efficiently extended matched-C primers than corresponding mismatched-A, -G or -T primers when annealed to either ND or damaged templates (Figure 7C). To further rule out a significant role for pol η in the bypass of this adduct, pol η -deficient COS-7 cells were generated by shRNA against *Pol η* and were used in the mutagenesis assay as described above [in collaboration with Irina G. Minko (OHSU), Robert W. Sobol (University of Pittsburgh), and Thomas G. Wood (University of Texas Medical Branch), unpublished]. No changes were detected in the AFB₁-FAPY mutation frequency or spectrum in pol η -depleted COS-7 cells compared to WT cells (data not shown). Collectively, these data suggest that human pol κ and η may only exert a limited role in cellular replication bypass of AFB₁-FAPY through either error-prone or error-free reactions.

Additionally, it was observed that human pol ι could not incorporate any nucleotides opposite AFB₁-FAPY, although it could extend matched-C primers annealed to AFB₁-FAPY more efficiently than the corresponding mismatched-A primers *in vitro* (data not shown). Taken together, these results suggest that

polymerases κ , η and ι are unlikely to be the primary contributors (but may serve as backup TLS polymerases) for processing AFB₁-FAPY adducts *in vivo*.

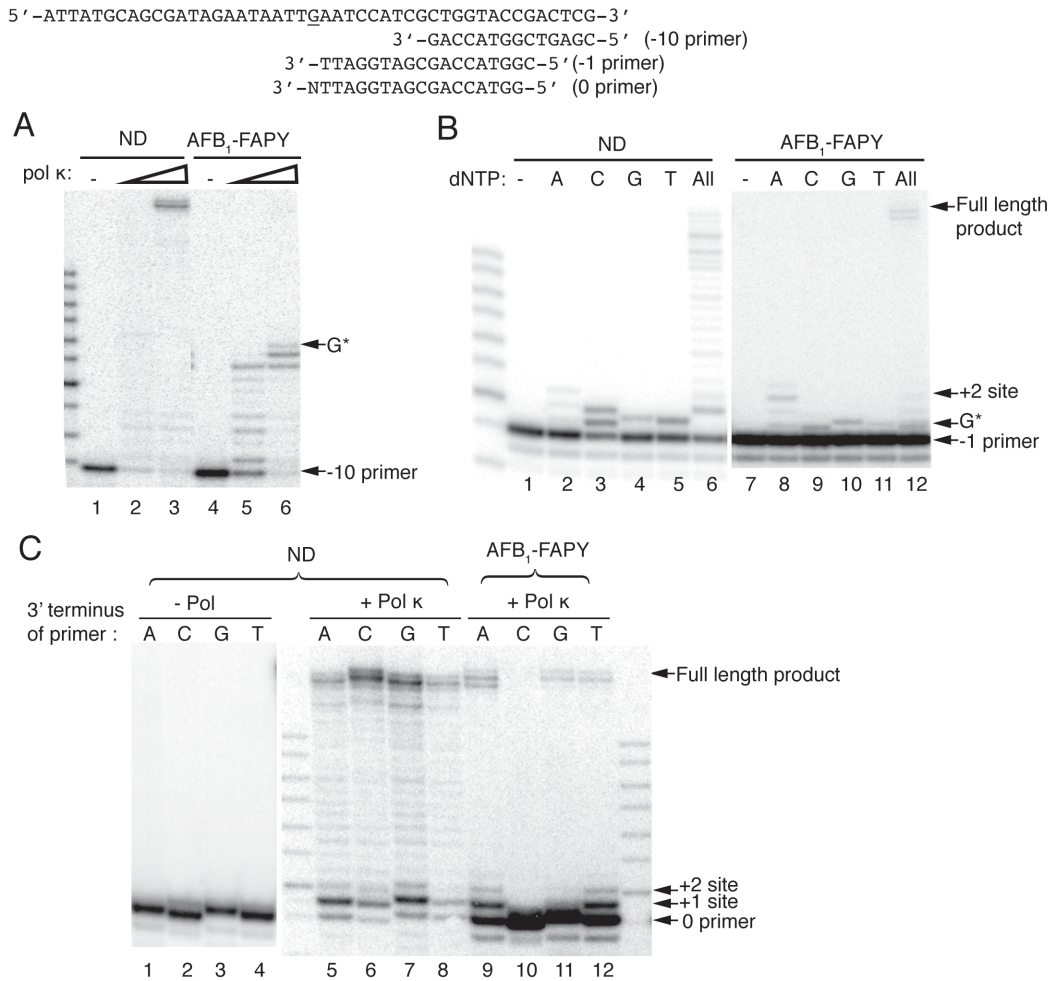


Figure 6. Replication bypass of AFB₁-FAPY by human pol κ . Oligodeoxynucleotide primers (-10, -1 or 0) with different 3' termini (designated as N, which represents either A, C, G or T) were annealed to ND or AFB₁-FAPY containing DNA templates. (A) Primer extension reactions were catalyzed by increasing concentrations of pol κ (2 or 10 nM) in the presence of 100 μ M dNTPs. (B) Single-nucleotide incorporation and primer extension reactions were conducted by 2 nM (ND) or 10 nM (AFB₁-FAPY) pol κ in the presence of 20 μ M (ND) or 100 μ M (AFB₁-FAPY) combined or individual dNTPs. (C) Primer extensions from the matched C or mismatched A, G, and T 3'

terminus opposite AFB₁-FAPY or ND were catalyzed by 10 nM or 0.5 nM pol κ in the presence of 20 μM dNTPs. G* indicates the position of the adducted site.

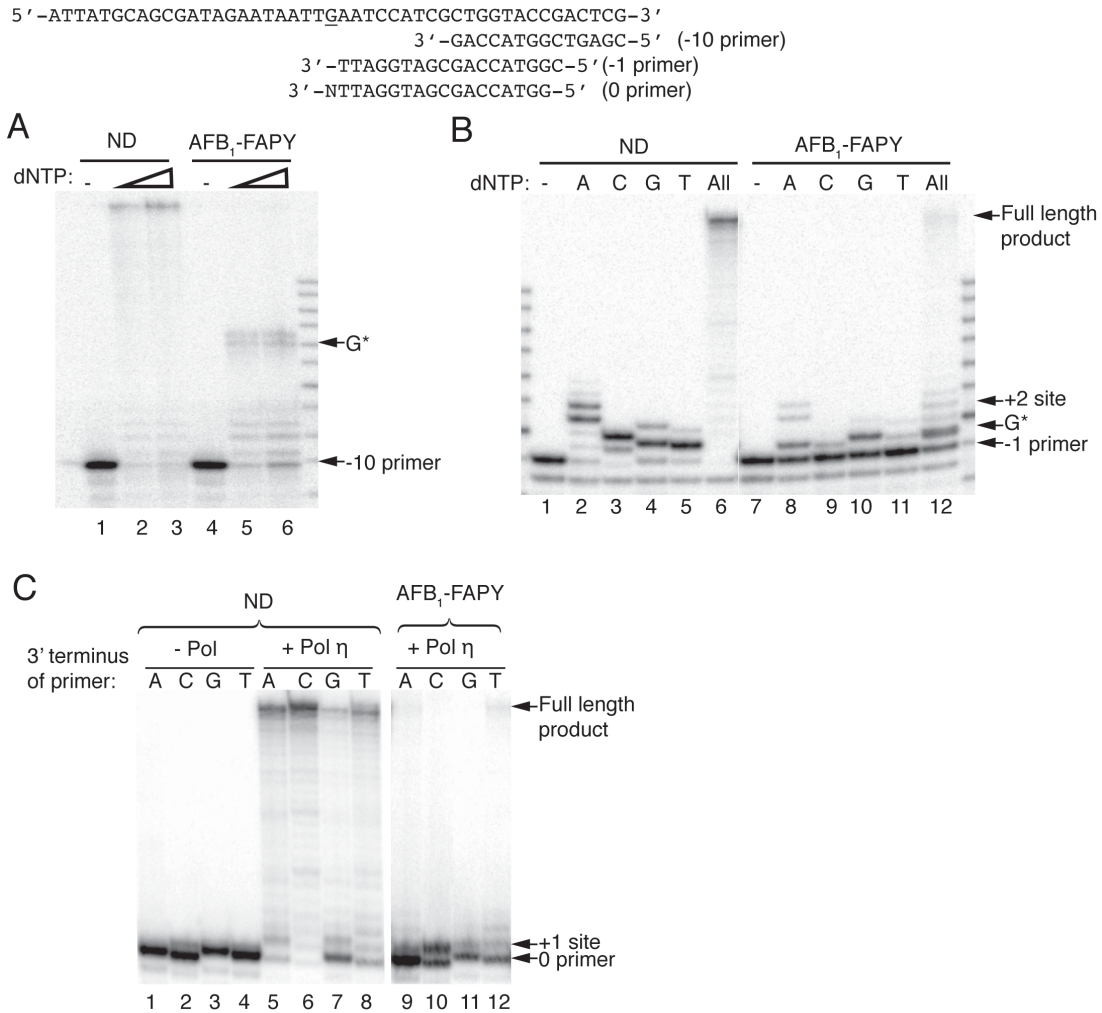


Figure 7. Replication bypass of AFB₁-FAPY by human pol η catalytic core.

Oligodeoxynucleotide primers (-10, -1 or 0) with different 3' termini (designated as N, that represents either A, C, G or T) were annealed to ND or AFB₁-FAPY adducted DNA templates. (A) Primer extension reactions were catalyzed by 0.5 nM pol η with increasing concentrations of dNTPs (20 or 100 μM). (B) Single-nucleotide incorporation and primer extension reactions were catalyzed by 2 nM pol η in the presence of 20 μM individual or combined dNTPs. (C) Primer extension reactions from the matched C or mismatched A, G, and T 3' terminus opposite AFB₁-

FAPY or ND were catalyzed by 0.5 nM pol η in the presence of 20 μ M dNTPs. G* indicates the position of the adducted site.

Resumption of efficient replication by pol δ

To test how far beyond the lesion site normal replication can resume, primer extension reactions were carried out with pol δ using ND or AFB₁-FAPY modified templates annealed to +2, +3, and +5 primers, containing either matched C or mismatched A opposite the lesion, mimicking the accurate and mutagenic bypass observed *in vivo* (Figure 8). When the correct C was positioned opposite control dG or an AFB₁-FAPY adduct, pol δ efficiently extended all primers (Figure 8A lanes 4-9). However, for the lesion containing templates, there was a small percentage of the primer resected primarily back to the +1 site. Furthermore, the extension efficiencies increased as the number of correct base pairs beyond the lesion increased. All primers with the ND template were completely utilized.

In contrast to the data with the correct C opposite the lesion, when a mispaired A was positioned opposite the adduct for the +2 or +3 primer, the exonuclease activity digested back to the -1 position (Figure 8B lanes 7-8). Appreciable amounts of full-length products were only obtained with the mispaired +5 primer (Figure 8B lane 9). Even under these conditions, some +5 primers were resected to the -1 site. In contrast, mismatched primers that were hybridized to the ND template were fully extended (Figure 8B lanes 4-6). Collectively, these data revealed that for pol δ , the balance between polymerization and exonucleolytic resection was affected by the location of the mispair in the duplex primer template. Thus, the balance between the exonuclease and polymerase activities

shifted towards extension when the mismatch was located deeper in the duplex. These data suggest that the TLS polymerase(s) need to continue several nucleotides beyond the lesion to preserve the mutagenic bypass before switching to a replicative polymerase.

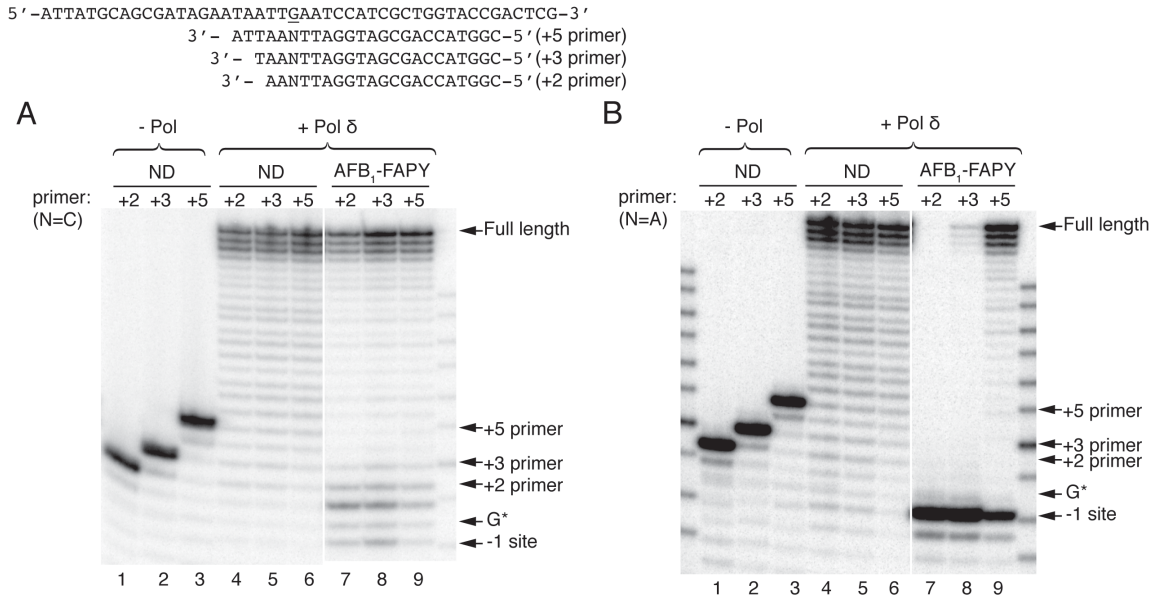


Figure 8. Resumption of replication by pol δ downstream of AFB₁-FAPY. +2, +3 or +5 oligodeoxynucleotide primers with either matched C or mismatched A opposite the lesion or control site were annealed to ND or AFB₁-FAPY containing DNA templates. (A-B) Primer extensions were catalyzed on matched and mismatched primers, respectively. All reactions were catalyzed by 50 nM pol δ in the presence of 100 μM dNTPs. G*, adducted site.

Discussion

Aflatoxin-associated HCCs represent an enormous global health crisis, with a significant percentage of the estimated 550,000-600,000 new cases of HCC per year attributed to aflatoxin exposure alone¹⁴. However, insights into the molecular

mechanisms driving this mutagenesis as an early event of hepatocellular carcinogenesis have not been elucidated in either non-human primate or human cells. In the current study, we addressed the following issues: 1) the mutagenicity of AFB₁-FAPY in primate cells using a site-specifically modified ss vector, and 2) the mechanism of replication bypass of AFB₁-FAPY adducts using *in vitro* replication assays catalyzed by eukaryotic replicative and TLS DNA polymerases δ , ζ , κ , η and ι .

The utility of pMS2 ss shuttle vector containing site-specific DNA adduct, combined with differential hybridization analysis, in mutagenesis studies of various carcinogens has been demonstrated by others and our laboratory¹⁸³⁻¹⁸⁷. This approach allows straightforward detection of mutation spectrum and frequency opposite the lesion within a designated region of the vector, but without biased selection and interference from DNA adduct formation and DNA repair processes.

The results of our mutagenesis assays in primate cells were in good agreement with previous prokaryotic-based studies¹⁶⁶, indicating that AFB₁-FAPY is a biologically relevant mutagenic DNA adduct, predominantly giving rise to G to T transversions (Table 1). These data also correlate well with previous observations of G to T transversions dominating the mutagenic spectrum of human AFB₁-associated HCC samples and in experimental model systems treated with AFB₁^{123,126,130,131,141,168,169}. Taken together, these data suggest a causative role of AFB₁-FAPY in the initiation of liver cancer through mutagenesis. More strikingly, the mutagenicity of AFB₁-FAPY lesions in primate cells appeared

to be much higher (97%, Table 1) than that previously observed in *E. coli* cells (32%)¹⁶⁶. These data indicate that primate cells, and by way of extension to human cells, are more susceptible to the mutagenic effect of AFB₁ than *E. coli*, thus emphasizing the carcinogenic potency of AFB₁ in animals and humans.

A limitation of the present study was that only one DNA sequence context was examined. The immediate 5' sequence context of the lesion was 5' TT**G** in which the G in bold was the site of the adduct. In this specific sequence, there could be two competing hypotheses for the molecular mechanisms underlying the high frequency G to T transversions. The first is a simple misinsertion of dA opposite the adduct and subsequent extension from that mispair, followed by correct base pairing of the following two nucleotides, both dAs. This reaction could conceivably occur as a continuous processive reaction, or as a series of associative/dissociative polymerization steps in which the incorporation of nucleotides would be distributive. Alternatively these data could also be anticipated if there was a transient DNA polymerase slippage mechanism in which the adducted nucleotide was expelled from the active site and the incorporation of dA would be opposite the 5' unadducted dT, followed by a slippage/realignment of the newly synthesized dA opposite the AFB₁-FAPY adduct. This would then be followed by normal base-pairing synthesis of the downstream sequences. This model could also possibly account for the G to T transversions. Of these two competing models, we favor the former for the following reasons. First, to the best of our knowledge, mutation hotspots have not been reported at G:C pairs that are adjacent to a run of consecutive dTs. Instead,

AFB₁-induced G to T mutation sites frequently arise at the third base of codon 249 (AGG in human) of the *p53* tumor suppressor gene and the first or middle base of codon 12 (GGC in human or GGA in trout) of the *ras* oncogene^{141,168,188}. In addition, Besaratinia et al. found that about half of the mutation sites of the predominant G to T transversions in the *cII* transgene in AFB₁-exposed Big Blue MEF cells occurred within CpG sequence contexts¹⁴³. Similarly, this sequence specificity was observed at nucleotide positions 101, 108, 115, 140, 208, and 320 as G to T mutation hotspots in the *gpt* gene in AFB₁-treated mouse liver¹²⁶. Therefore, it seems more likely that the G to T transversions detected in the current sequence context are caused by the combination of a misincorporated dA opposite the AFB₁-FAPY lesion and extension from the misinsertion by DNA polymerase(s) as discussed below.

Systematic biochemical studies suggest a model of TLS across AFB₁-FAPY adducts (Figure 9). Upon encountering an AFB₁-FAPY adduct during replication, synthesis by the replicative polymerases (here represented by pol δ) are hypothesized to be blocked, resulting in a switch to pol ζ to insert an A opposite and extend beyond the lesion. This model predicts that, following synthesis of a short stretch of DNA, normal replicative polymerases could resume replication to preserve the mismatch. A subsequent round of DNA replication would be required to make permanent the G to T mutation that occurred in our system with 97% probability. Although pol κ exhibited marginal preference for extending the mismatched A primer terminus, which could potentially contribute to G to T mutations, experimental proof of a combined two-polymerase bypass mechanism

using pol ζ and κ was not evident (data not shown). These data are also in accordance with the observation that pol ζ was involved in AFB₁-induced mutagenesis when human cytochrome P450 1A2 enzyme was expressed in yeast cells to metabolically activate AFB₁¹⁸⁹.

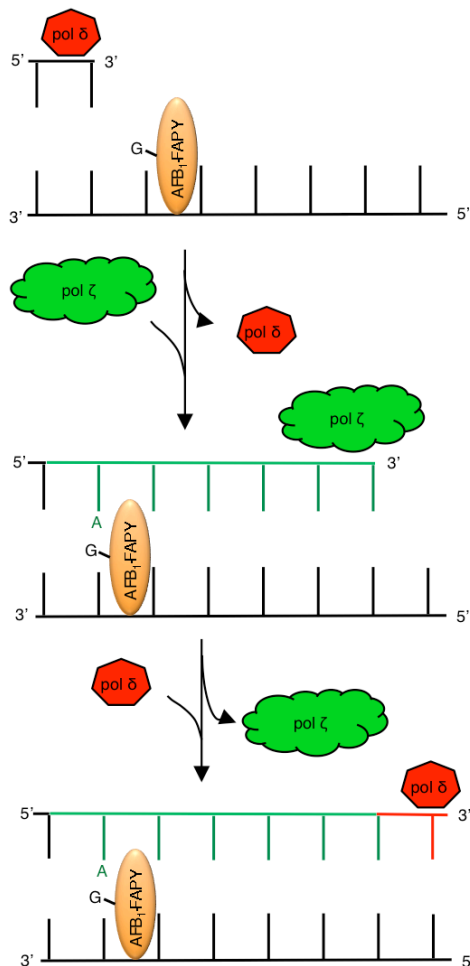


Figure 9. Proposed model of TLS past AFB₁-FAPY. The mutagenic bypass of AFB₁-FAPY by pol ζ . The current model suggests that pol δ can synthesize up to one nucleotide prior to the lesion, followed by a polymerase switch to pol ζ . Pol ζ is proposed to preferentially insert an A opposite the lesion and extend synthesis several nucleotides downstream from the inserted A (indicated by dark green lines). This would be followed by a second polymerase switch to pol δ that catalyzes resumption of normal DNA replication.

As an overall trend, the DNA polymerases tested in the present study appeared to bypass AFB₁-FAPY adducts *in vitro* with minimal efficiency. Although REV1 and PCNA have been shown to interact with these replicative and TLS polymerases to enhance their ability in processing certain DNA lesions¹⁴⁵, our results demonstrated the intrinsic actions of these DNA polymerases when encountering AFB₁-FAPY adducts. By comparing the qualitative *in vitro* bypass data, only pol ζ displayed the corresponding mutagenic bypass specificity for G to T transversions. These results also provided support for the mechanism of direct misinsertion/extension across the lesion by DNA polymerases, rather than the polymerase slippage model. Potentially, in the cellular context, there may be yet unknown accessory and/or regulatory proteins involved in facilitating the bypass process since the mutation was readily detected in the primate cells (Table 1). Further studies are needed to examine this possibility.

Based on crystallographic studies, it has been proposed that the mutagenic bypass of AFB₁-FAPY may be due to the structural restriction for an incoming dCTP access. The conformation of the AFB₁ moiety within the active site of the polymerase Dpo4 appeared with a distinct orientation about the N⁵-C8 bond of the AFB₁-FAPY adduct¹⁸¹. The rotation about the C5-N⁵ the bond of the pyrimidinyl moiety allows the AFB₁ moiety to be parallel to the FAPY base since the N⁵-C8 bond was out of plane, shifting to the 5'-direction in respect to the FAPY base. This led to a stronger stacking ability of AFB₁-FAPY, that may hinder the access of the incoming dNTP within the active site^{99,181,190}. However, a more

detailed understanding of the mechanism of action of polymerases on AFB₁-FAPY adducts awaits the crystal structure of the cognate polymerase in complex with this lesion.

There are two anomers of AFB₁-FAPY, α and β forms at the deoxyribose, that have been detected in oligodeoxynucleotides^{93,166}. The equilibrium ratio of α : β is 2:1 in ss DNA. The β anomer has been shown to be mutagenic in *E. coli*, in contrast to the α form, which acts as a replication block¹⁶⁶. Theoretically, the site-specific AFB₁-FAPY adducts in the ss pMS2 vector consisted of a mixture of α and β anomers; however, we could not determine which anomer induced each mutation in primate cells. Thus, although it is not yet known which form(s) of AFB₁-FAPY could be bypassed in mammalian cells, extrapolation of the data derived from the *E. coli* system would postulate that the mutagenic anomer would be in the β -configuration.

In the present report, we demonstrate that the AFB₁-FAPY adduct is a biologically relevant DNA modification causing G to T transversions. We also provide biochemical evidence of DNA replication bypass of AFB₁-FAPY adducts. Insights gained from these biochemical studies have laid the foundation for *in vivo* assays that can elucidate the cellular pathways involved in replication bypass of AFB₁-FAPY adducts in mammalian cells. Our data suggest that pol ζ is the most likely TLS polymerase that is responsible for AFB₁-induced mutagenesis, which is believed to be the initiating event of AFB₁-associated HCC.

CHAPTER 3

Error-prone replication bypass of the primary aflatoxin B₁ DNA adduct, AFB₁-N7-Gua

Ying-Chih Lin^{1,2}, Liang Li³, Alena V. Makarova⁴, Peter M. Burgers⁴, Michael P. Stone³, R. Stephen Lloyd^{2,5} (2014) Error-prone replication bypass of the primary aflatoxin B₁ DNA adduct, AFB₁-N7-Gua, *J. Biol. Chem.* 289, 18497-18506.

¹ Cancer Biology Program and

² Oregon Institute of Occupational Health Sciences, Oregon Health & Science University, Portland, OR 97239, USA

³ Department of Chemistry, Vanderbilt University, Nashville, TN 37235, USA

⁴ Department of Biochemistry and Molecular Biophysics, Washington University School of Medicine, St. Louis, MO 63110, USA

⁵ Department of Molecular and Medical Genetics, Oregon Health & Science University, Portland, OR 97239, USA

Preface

This work is published in *The Journal of Biological Chemistry*.

The author's contributions to this work included conception, design and performance of experiments, data analyses, and writing of the manuscript.

Liang Li and Michael P. Stone provided AFB₁-N7-Gua adducted oligonucleotides and contributed to the critical reading of the manuscript.

Alena V. Makarova and Peter M. Burgers provided yeast pol δ and pol ζ_4 , and contributed to the critical reading of the manuscript.

R. Stephen Lloyd contributed to the conception of the project, experimental design, the editing and critical reading of the manuscript, and provided funding and lab space for the execution of this work.

Adapted and modified with permission from

Ying-Chih Lin, Liang Li, Alena V. Makarova, Peter M. Burgers, Michael P. Stone, R. Stephen Lloyd (2014) Error-prone replication bypass of the primary aflatoxin B₁ DNA adduct, AFB₁-N7-Gua, *J. Biol. Chem.* 289, 18497-18506.

Copyright (2014) American Society for Biochemistry and Molecular Biology

Introduction

HCC are the most common form of liver cancer and the third leading cause of cancer death worldwide, with about half a million new cases diagnosed each year. Most cases occur in sub-Saharan Africa, Southeast Asia and China because of the high prevalence of HBV infection and dietary exposure to AFB₁^{3,167}. Chronic exposure to AFB₁ in HBV-infected patients has been shown to correlate with onset of HCC 20 years earlier than in individuals who suffer from HBV infection alone¹⁷. Thus, it is essential to understand the mechanism of action of AFB₁ in hepatocellular carcinogenesis for the development of future effective intervention and therapeutic strategies.

AFB₁ is the most potent hepatocarcinogen of the known natural aflatoxins, and is produced as a secondary metabolite by *Aspergillus flavus* and *Aspergillus parasiticus*. These fungi commonly contaminate agricultural crops such as corn and peanuts during their growth in the field and during post-harvest storage^{3,191}. Upon ingestion, liver metabolic CYP450 enzymes convert AFB₁ to the reactive intermediate, AFB₁-8,9-epoxide^{36,41}, which can conjugate on the N7 atom of deoxyguanosine in DNA to form a quantitatively abundant AFB₁-DNA adduct, AFB₁-N7-Gua^{78,79,81} (Figure 2). This primary DNA adduct is chemically unstable due to the positive charge on the imidazole ring, which further promotes rearrangement to the open-ring form of AFB₁-FAPY or depurination to generate an abasic site (AP)^{82,93}. Kinetic analyses of the formation and fate of these aflatoxin DNA adducts were determined from rat liver DNA after a single dose exposure. These data revealed that the maximum level of AFB₁-N7-Gua adducts

was attained at or before 2 hr, with a half-life of 7.5 hr. In 24 hr, about 20% of the initial AFB₁-N7-Gua was converted to the persistent AFB₁-FAPY adduct, which was continuously detected during the 72-hr period studied⁹⁴. Thus, the timing of DNA replication in cells relative to the time of the initial adduct formation would significantly determine whether the DNA polymerase would encounter the AFB₁-N7-Gua, or AFB₁-FAPY adducts, AP sites, or a mixture of all types of DNA lesions.

Mutagenesis that arises from replication of a damaged DNA template in tumor suppressor genes or oncogenes is considered to be the initial step of cancer development. Analyses of two surveys conducted in regions with high prevalence of HBV infection and aflatoxin exposure revealed that more than half of the HCC samples contained a G to T mutation at the third position in codon 249 (AGG) of the *p53* tumor suppressor gene^{130,131}. This mutation represents a biomarker of aflatoxin exposure, as it is not detected in solely HBV-associated HCC. Multiple experimental mutagenesis studies have shown that the predominant mutation caused by AFB₁ exposure is G to T transversion^{123,128,141,168}. Among the three AFB₁-induced DNA lesions mentioned above, AP sites appear to make only a minor contribution to the observed G to T mutation in *E. coli*¹⁶⁵. Recently, our group and others have demonstrated that AFB₁-FAPY adducts are highly mutagenic precursors in both primate cells and *E. coli* (mutation frequencies of 97% and 32%, respectively), with the G to T transversion being the predominant type of mutation^{39,166}. However, the primary AFB₁-N7-Gua adducts appear to be only slightly mutagenic in *E. coli*, with an error rate of 4%¹⁶⁵. There are no reports

regarding the mutagenic potential of AFB₁-N7-Gua in mammalian cells, thus prompting this investigation.

DNA lesions that stall the progression of replication fork can be bypassed using specialized TLS polymerases. However, this bypass may occur at the detriment of genome stability, with the mutation outcome, depending on the type of DNA damage and the TLS polymerase utilized^{145,173,174}. Recently, pol ζ has been suggested to play a role in replication bypass of AFB₁-FAPY adducts, contributing to the predominant G to T transversions³⁹. There is only limited information regarding how DNA polymerases process the AFB₁-N7-Gua adducts. The Klenow fragment (*exo*⁻) of bacterial DNA pol I could insert either a correct C or a mismatched A opposite AFB₁-N7-Gua *in vitro*, but only the mispaired A allowed full-length extension, a result consistent with the observation of G to T mutations¹⁹². In contrast, the archaea *Sulfolobus solfataricus* DNA polymerase IV (Dpo4), a homolog of human pol κ, exhibits error-free bypass of AFB₁-N7-Gua *in vitro*¹⁸¹.

The present study was designed to examine the mutagenic potential of AFB₁-N7-Gua adducts in primate cells using a site-specific mutagenesis approach and subsequently test the potential role of eukaryotic DNA polymerases in replication bypass of this lesion by *in vitro* replication assays.

Experimental procedures

Materials

The following materials and reagents were purchased: uracil DNA glycosylase, T4 DNA polymerase, T4 polynucleotide kinase, T4 DNA ligase and *EcoRV* (New England BioLabs); [γ -³²P]ATP (PerkinElmer Life Sciences); 100 mM dNTPs (GE Healthcare Life Sciences); COS-7 cells (American Type Culture Collection); Cell culture media, transfection reagents and *E. coli* Max Efficiency DH5 α cells (Invitrogen); human pol κ and ι (Enzymax, LLC). The pMS2 shuttle vector was kindly given by Dr. Masaaki Moriya (State University of NY, Stony Brook, NY). Human pol η catalytic cores were generously given by Dr. Robert Eoff, University of Arkansas¹⁹³. WT and the exonuclease-deficient form of pol δ holoenzymes and pol ζ_4 (Rev3–Rev7–Pol31–Pol32) of *Saccharomyces cerevisiae* were expressed and purified as previously described^{182,194}. Human AP endonuclease was a generous gift from Dr. David Wilson (National Institute on Aging, National Institutes of Health, Baltimore, MD).

Oligodeoxynucleotides

Oligodeoxynucleotides (5'-ATAATTXAATCC-3') adducted with AFB₁-N7-Gua (Fig. 1) at the position of X were prepared as previously described^{36,195}. Nondamaged (ND) oligodeoxynucleotides (12- and 46-mers) with a dG in place of AFB₁-N7-Gua and primer DNAs were obtained from Integrated DNA Technologies, Inc. The stability of the AFB₁-N7-Gua adduct in the 12-mer oligodeoxynucleotides was tested by assaying for spontaneous depurination. Single stranded (ss) DNAs

were dissolved in a buffer consisted of 10 mM Tris-HCl (pH 7.5) and 1 mM EDTA, and after three months digested with human AP endonuclease in 50 mM HEPES, 150 mM KCl and 2 mM MgCl₂. Following electrophoretic separation of the DNAs, there was no evidence of any site-specific depurination of the AFB₁-N7-Gua site, suggesting that spontaneous depurination rates are negligible under the storage and manipulation conditions used throughout this study.

Site-specific mutagenesis in COS-7 cells

The insertion of modified oligodeoxynucleotide (12-mer) containing an AFB₁-N7-Gua adduct into ss pMS2 shuttle vector, cellular transfection, extraction of replicated progeny and differential hybridization analyses were performed as previously reported³⁹. Briefly, the 12-mer oligodeoxynucleotide was ligated into an EcoRV linearized ss pMS2 vector through the complementarity to the center of a 44-mer scaffold DNA (indicated in bold) (5'-CUCGAGGGCCCCUGCAAGC **GAUGGAUUCAAUUAUAUCGCUGGUACCGAGCUCGAAUUC**-3'), while the flanking sequences were annealed to the linearized vector sequences upon EcoRV cleavage of the spontaneous duplex hairpin. Subsequently, the scaffold DNA was removed by uracil DNA glycosylase and T4 DNA polymerase treatments in the absence of dNTPs. Following transfection of site-specifically AFB₁-N7-Gua modified ss pMS2 vector into COS-7 cells, replicated DNAs were extracted and used to transform *E. coli* DH5α cells. Individual colonies were grown in liquid culture and lysed, then the DNA was cross-linked to a Hybond membrane using a UV Stratalinker.

Differential DNA hybridizations were carried out using a total of four 5'-radiolabeled probes (5'-GATATAATTNAATCCATCGCTT-3', where N refers to G, T, A, or deletion) at 44°C overnight. To confirm the successful insertion of the 12-mer oligodeoxynucleotides, a bridge probe (5'-ATCCATCGCTTGCAGGGG-3') complementary to the sequence at the joint of the vector and insert was used. DNAs that contained the 12-mer insert, but did not hybridize with any of the mutation or deletion probes were analyzed by DNA sequencing.

Construction of linear templates for in vitro replication assay

Linear DNAs (46-mers) modified with AFB₁-N7-Gua at a specific site were prepared as reported³⁹. Briefly, the adducted 12-mer oligodeoxynucleotide was ligated between a 16-mer (5'-ATTATGCAGCGATAGA-3') and an 18-mer (5'-ATCGCTGGTACCGACTCG-3') at the 5' and 3' ends, respectively, due to their sequential complementarities to a 42-mer scaffold DNA (5'-AGTCGGTACCAGC GATGGATTCAATTATTCTATCGCTGCATA-3'). The correctly ligated products were purified by gel electrophoresis. The complete sequence of the 46-mer was: 5'-ATTATGCAGCGATAGAATAATTXAATCCATCGCTGGTACCGACTCG-3', where X is AFB₁-N7-Gua.

In vitro DNA replication assay

A series of primers whose 3' end was designed to hybridize either upstream (-), opposite (0), or downstream (+) of the lesion site were used to anneal to different regions of the 46-mer template as previously described³⁹ and shown in figure

insets. Three additional variations of the 0 primer were designed to contain a mismatched nucleotide at the 3' end (0-A, 0-T, 0-G primers, respectively). The primers were ^{32}P labeled and annealed to the 46-mer template at a 1:2 molar ratio in the presence of 40 mM NaCl, heated at 90°C for 2 min and cooled to room temperature. The components of the *in vitro* primer extension reactions for pol δ , κ , η and ι were generally designed from previous studies and included 5 nM primer-template duplex in 25 mM Tris-HCl (pH 7.5), 8 mM MgCl_2 , 10% glycerol, 100 $\mu\text{g/ml}$ bovine serum albumin, 8 mM NaCl and 5 mM dithiothreitol^{187,196,197}. For pol ζ_4 , a different buffer was used, containing 40 mM Tris-HCl, pH 7.6, 0.2 mg/ml bovine serum albumin, 8 mM magnesium acetate, and 120 mM NaCl¹⁹⁴. All the reactions were conducted at 37°C for 30 min unless specified in the figure legends. Concentrations of dNTP(s) and polymerases are given in the figure legends. An equal volume of a solution containing 95% (v/v) formamide, 20 mM EDTA, 0.02% (w/v) xylene cyanol, and 0.02% (w/v) bromophenol blue was added to terminate the reaction. The reaction products were resolved by electrophoresis through 15% acrylamide denaturing gels containing 8 M urea and visualized by a GE PhosphorImager screen.

Results

Mutagenic potential of AFB₁-N7-Gua adducts in primate cells

To assess whether the AFB₁-N7-Gua adducts (Figure 2) are mutagenic precursors in mammalian cells, we generated a ss shuttle vector pMS2 containing site-specific AFB₁-N7-Gua adduct or ND dG control; the vector was

subsequently transfected into African green monkey kidney COS-7 cells. The utilization of a ss vector, which was not a suitable substrate for DNA repair, allowed for a reliable determination of the mutagenic frequency and spectra derived from the replication bypass of the lesion. After a 48 hr incubation period, the replicated plasmid progenies were extracted and transformed into *E. coli* to form individual colonies. DNAs extracted from bacteria were further hybridized with various DNA probes that were designed to recognize the accurate or mutated sequence at the AFB₁-N7-Gua adduct or ND dG insertion region. A bridge probe, spanning both the 12-mer insert and the vector, was used to ensure the successful construction of a ss pMS2 vector containing either AFB₁-N7-Gua or ND dG. Thus, a mutagenic spectrum could be inferred through the results of differential hybridization. Representative colonies were picked for DNA sequencing to verify the correct identification of the mutation by each sequence-specific probe. If the bacterial DNA only hybridized with the bridge probe, indicative of the presence of the adducted 12-mer, but not with any sequence-specific mutation probes, plasmid DNAs were extracted for DNA sequencing across the region of the insert to determine the sequence of the progeny DNA. Analyses of these data revealed that replication past the AFB₁-N7-Gua adduct resulted in a high error frequency ~45% (Table 2). No mutations were observed with the control sequence (Table 2). The mutation spectrum included single base substitutions and deletions, with the predominant mutations being G to T transversions, accounting for 82% of all mutations scored. The second most common mutation type was G to A transitions (~10%), followed by G to C

transversions and deletions (< 3%). Taken together, these data indicate that AFB₁-N7-Gua is a highly mutagenic precursor in primate cells, predominantly inducing a G to T transversion, which is consistent with observations of HCC patient samples from areas experiencing high aflatoxin exposure^{130,131}.

DNA modification	Colonies scored	Mutated	Single base substitutions			Deletions	Other position substitution	Frequency of mutation (%)
			G to T	G to A	G to C			
ND ^a	189	0	0	0	0	0	0	0
AFB ₁ -N7-Gua	216	98	80 (81.6%) ^b	12 (12.2%) ^b	1 (1%) ^b	3 (3.1%) ^b	2 (2%) ^b	45.4

Table 3. Mutation spectrum and frequency following replication past AFB₁-N7-Gua adducts in COS-7 cells.

^a Replication through nondamaged dG in COS-7 cell, adapted from³⁹

^b The percentage of total mutated colonies

Accurate replication bypass of AFB₁-N7-Gua by pol δ

In light of the *in vivo* mutagenesis results, studies were initiated to determine which replicative or TLS DNA polymerases may be involved in synthesis past the AFB₁-N7-Gua adducts in COS-7 cells using *in vitro* replication assays. Although the AFB₁-FAPY adduct was highly effective in blocking replication bypass by pol δ³⁹, it was important to establish whether the ring-closed AFB₁-N7-Gua adduct was similarly effective in blocking. Primer extension reactions were carried out using pol δ on control ND or AFB₁-N7-Gua-modified templates under running (-10 primer) and standing (-1 primer) start conditions. Under the conditions in which primers annealed to ND templates were efficiently extended, synthesis by pol δ was predominantly inhibited one nucleotide prior to AFB₁-N7-Gua (Figure 10A). Surprisingly, unlike comparable replication studies using DNAs containing

the AFB₁-FAPY adduct, pol δ generated small amounts of full-length bypass product of AFB₁-N7-Gua (Figure 10A, lane 6). In addition, the presence of the adduct also prevented efficient loading of pol δ at low concentrations, as evidenced by significant reductions in primer utilization (Figure 10A, comparison of lanes 2 and 5).

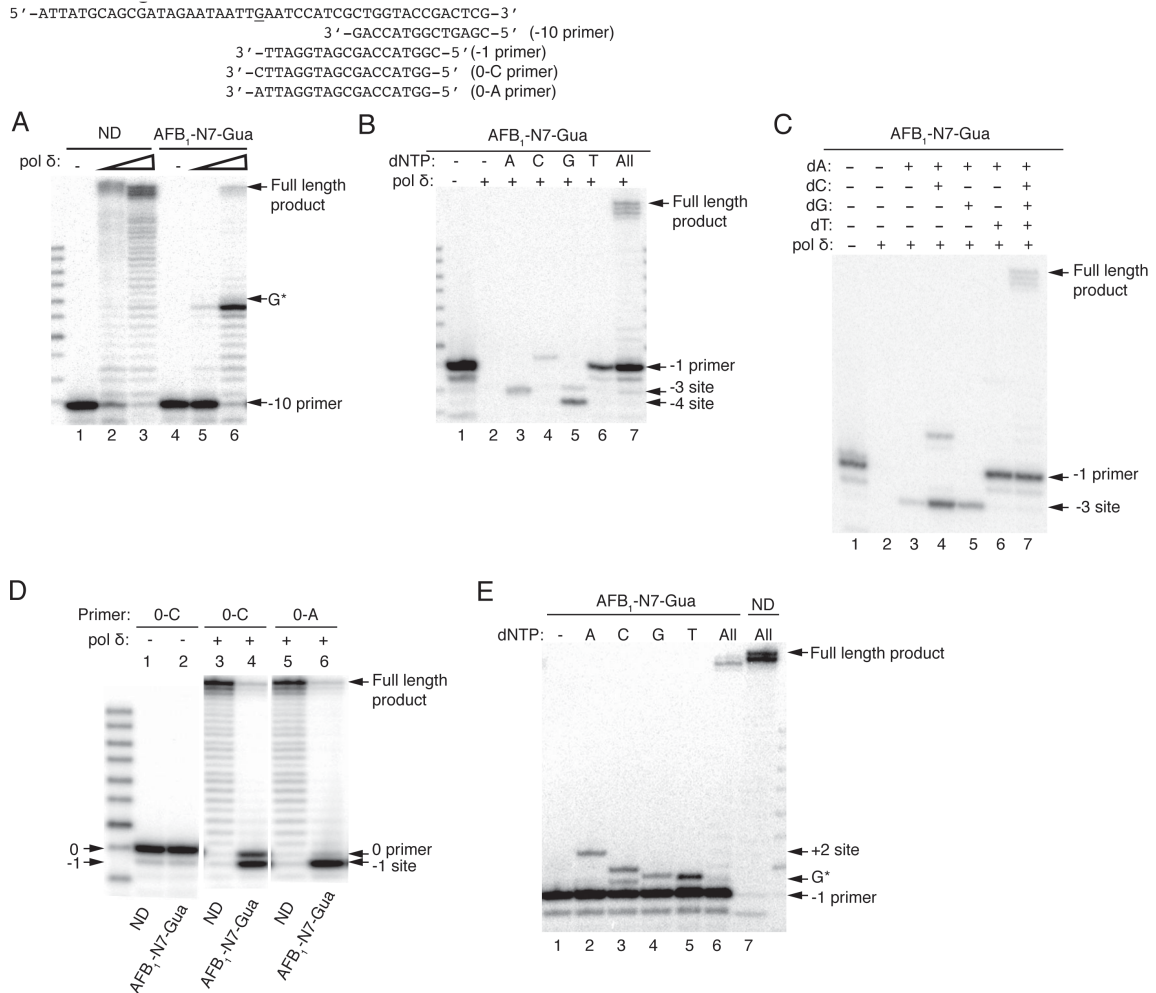


Figure 10. Replication bypass of AFB₁-N7-Gua by pol δ . The -10, -1, or 0 primers with either C or A at the 3' end were annealed to ND or AFB₁-N7-Gua adducted DNA templates. (A) Primer extensions were catalyzed by 1 nM (lane 2, 5) or 50 nM (lane 3, 6) pol δ in the presence of 100 μ M dNTPs. G*, adducted site. (B) Single-nucleotide incorporations and primer extensions were conducted by 50 nM pol δ in the presence of combined or individual dNTPs at a final concentration of 100 μ M. (C) dNTP combination and primer extension reactions were catalyzed by 50 nM pol δ in the presence of different combinations of 100 μ M individual dNTPs. (D) Primer extensions from the 3' end of the 0 primer with a matched C or mismatched A annealed opposite ND or AFB₁-N7-Gua were catalyzed by 50 nM pol δ in the presence of 100 μ M dNTPs in a buffer containing 40 mM HEPES-KOH, pH 6.8, 10% glycerol, 0.2 mg/ml bovine serum albumin, 1 mM DTT and 8 mM MgCl₂ for 1 hr at 37°C. (E) Single nucleotide insertion opposite AFB₁-N7-Gua by pol δ -Exo. Primer extension reactions were catalyzed by 20 nM pol δ -Exo in the presence of 100 μ M individual or all dNTPs.

Single-nucleotide incorporation reactions were conducted to determine the specificity of the insertion by pol δ opposite the lesion. As shown in Figure 10B, using the -1 primer, the overall reaction was dominated by the exonucleolytic

activity of pol δ (as evidenced by significant degradation of the -1 primers). However, when primer extension was observed, pol δ exclusively inserted the correct C opposite AFB₁-N7-Gua, and full-length bypass products were observed in the presence of all dNTPs. In reactions containing only dATP or dGTP, the -1 primer was degraded by the exonuclease proofreading activity of pol δ to -3 or -4 sites, respectively. In the presence of dTTP, primer degradation paused due to polymerase idling at the -1 site. These data suggested that under conditions restricting dNTP availability, the exonuclease reaction dominated the polymerization reaction when pol δ encountered AFB₁-N7-Gua adducts. Although these data suggested that pol δ insertion was primarily error-free, an additional experimental strategy was used to corroborate this conclusion. Since the two downstream template nucleotides were both T, it was hypothesized that addition of dATP with the other individual dNTPs in the reaction could facilitate extension beyond the nucleotide that had been inserted opposite the lesion. As shown in Figure 10C, correct C insertion opposite the lesion followed by incorporation of two additional nucleotides by pol δ was observed, yielding a product band at the +2 site (Figure 10C, lane 4). All other permutations of two nucleotides resulted in exonuclease resection back to the nearest complementary nucleotide (Figure 10C, lane 3 and 5). However, when pol δ -Exo was assayed, it inserted all four dNTPs opposite AFB₁-N7-Gua and readily extended the misinserted A (Figure 11), indicating that the presence of the pol δ proofreading function plays a critical role in preventing mutagenesis of AFB₁-N7-Gua.

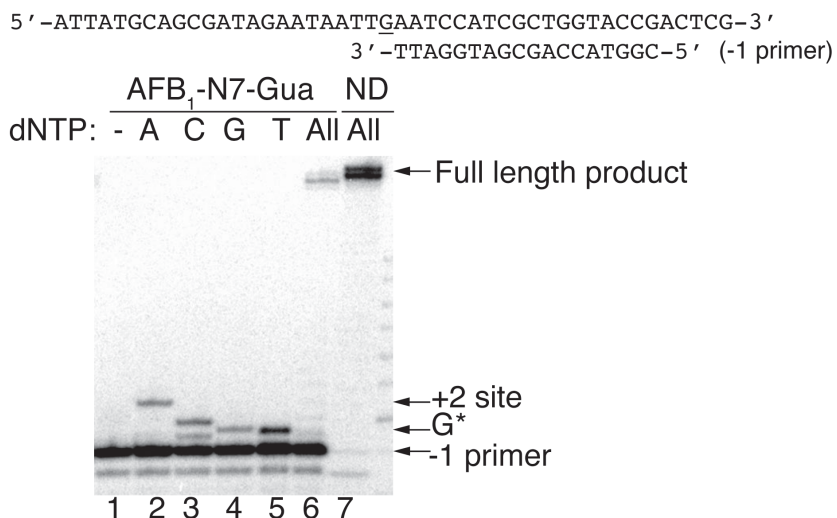


Figure 11. Single nucleotide insertion opposite AFB₁-N7-Gua by pol δ -Exo. The -1 primers were annealed to ND or AFB₁-N7-Gua-containing DNA templates. Primer extension reactions were catalyzed by 20 nM pol δ -Exo in the presence of 100 μ M individual or all dNTPs. G* indicates the position of the adducted site.

Although these data suggested that pol δ catalyzed high fidelity replication, the results did not eliminate the possibility that, if another polymerase inserted an A opposite the adduct, then pol δ could extend it, contributing to the predominant G to T mutations induced by AFB₁-N7-Gua in COS-7 cells (Table 2). To determine whether pol δ was capable of extending a primer constructed with a mispaired-A opposite the lesion, as compared to a primer with a matched C, primer extension reactions were carried out. Consistent with the data in Figure 10B-C, for both primers, the exonucleolytic reaction was more efficient than the extension when replicating through AFB₁-N7-Gua. However, the mispaired primer was totally resected to the -1 site (Figure 10D, lane 6), whereas the matched C primer was more resistant to the exonuclease processing (Figure 10D, lane 4). Although both reactions resulted in full-length products, the abundance was greater for the

matched primer. Given the efficiency of the exonucleolytic reaction on the mispaired primer, it is inferred that the full-length products were generated from the resected -1 position.

Thus, these data reveal for the first time that pol δ can replicate past AFB₁-N7-Gua by accurate incorporation opposite, and extension beyond, the lesion. These data suggested that pol δ could be involved in limiting mutagenesis of AFB₁-N7-Gua *in vivo* and contributing to the error-free portion of the replication (Table 2).

Replication bypass of AFB₁-N7-Gua by TLS polymerases

Given that nearly 50% of the DNA synthesis past AFB₁-N7-Gua in COS-7 cells was mutagenic (Table 2), and that pol δ catalyzed high fidelity bypass of the lesion (Figure 10), it was hypothesized that one or more of the specialized TLS polymerase(s) may play a role in the AFB₁-N7-Gua-induced mutagenesis. To determine the identity of the nucleotide inserted opposite the lesion, single-nucleotide incorporation reactions were carried out with yeast pol ζ_4 , human pol κ , η , and ι .

As shown in Figure 12A lane 9, pol ζ_4 preferentially inserted the correct C opposite the lesion, while A, G, and T were utilized, albeit less efficiently (Figure 12A lanes 8, 10, 11, respectively). With the same experimental approach, pol κ displayed no nucleotide preference (Figure 12B, lanes 8-11), while pol η preferentially incorporated A and G (Figure 12C). In contrast, pol ι preferred insertion of C and T (Figure 12D).

5' -ATTATGCAGCGATAGAATAATTGAATCCATCGCTGGTACCGACTCG-3'
 3' -TTAGGTAGCGACCATGGC-5' (-1 primer)

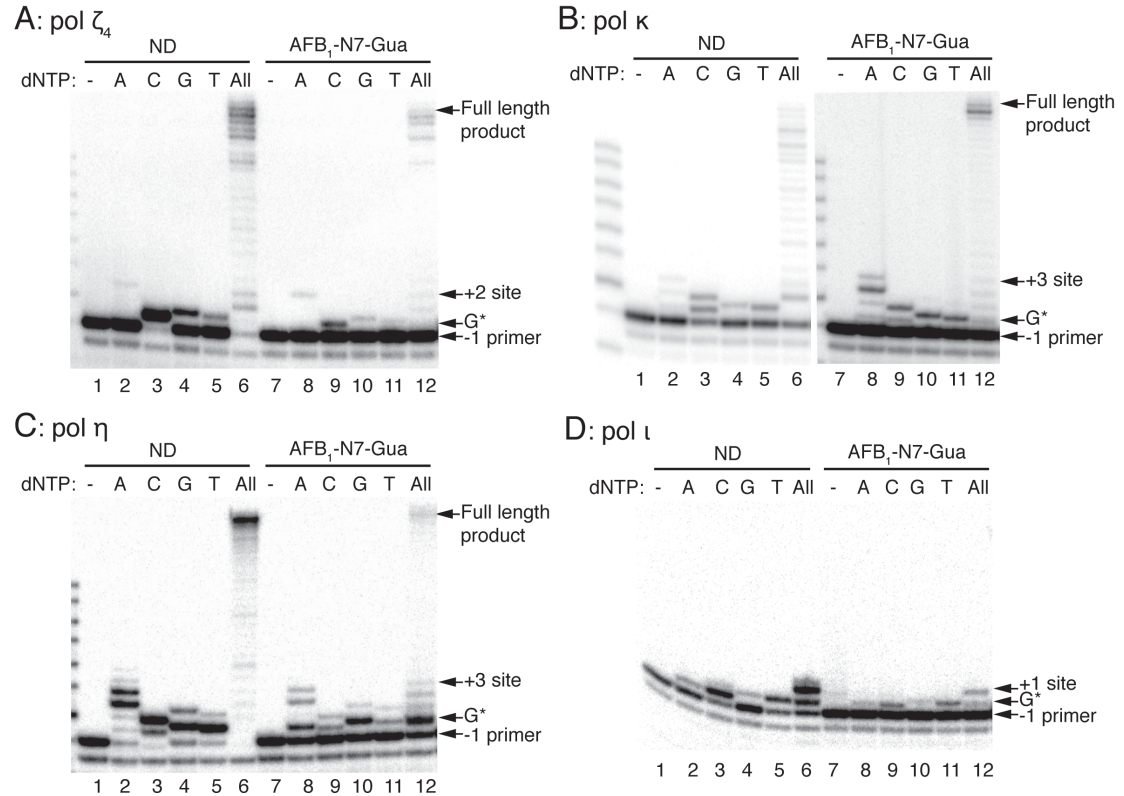


Figure 12. Single-nucleotide incorporations and primer extensions opposite AFB₁-N7-Gua by yeast pol ζ_4 and human pol κ , η and ι . The -1 primer was annealed to DNA templates containing ND or AFB₁-N7-Gua. (A-D) Reactions were catalyzed by 10 nM pol ζ_4 , 2 nM (ND) and 10 nM (AFB₁-N7-Gua) pol κ , 2 nM pol η catalytic core and 1 nM pol ι , respectively. 100 μ M individual or all dNTPs were used in panel A, B (AFB₁-N7-Gua) and D, while 20 μ M were added in panel C and B (ND).

Given that none of the TLS polymerases tested above exhibited selectivity of insertion of dA opposite the AFB₁-N7-Gua adduct, which could play a major role in contributing to the predominant AFB₁-N7-Gua-induced G to T mutation, it was hypothesized that TLS polymerases (pols ζ_4 , κ , η , and ι) could preferentially extend a mispaired primer opposite the lesion. To experimentally test this, 4 primers were synthesized such that the 3' nucleotide represented the matched C and the 3 mismatches (Figure 13). Comparative analyses revealed that pol ζ_4 extended the accurate base paired C primer somewhat more efficiently than any

of the other three mispaired primers annealed to the damaged template (Figure 13B).

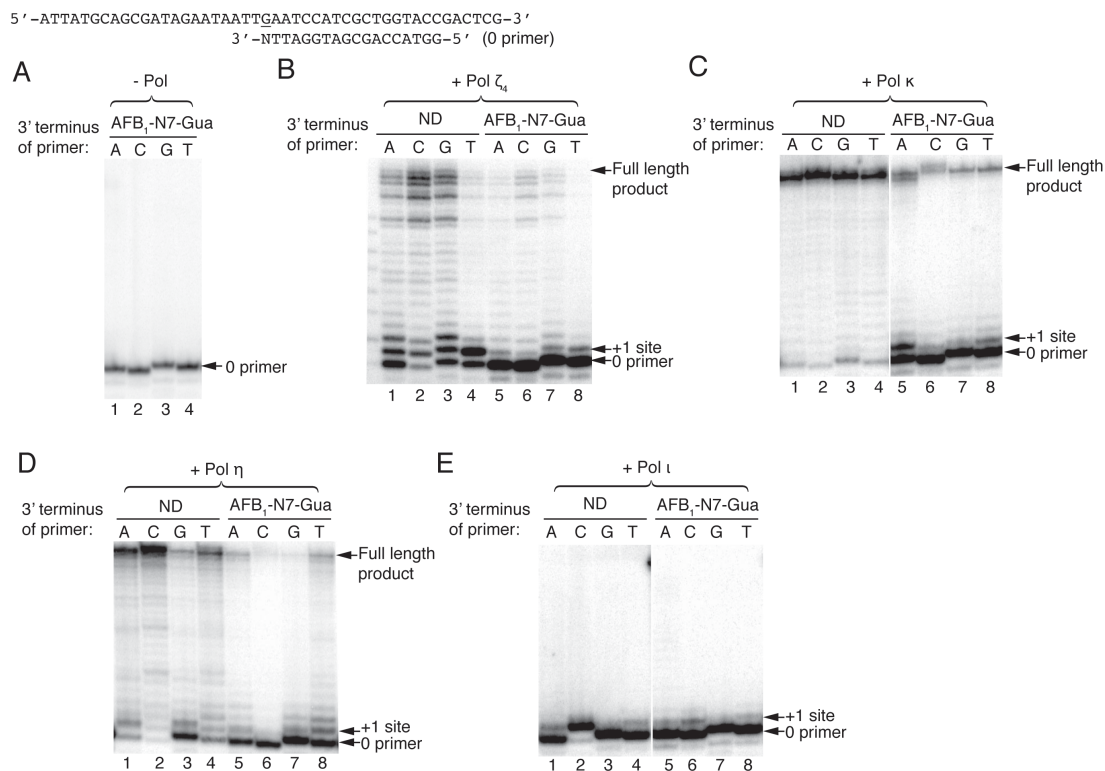


Figure 13. Primer extensions past AFB₁-N7-Gua catalyzed by yeast pol ζ_4 and human pol κ , η and ι . Four 0 primers with different 3' end (where N represents either A, C, G or T) were annealed to ND or AFB₁-N7-Gua adducted DNA templates. (A) Control reactions contained no polymerase. (B-E) Reactions were catalyzed by 5 nM pol ζ_4 , 1 nM pol κ , 0.5 nM pol η and 10 nM pol ι , respectively. Reactions in panel A, B, C and E were conducted in the presence of 100 μ M dNTPs, while 20 μ M were used in panel D.

In the case of pol κ , although full-length bypass products were detected from all four primers hybridized with the damaged template, there was an increased preference for extension from the mispaired-A primer (Figure 13C, lanes 5-8). However, using conditions to observe these extensions on damaged DNA, all primers were extended on ND templates (Figure 13C, lanes 1-4). Similar to that observed for pol κ , pol η preferentially catalyzed primer extension from the

mismatched-A and -T primers for the adducted template (Figure 13D, lane 5 and 8). Moreover, a pol η -deficient COS-7 cell line was made available [in collaboration with Irina G. Minko (OHSU), Robert W. Sobol (University of Pittsburgh), and Thomas G. Wood (University of Texas Medical Branch), unpublished] to test for evidence for a role of pol η in the bypass of this lesion. Using the same site-specific mutagenesis strategy as described above, no differences were observed in the mutation frequency or spectrum in the pol η -defective cells compared to WT cells. The mutation frequency of AFB₁-N7-Gua was 50% in pol η -deficient cells with the predominant mutation type being G to T transversions as 89% of all mutants followed by 11% of G to A transitions.

Consistent with the results obtained for pol ζ_4 , pol ι preferentially extended the matched-C primers using either the ND or AFB₁-N7-Gua-modified template, albeit inefficiently on the damaged substrate (Figure 13E). In summary, these data provide the first biochemical evidence supporting the possible role of pol ζ_4 , in addition to pol δ , in accurate TLS past AFB₁-N7-Gua. Pol κ may contribute to misinsertion opposite the adduct and extension from the mispaired A, thus accounting for the predominant G to T mutation in mammalian cells.

Resumption of efficient replication by replicative polymerase

To address how close to the adduct normal DNA synthesis by replicative polymerase can resume, primer extension reactions were carried out with pol δ using ND or AFB₁-N7-Gua modified templates annealed to +2, +3, and +5 primers. These primers contained either matched C or mismatched A opposite

the lesion, representing the accurate and mutagenic bypass observed *in vivo*, respectively (Figure 14). Pol δ extended all primers efficiently when the correct C was paired across control dG or the adduct (Figure 14A, lanes 4-9). However, a small percentage of the primer annealed to the templates containing the lesion was resected, primarily back to the +1 site, with slightly higher exonucleolytic activity on the +2 primer. Thus, the extension efficiencies increased as the number of correct base pairs beyond the lesion increased. All primers with the ND template were completely utilized. Conversely, minimal amounts of full-length products were observed when a mispaired A was placed opposite the lesion in the +2 or +3 primer; the exonuclease digested back to the -1 position (Figure 14B, lanes 7-8). Interestingly, when the primer terminus was 5 nucleotides downstream from the mismatched A across the lesion, substantial amount of full-length extended products were readily detected, with some portion of the +5 primers still excised to the -1 site (Figure 14B, lanes 9). Moreover, pol δ efficiently extended all the mismatched primers annealed to the ND template (Figure 14B, lanes 4-6).

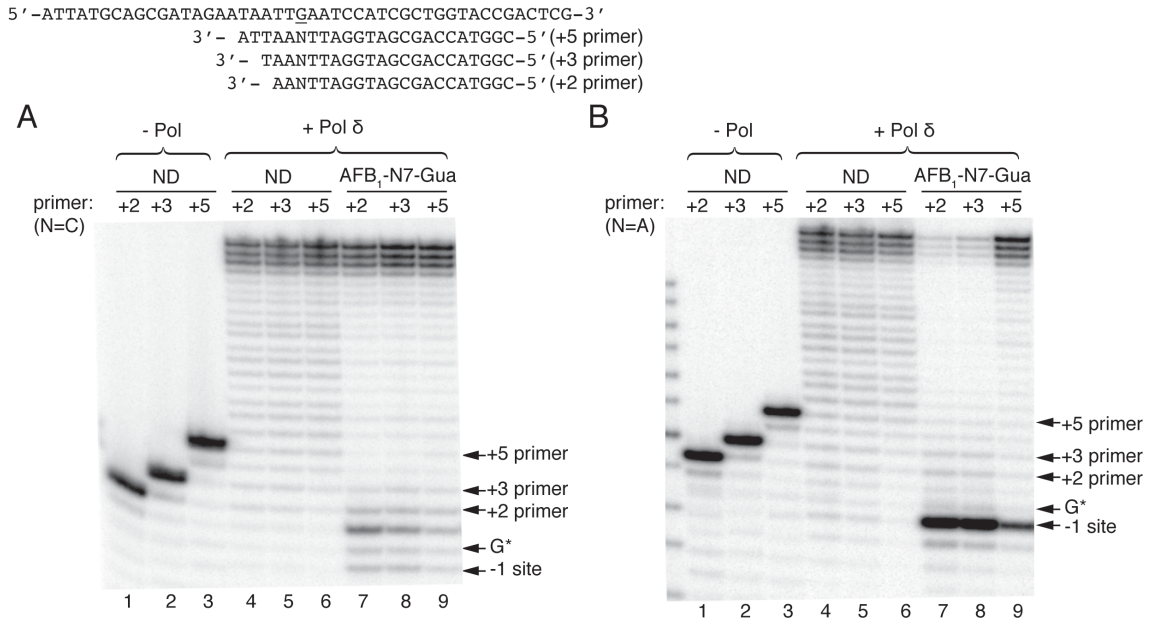


Figure 14. Resumption of replication by pol δ downstream of AFB₁-N7-Gua. +2, +3 or +5 primers with either matched C or mismatched A opposite the lesion or control site were annealed to ND, AFB₁-N7-Gua containing DNA templates. (A-B) Primer extensions were catalyzed on matched and mismatched primers, respectively. All reactions were catalyzed by 50 nM pol δ in the presence of 100 μ M dNTPs. G*, adducted site.

In summary, these data revealed that the position of the mispair across the lesion upstream of the primer terminus could affect the DNA synthesis ability of pol δ . The balance between the exonuclease and polymerase activities shifts towards extension when the mismatch was located deeper in the duplex, suggesting the requirement of continuous synthesis by TLS polymerase(s) beyond the lesion to reserve the mutagenic bypass before switching to replicative polymerase.

Discussion

Exposure to aflatoxin, the most potent environmental chemical carcinogen, poses a great risk to public health for the development of HCC. About 4.6-28.2%

of more than half a million new HCC cases worldwide each year can be attributed to aflatoxin exposure alone¹⁴. Despite intense studies to identify the DNA adducts, mutagenesis, and carcinogenesis induced by aflatoxin, the underlying molecular mechanisms driving these processes are far from completely understood. Recently, we reported that the AFB₁-FAPY adducts are highly mutagenic in primate cells³⁹. The current study utilized exactly the same sequence context and site-specific mutagenesis approach to demonstrate that the primary AFB₁-DNA adduct, AFB₁-N7-Gua, was also highly mutagenic (Table 2), although it was about half of that measured for AFB₁-FAPY adducts³⁹. Consistent with the observation made for AFB₁-FAPY, the mutagenicity of AFB₁-N7-Gua in primate cells was much higher (Table 2) than that in *E. coli* cells (4%)¹⁶⁵. This underscores the advantage of our biologically relevant system to address the mutagenic effects of aflatoxin in animals and humans.

Furthermore, the predominant G to T transversion at the lesion site measured in primate cells was in agreement with that reported in *E. coli*¹⁶⁵. The mutation spectrum also correlated well with other mutagenesis studies in various experimental model systems^{123,127,128,141,143} and aflatoxin-related HCC samples^{130,131}. However, no base substitutions located at the 5' base of AFB₁-N7-Gua were detected in our study, suggesting that the mutation at the 5' base of the lesion identified in *E. coli*¹⁶⁵ could be sequence-context dependent; we can rule out the possible effect of DNA adduct formation and DNA repair on the mutagenesis of this lesion since a ss vector that had been modified by the adduct at a specific-site was used. Alternatively, it could also be cell-type specific,

considering the differences between primate and SOS-induced bacterial DNA polymerases that may be involved in TLS across AFB₁-N7-Gua adducts. Overall, our results support the following conclusions: 1) AFB₁-N7-Gua could serve as a mutagenic precursor contributing to the commonly observed G to T transversion as the initiating event of hepatocellular carcinogenesis, and 2) primate cells, and by inference human cells, are more susceptible to the mutagenic effect of AFB₁ than *E. coli*, thus providing a basis for AFB₁-associated HCC carcinogenesis. We speculate that the data derived from replication of these single-stranded vectors in African green monkey cells are germane to mutagenic processes in human cells based on a very high degree of sequence identity between human and African green monkey. This assumption is based on unpublished data in which we have cloned and sequenced 16 DNA repair and replication genes from COS-7 cells and overall, the conservation was 97% for DNA sequence and 98% for amino acid identity (RS Lloyd, IG Minko and TG Wood, unpublished data).

A model of TLS past AFB₁-N7-Gua adducts was inferred based on the biochemical studies (Figure 15). High fidelity replication bypass of the AFB₁-N7-Gua adduct occurred in about half of the progeny, and these data are consistent with a bypass mechanism mediated by pol δ or pol ζ_4 (Figure 15, top). If, however, the AFB₁-N7-Gua adduct causes blockage of the replicative polymerase, this could lead to the recruitment of pol κ that would subsequently catalyze incorporation of all dNTPs opposite the lesion and preferentially extend the mismatched dA (Figure 15, bottom). We favor this explanation to account for the G to T transversion over a slippage-realignment model, in which the 5' dT

would be used as the template for the exclusive insertion of dA. The insertion of all dNTPs equally by pol κ without preference for dA (Figure 12B) argues against the slippage-realignment model; instead, the preferential extension off of dA by pol κ could potentially account for the observed mutagenesis. These results will aid us in focusing future studies into the biological role of these polymerases in the bypass of AFB₁-DNA adducts.

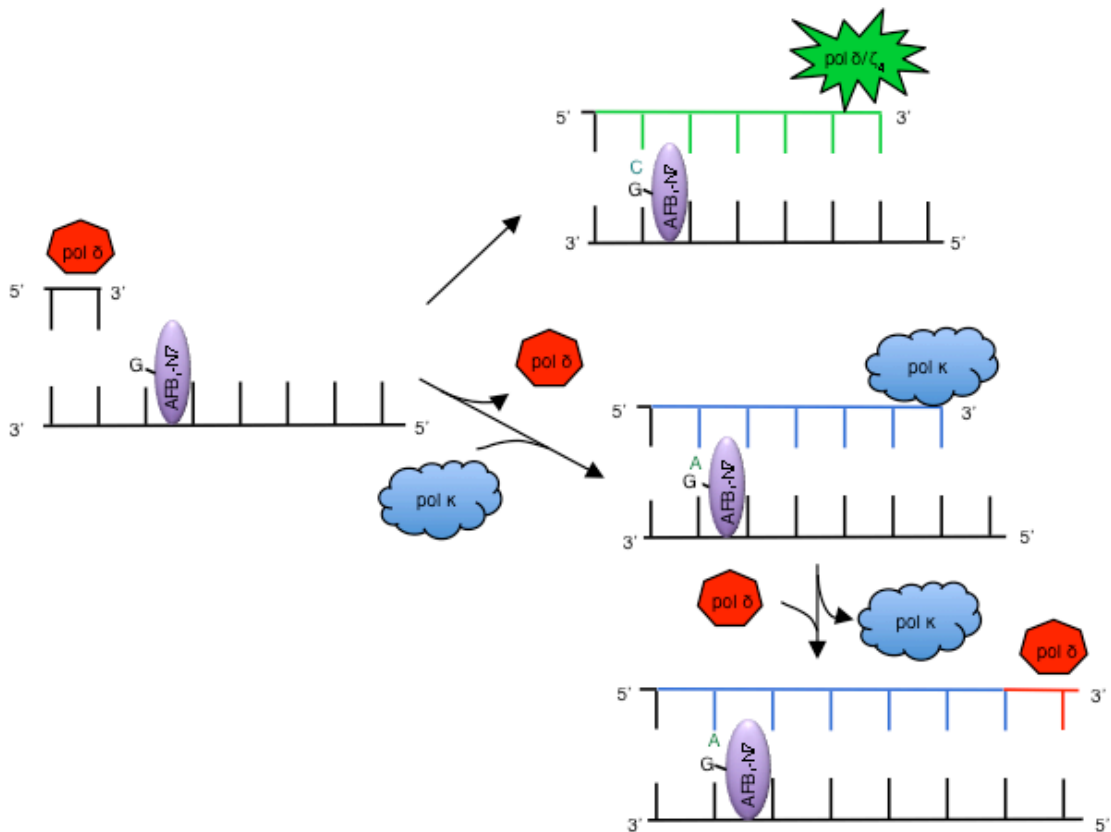


Figure 15. Proposed model of TLS past AFB₁-N7-Gua. The accurate and error-prone bypass of AFB₁-N7-Gua by pol δ or ζ_4 and pol κ , respectively. For this lesion, the model proposes that pol δ can replicate past the lesion by correct insertion and extension from the damage site. Alternatively, if pol δ is blocked and dissociates one nucleotide prior to the adduct, pol ζ_4 can preferentially insert a correct base opposite and extend from the lesion (green lines). The mutagenic pathway involves the blocking of pol δ one nucleotide prior to the lesion, followed by recruitment of pol κ to catalyze the insertion step and the more efficient extension from a mismatched A: G terminus (blue lines). Efficient resumption of normal replication by pol δ after the second polymerase switch is proposed to occur at least 5 nucleotides downstream of the mismatched site (red lines).

Although both AFB₁-N7-Gua and AFB₁-FAPY adducts intercalate at the 5' face of the modified base in duplex DNA^{95,97}, potentially explaining the similar mutation spectrum, with predominant mutation being G to T transversion, it does not provide insight for the differential mutagenic potential between these two lesions (Table 1-2)³⁹. Recently, crystallographic studies revealed that the conformation of the AFB₁ moiety within the active site of the archaea polymerase Dpo4 differed between AFB₁-N7-Gua and AFB₁-FAPY, due to the distinct orientations of the N7-C8 bond of AFB₁-N7-Gua compared to the N⁵-C8 bond of AFB₁-FAPY¹⁸¹. In order to keep the N7-C8 bond of AFB₁-N7-Gua in plane with the adducted dG, the AFB₁ moiety of AFB₁-N7-Gua is 16° out of plane relative to the modified dG, forming a wedge in the DNA; this is believed to allow better access for the incoming dCTP¹⁸¹. This could be a plausible mechanism underlying the more accurate bypass of AFB₁-N7-Gua that was observed in this study. However, bacterial DNA pol I Klenow *exo*⁻ has been shown to be capable of inserting both dA and dC opposite AFB₁-N7-Gua, with the exclusive extension from the mispaired primer template¹⁹². Thus, it warrants further investigation of crystal structures of these eukaryotic polymerases in complex with AFB₁-N7-Gua adducts to elucidate the mechanisms that may contribute to the mutagenic outcome in mammalian cells.

In the current report, we established that AFB₁-N7-Gua lesions are biologically relevant DNA adducts causing primarily G to T transversions, the predominant mutation induced by AFB₁ exposure, in primate cells. Furthermore, biochemical evidence of DNA replication bypass of these adducts was provided, and from

which attention could be focused particularly on pol δ , ζ , and κ for *in vivo* assays to advance our understanding of cellular pathways that involve in AFB₁-induced mutagenesis as the initiation of AFB₁-related HCC.

CHAPTER 4

The critical role of mammalian pol ζ in response to aflatoxin B₁ exposure

Ying-Chih Lin^{1,2}, Sabine S. Lange³, Richard D. Wood³, R. Stephen Lloyd^{2,4}

¹ Cancer Biology Program and

² Oregon Institute of Occupational Health Sciences, Oregon Health & Science University, Portland, OR 97239, USA

³ Department of Molecular Carcinogenesis, The University of Texas MD Anderson Cancer Center Science Park, and the Graduate School of Biomedical Sciences at Houston, Smithville Texas, TX 78957, USA

⁴ Department of Molecular and Medical Genetics, Oregon Health & Science University, Portland, OR 97239, USA

Preface

This is currently a work in progress.

The author's contributions to this work included conception of the project, design and performance of experiments and data analyses, and manuscript writing.

Sabine S. Lange and Richard D. Wood provided immortalized *Rev3L^{+/-}*, *Rev3L^{-/-}* and *Rev3L^{-/-}* supplemented with human REV3L MEFs.

R. Stephen Lloyd contributed to the conception of the project, experimental design, and provided funding and lab space for the execution of this work.

Introduction

AFB₁ is a fungal toxin generated primarily by *A. flavus* and *A. parasiticus* that frequently contaminates food supplies consumed by humans and livestock. Exposure to AFB₁ is a major risk factor for liver cancer in sub-Saharan Africa, Southeast Asia and China, where HBV infection is also endemic^{3,9}. Liver cancer is the second leading cause of cancer-related death worldwide¹, with HCC being the predominant histological subtype in liver cancer. About 4.6-28.2% of the more than 500,000 new HCC cases each year may be attributable to aflatoxin exposure alone¹⁴. Thus, understanding the pathogenesis of AFB₁-associated HCC should provide some insight for the development of preventative screening methods and therapeutic approaches.

The mechanism of AFB₁-initiated carcinogenesis is thought to be related to its potency to induce mutation and genomic instability. Human epidemiological studies revealed a mutation hotspot at the third position of codon 249 (AGG->AGT, R249S) in tumor suppressor *TP53* gene associated with AFB₁ exposure^{130,131}. Experimental results from AFB₁-treated human hepatocytes corroborated the causal relationship of AFB₁ for R249S mutation in *TP53*^{141,142}. The major point mutation induced by AFB₁ is G to T mutation^{123,141,170}, which is consistent with the observed genotoxicity of AFB₁, as the metabolically activated AFB₁-epoxide can conjugate on the N7 atom of guanine in DNA to form AFB₁-N7-Gua. This is further converted to AFB₁-FAPY, a more persistent DNA lesion^{78,79,93,94}. Previously, we and others have shown that AFB₁-FAPY adducts are more mutagenic than AFB₁-N7-Gua for G to T transversion in bacterial and

primate cells, with a mutation frequency of 32% and 97%, respectively^{39,166}. The mechanism by which the FAPY adduct of AFB₁ induces G to T mutation remains unclear. A systematic examination of eukaryotic TLS DNA polymerases for their ability to replicate past AFB₁-DNA adducts indicated that yeast pol ζ preferentially misincorporates an A opposite and extends beyond the mispaired AFB₁-FAPY lesion *in vitro*³⁹, whereas AFB₁-N7-Gua appeared to be bypassed by pol ζ in an error-free manner¹⁹⁸. These results suggest a role for pol ζ in TLS across AFB₁-DNA adducts *in vivo*.

Pol ζ is a member of the B family DNA polymerases, which includes the replicative DNA polymerases α, δ, and ε. Unlike other members in the family, pol ζ lacks a 3' → 5' proofreading exonuclease activity and has low fidelity in copying nondamaged (ND) DNA, with an error frequency of 10⁻³-10⁻⁵. This enzyme was thought to consist of two subunits, the accessory protein Rev7 and the catalytic subunit Rev3^{174,199}. Recently, both yeast and human pol ζ have been shown to form a four-subunit complex, with the two additional subunits previously known as accessory proteins of pol δ^{194,200-202}. It was proposed that sharing the accessory proteins allows the switch between pol δ and pol ζ at a DNA lesion when a replication fork is stalled. Mammalian *Rev3L* encodes an ~350 kDa protein, which is twice as large as the yeast Rev3 protein, and posed a challenge for protein purification. Almost all previous biochemical studies were performed using yeast pol ζ. Successful purification of human Rev3L was recently demonstrated by Lee et al²⁰². The importance of pol ζ in TLS is generally considered as a proficient extender from mismatches formed when incorrect

nucleotides are inserted by other TLS polymerases opposite DNA lesions. The TLS function of pol ζ has been demonstrated with a variety of DNA lesions, including UV- and cisplatin-induced DNA damage²⁰³⁻²⁰⁵.

Pol ζ deficiency in yeast results in viable cells with decreased spontaneous and induced mutagenesis, as well as increased sensitivity when exposed to genotoxic stress. In marked contrast, disruption of *Rev3L* causes embryonic lethality in mice²⁰⁶, a result that is unique among TLS polymerases. *Rev3L* knockout (KO) mouse embryonic fibroblasts (MEF) are only viable in a *TP53*-null background^{207,208}. These cells showed increased chromosomal instability, such as translocations, and sensitivity to a diversity of DNA-damaging agents compared to *Rev3L* proficient MEFs. Similarly, primary MEFs following conditional deletion of *Rev3L*, exhibited a growth defect with increased double-strand breaks (DSB) and chromatid aberrations. These cells subsequently became senescent or apoptotic. Immortalization by expression of simian virus 40 (SV40)-T antigen (TA_g) allowed continuous cell growth in culture²⁰⁹. These data highlight the distinctive function of mammalian pol ζ in tolerating endogenous DNA damage for normal cell growth. In addition to TLS, pol ζ has been shown to be involved in homologous recombination (HR)²¹⁰ and repair of interstrand cross-links (ICL)^{211,212}.

The current study was designed to investigate the TLS function of pol ζ for AFB₁-FAPY adducts *in vivo* and characterize the cellular response to AFB₁ in the absence of pol ζ .

Experimental procedures

Materials

The following materials and reagents were purchased: AFB₁, nicotinamide adenine dinucleotide 2'-phosphate reduced tetrasodium salt hydrate (NADPH) (Sigma-Aldrich); aroclor-induced rat liver microsome S9 (Moltox); CellTiter-Glo luminescent cell viability assay (CTG) (Promega); media and reagents for cell culture, propidium iodide (PI), DNase I, Amplification Grade (Life Technologies); fetal bovine serum (FBS) (Atlanta Biologicals); HiPerfect transfection reagent, RNase A and RNeasy Mini kit (Qiagen); electroporation cuvettes (Fisher Scientific); On-TARGETplus SMARTpool siRNA targeting human *Rev3L* (Dharmacon); iScript reverse transcription supermix for RT-qPCR and SYBR Green PCR (Bio-Rad); primers (Integrated DNA Technologies); 5-bromo-4-chloro-3-indolyl-beta-D-galacto-pyranoside (X-gal) (Roche); isopropyl-β-D-thiogalactopyranoside (IPTG) (Research Organics); all other chemicals used for these experiments (Sigma-Aldrich or Fisher Scientific). The pMS2 shuttle vector was a generous gift from Dr. Masaaki Moriya (State University of NY, Stony Brook, NY). The pSP189 plasmid and *E. coli* MBM7070 cells were gifts from Dr. Michael Seidman (National Institute of Aging).

Cell culture

Mouse embryonic fibroblasts (MEF) with *Rev3L* deletion, *Rev3L*^{+/ Δ} and *Rev3L*^{-/ Δ} , were established from SV40 TAg-immortalized *Rev3L*^{+/*lox*} and *Rev3L*^{-/*lox*} MEFs following Cre recombinase expression via adenovirus infection to remove the

floxed allele of the *Rev3L* gene^{209,213}. *Rev3L*^{-Δ} MEFs were then supplemented with exogenously expressed human REV3L (*Rev3L*^{-Δ} +*hRev3L*) using pOZ expression system with IL2R as a selectable marker. Cells were cultured in Dulbecco's modified Eagle's medium (DMEM, 4.5 g/L glucose) with 10% FBS, 100 units/ml of penicillin, 100 μg/ml streptomycin, 0.25 μg/ml Fungizone antimycotic, and 4 mM GlutaMax in 5% CO₂ at 37°C.

AFB₁ treatment and growth inhibition assay

AFB₁ was dissolved in dimethyl sulfoxide (DMSO) and stored in 4°C. Working dilutions were prepared fresh in serum-free media. Growth inhibition effect of AFB₁ was determined by CTG assays to measure ATP, which is present in all metabolically active cells. Cells were seeded in 96-well plates 18-22 h prior to treatment, then exposed to various concentrations (50, 100, 150, 200 and 500 nM) of AFB₁ in serum-free media with antibiotic-antimycotic, 1 mM NADPH and 1% aroclor-induced rat liver microsome S9 (0.36-0.42 mg/ml protein) for 1.5 h at 37°C. Fresh complete media was added after removal of treatment media, and cells were allowed to grow for 48 h, after which a CTG assay was performed according to the manufacturer's protocol on a Tecan microplate reader for luminescence signal. Results were expressed as the average luminescence signal of the quadruple AFB₁ treated wells relative to that of control 1% DMSO treated wells (% of control).

Flow cytometry

For cell cycle analyses, cells were seeded in 100 mm dishes, treated as described above, harvested 24 h post treatment and fixed in 70% of alcohol at -20°C overnight. Cells were washed twice with cold 1X PBS and resuspended in PBS containing 10 µg/ml RNase A and 50 µg/ml PI. The cells were analyzed by FACSCalibur (Becton Dickinson) for DNA content in the flow cytometry core facility at Oregon Health & Science University. Cell cycle analyses were performed by FlowJo software.

Results

Sensitivity of DNA pol ζ null cells to AFB₁

Our previous biochemical data indicated that yeast pol ζ could catalyze bypass of AFB₁-FAPY and AFB₁-N7-Gua in an error-prone and high fidelity manner, respectively, providing the basis for the hypothesis that pol ζ may be necessary for replication past AFB₁-DNA adducts *in vivo*. To assess the importance of pol ζ in the cellular response to AFB₁, the *Rev3L* null MEFs immortalized by SV40 TAG were assayed for growth and survival by measuring ATP levels after AFB₁ treatment. Since MEFs do not possess the required metabolic enzymes to activate AFB₁, aroclor-induced rat liver microsome S9 and co-factor NADPH was used to activate AFB₁ in culture. As shown in Figure 16, *Rev3L*^{-Δ} MEFs appeared to be more sensitive to AFB₁ than *Rev3L*^{+Δ} cells in a dose-dependent manner, and the effect was specifically related to the presence of Rev3L as evidenced by the reverse of the sensitive phenotype in human *Rev3L*

complemented cells. These results indicate that mammalian pol ζ confers resistance to AFB₁-induced cytotoxicity, presumably by copying past AFB₁-DNA adducts, in a cellular context where the functions of p53 and retinoblastoma (Rb) were impaired by SV40 TAg²¹⁴.

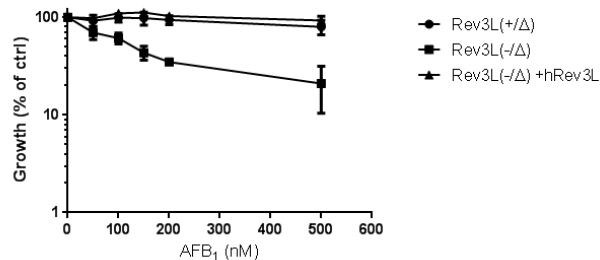


Figure 16. Disruption of pol ζ confers hypersensitivity to AFB₁. *Rev3L^{+Δ}*, *Rev3L^{-Δ}*, and *Rev3L^{-Δ} + hRev3L* cells were seeded in quadruplicate in 96-well plates followed by AFB₁ exposure in the presence of metabolic activation system as described in the Material and Methods. After 48 h, cell survival was measured by quantification of ATP levels using CTG assay. Data are presented as the mean \pm SD from three independent experiments.

Deletion of *Rev3L* triggers cell cycle distribution change by AFB₁

To test whether failed bypass of AFB₁-DNA adducts in the absence of pol ζ may interrupt cell cycle progression by checkpoint activation, cell cycle profiling by PI staining for DNA content in MEFs was performed. According to the results shown in Figure 16, administration of a sub-lethal dose, followed by a 24 h post-treatment time period that allows one population doubling was used to evaluate the effect of AFB₁ on cell cycle progression in pol ζ deficient cells. A snapshot of the cell cycle profiles (Figure 17) revealed that the *Rev3L* null MEFs had a change in cell cycle distribution 24 h after activated AFB₁ treatment. An increase

in the fraction of *Rev3L*^{-Δ} cells in the S and G2/M phase was accompanied by a reduction of the G1 phase, suggesting a delayed progression through or an arrest in S and G2/M phases. In contrast, no such change was detected in *Rev3L*-proficient cells. The specificity of this effect was further confirmed by the results observed in *hRev3L*-supplemented *Rev3L*^{-Δ} cells, which behaved similarly to pol ζ-proficient cells. Regardless of the status of *Rev3L*, inactive AFB₁ or DMSO control exerted no effect on the cell cycle profiles in these MEFs. Consistent with the notion that SV40 TAg blocks p53-mediated growth inhibition²¹⁴, no G1 arrest was observed in these AFB₁-exposed MEFs. Consistent with a role in TLS across AFB₁-DNA adducts, pol ζ deficiency resulted in DNA damage checkpoint responses to delay or completely block cell cycle transitions.

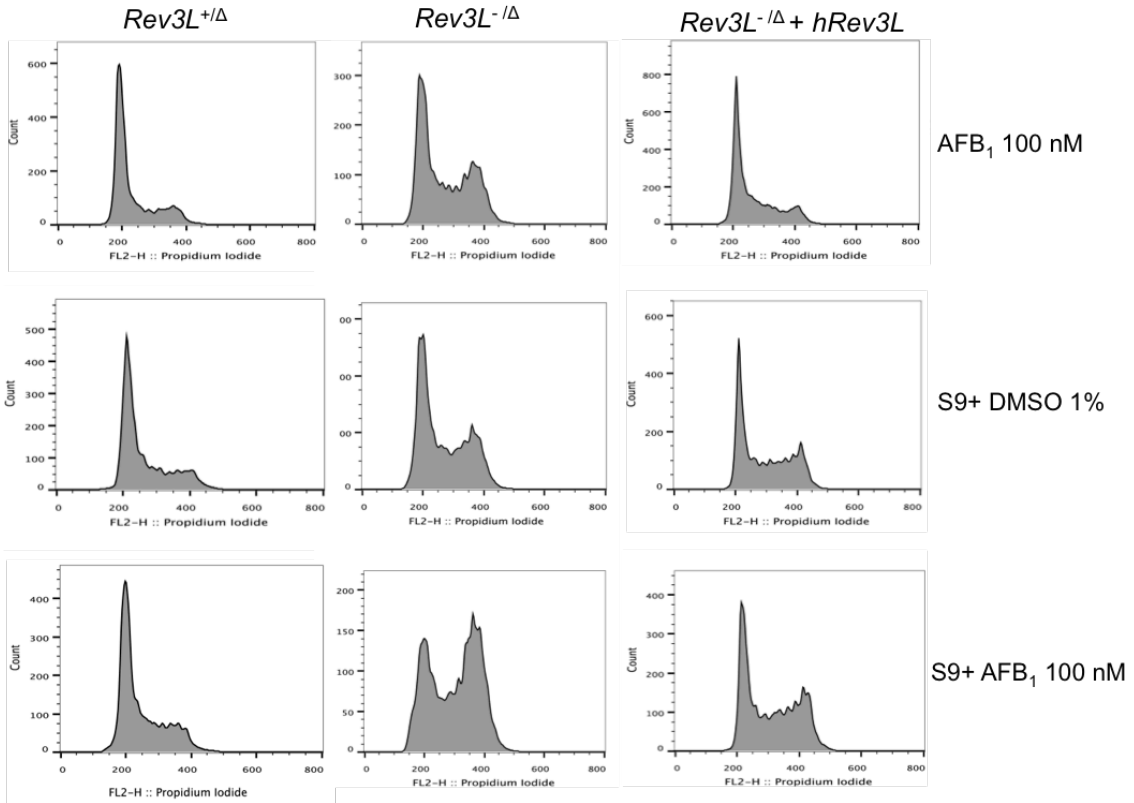


Figure 17. *Rev3L* deletion changes cell cycle distribution following AFB₁ exposure. TAG-immortalized control, *Rev3L*-deleted or human *Rev3L* complemented MEFs were exposed to DMSO control or 100 nM AFB₁ with or without metabolic activation system (S9) for 1.5 h. Cells were subjected to PI-staining for cell cycle analysis by flow cytometry to measure DNA content per cell 24 h after AFB₁ treatment. Results are representative histograms of one of three independent experiments.

Discussion

Our current SV40-immortalized cell model provides a biologically relevant system to study the role of pol ζ in maintaining genome stability following exposure to AFB₁ in a background of compromised checkpoints, mimicking the impaired functions of p53 and Rb due to the high prevalence of *R249S* mutation in *TP53* gene and HBV infection, which is known to inactivate Rb²¹⁵, in AFB₁-related

HCCs^{3,9}. In the present report, we provided the first evidence for the essential role of mammalian TLS pol ζ in cell survival in response to AFB₁ exposure (Figure 16). In contrast, yeast *rev3* mutant only exhibited a decrease in AFB₁-induced mutagenesis with comparable viability as the wild-type (WT) cells when expressing human metabolic enzyme CYP1A2 to activate AFB₁¹⁸⁹. This indicates that mammalian pol ζ provides an indispensable function, whereas yeast possess an alternative pathway to process AFB₁-induced DNA damage in an error-free manner that allows cell survival. Further studies are needed to confirm that the growth inhibition by AFB₁ in pol ζ null MEFs was due to apoptosis and/or a reduction in proliferation. On the other hand, the resistant phenotype of Rev3L proficient MEFs to AFB₁ is in accordance with previous observation of transgenic Big Blue MEFs that displayed sensitivity when exposed to ≥ 1 μ M AFB₁¹⁴³.

The effect of AFB₁ on cell cycle progression has been studied in a few experimental systems. Budding yeast *Saccharomyces cerevisiae*, expressing human metabolic enzyme CYP1A2, exhibited a transient delay in progression through S phase following exposure to 50 μ M AFB₁^{216,217}. In contrast, human liver carcinoma HepG2 cells with WT p53 displayed cell cycle arrest in G1 and G2/M phases with an inability to recover from inhibition of DNA synthesis 48 h after 9.6 μ M AFB₁ treatment²¹⁸. Interestingly, only transient accumulation in S phase, but no p53-dependent G1 arrest or sustained G2/M arrest, was observed when these cells were exposed to 5 μ M AFB₁, which is a dose causing single- and double-strand breaks without cytotoxic effect²¹⁹. Similarly, no cell cycle distribution change was detected in control Rev3L proficient MEFs when

exposed to 100 nM AFB₁ in the current report. It is tempting to speculate that depleting pol ζ by siRNA in HepG2 cells may sensitize them to the low dose of AFB₁ with a cell cycle effect.

Several models have been utilized to study the effect of Rev3L loss on the cell cycle progression. In particular, *Rev3L*-KO MEFs in a *p53*-null background exhibited a decreased frequency in S phase, and an increased proportion in G2/M phase and sub-G1 apoptotic population compared to control cells²⁰⁷. Moreover, the KO MEFs were sensitive to ultraviolet irradiation and cisplatin accompanied by a G2/M arrest in comparison to control. Consistently, conditional deletion of *Rev3L* in primary MEFs resulted in a reduction of S phase cells and an increase in cell death and senescence²⁰⁹. The current results showed that immortalization of *Rev3L*-KO MEFs by SV40 TAg restored a cell cycle profile similar to that of *Rev3L*-proficient cells (Figure 17). In agreement with the phenotype observed in *p53*-null *Rev3L*-KO MEFs²⁰⁷, cell cycle perturbation was detected after AFB₁ exposure in SV40 TAg-immortalized *Rev3L*-deleted MEFs; cells potentially were arrested in S and G2/M phases(Figure 17). Detailed time-course cell cycle studies are necessary to confirm whether AFB₁ induces S and G2/M cell cycle arrests in the absence of functional Rev3L.

In the context of cancer, suppression of *Rev3L* expression by RNA interference revealed inconsistent results. A number of cancer cell lines demonstrated susceptibility to the proliferation-inhibitory effect of Rev3L loss without external challenges as in MEFs. Depending on their p53 status, G1 arrest with senescence or G2/M arrest with growth inhibition was observed²²⁰.

Interestingly, the cell cycle profile of *Rev3L*-knockdown (KD) HeLa cells, deficient in G1 checkpoint, exhibited a G2 arrest in response to ionizing radiation²¹⁰. Otherwise, it appeared comparable to that of control siRNA treated cells. These observations may be reflective of various degrees of inhibition of *Rev3L* expression and dependence of pol ζ function in different cancer cell contexts. Nevertheless, these data highlight the essential role of mammalian pol ζ in tolerance of spontaneous and induced DNA damage for normal and cancerous cells growth. The implication of the current findings is that AFB₁-exposed hepatocytes with defective DNA damage responses and uncontrolled proliferation may accumulate genetic alterations through the pol ζ -mediated DNA damage tolerance mechanism. Under chronic dietary exposure, these cells may acquire critical combinations of genetic changes to induce transformation and tumor development.

CHAPTER 5

Removal of aflatoxin B₁- formamidopyrimidine adducts by human DNA glycosylase Nei endonuclease VIII-like 1 (hNEIL1)

Vladimir Vartanian¹, **Ying-Chih Lin**^{1,2}, Liang Li³, Michael P. Stone³, R. Stephen Lloyd^{1,4}

¹ Oregon Institute of Occupational Health Sciences and,

² Cancer Biology Program, Oregon Health & Science University, Portland, OR 97239, USA

³ Department of Chemistry, Vanderbilt University, Nashville, TN 37235, USA

⁴ Department of Molecular and Medical Genetics, Oregon Health & Science University, Portland, OR 97239, USA

Preface

This write-up will be part of a manuscript with the listed authors above.

The author's contributions to this work included conception, design and performance of experiments and data analyses of kinetic studies.

Vladimir Vartanian contributed to design and performed experiments and data analysis in NEIL1 knockout mice tumorigenesis studies.

Liang Li and Michael P. Stone provided AFB₁-FAPY adducted oligonucleotides.

R. Stephen Lloyd contributed to the conception of the project, experimental design, carcinogenesis data analyses and provided funding and lab space for the execution of this work.

Introduction

Currently, the second leading cause of cancer death worldwide is liver cancer¹, and the major histological subtype is HCC, which commonly occurs in developing countries, particularly in sub-Saharan Africa, Southeast Asia and China. AFB₁ exposure and HBV infection have been identified as the major risk factors in those regions. AFB₁, generated by some *Aspergillus* fungi, represents one of the most potent hepatocarcinogens that commonly contaminate our food^{3,9}.

It is well recognized that AFB₁ can cause DNA damage and induce genetic changes that are implicated in the initiation of hepatocarcinogenesis. Following ingestion and activation by liver metabolic enzymes, the intermediate AFB₁-epoxide can form a covalently bound adduct on the N7 atom of guanine in DNA^{78,79,81}. Kinetic analyses of the formation and disappearance of AFB₁-DNA adducts in rat revealed that about 20% of the initial, quantitatively abundant AFB₁-N7-Gua lesions convert to the secondary AFB₁-FAPY adducts 24 h after a single dose of AFB₁. These FAPY adducts became the dominant DNA damage detected in cellular DNA 72 h later, comprising up to 80% of all known lesions⁹⁴. Similar results were observed in cultured human fibroblasts treated with AFB₁ in the presence of a metabolic activation system¹⁰⁸. These data indicate that AFB₁-FAPY adducts are more resistant to loss by spontaneous or repair processes than the initial AFB₁-N7-Gua lesions in mammalian tissues. Moreover, AFB₁-FAPY appeared to be more mutagenic than AFB₁-N7-Gua in bacterial and primate cells, inducing G to T transversion at frequencies of 32% and 97%, respectively^{39,166}. This mutation signature is consistent with mutation data

derived from AFB₁-associated HCCs^{130,131} and thus underscores a causative link between replication of these adducts and genetic alteration associated with these cancers.

Cells have evolved to utilize various DNA repair processes to protect themselves from DNA damage induced endogenously and exogenously. The DNA lesions generated after exposure to AFB₁ are considered to be bulky DNA adducts and indeed, the nucleotide excision repair (NER) pathway has been shown to remove both AFB₁-N7-Gua and AFB₁-FAPY in *E. coli* with similar efficiencies¹⁰⁵. The involvement of NER for the removal of AFB₁-N7-Gua in human cells is evident since more AFB₁-N7-Gua adducts accumulated in XPA than in normal fibroblasts 48 h post treatment¹⁰⁸. However, the case for NER-mediated AFB₁-FAPY repair does not seem as clear, even though a similar observation was noted¹⁰⁸. These data are inconclusive since there is no evidence to support whether their accumulation was a direct consequence of impaired NER function for AFB₁-FAPY or an indirect outcome of conversion of additional unrepaired AFB₁-N7-Gua to AFB₁-FAPY in XPA cells. Further studies of how cells repair the persistent and miscoding AFB₁-FAPY lesions to prevent the mutagenic events and subsequent carcinogenesis of HCC are necessary.

The role of base excision repair (BER) in removal of the AFB₁-FAPY lesion has only been investigated using the *E. coli* Fpg DNA glycosylase, and so far, the evidence appears to be contradictory with regard to the ability of Fpg to initiate repair of this adduct^{105,118}. Human NEIL1 (hNEIL1) DNA glycosylase is an ortholog of Fpg, with enzymatic activity towards oxidized pyrimidines, Fapy-dA

and Fapy-dG adducts^{120,221}. In addition, this enzyme exhibits distinct structural preference for repairing lesions that are located within a DNA bubble structures that are reminiscent of the DNA structures during transcription and replication²²². Therefore, based on the structural similarity between Fapy-dG and AFB₁-FAPY, we hypothesized that AFB₁-FAPY can be repaired by NEIL1 as the first step of the BER pathway. The current work was designed to determine whether hNEIL1 could cleave AFB₁-FAPY adducts in both duplex and bubble oligodeoxynucleotide substrates with further characterization of the catalytic efficiency of the enzyme.

Experimental procedures

Materials

The following materials and reagents were purchased: T4 polynucleotide kinase and bovine serum albumin (BSA) (New England BioLabs); [γ -³²P]ATP (PerkinElmer Life Sciences); Micro Bio-spin 6 column (Bio-Rad); all other chemicals used for these experiments (Sigma-Aldrich or Fisher Scientific). hNEIL1 was purified as previously described²²³ and total concentration of the protein was determined by the Bradford assay using BSA as the standard.

Substrate DNA preparation

The AFB₁-FAPY containing oligodeoxynucleotides were synthesized as previously described¹⁸¹. All non-adducted oligodeoxynucleotides were obtained from Integrated DNA Technologies, Inc. Sequences of the oligonucleotides for

constructing the duplex and bubble DNA substrates are shown in Figure 18. Oligodeoxynucleotides were dissolved in a buffer composed of 10 mM Tris-HCl (pH 7.5) and 1 mM EDTA. For all experiments, lesion-containing oligodeoxynucleotides were radiolabeled using [γ - 32 P]ATP with T4 polynucleotide kinase at 37°C. Following removal of excess [γ - 32 P]ATP with a Micro Bio-spin 6 column, labeled oligodeoxynucleotides were annealed to the complementary strand to form either a duplex or a five-nucleotide bubble DNA structure at a molar ratio of 1:1.2 in the presence of 50 mM NaCl by heating at 90°C for 2 min and allowing to gradually cool to room temperature.

Duplex (1) 5' -ACCACTACTATXATTCATAACAAC-3'
 (2) 3' -TGGTGATGATACTAAGTATTGTTG-5'

Bubble (1) 5' -ACCACTACTATXATTCATAACAAC-3'
 (3) 3' -TGGTGATGAGCTGCAGTATTGTTG-5'

X= AFB₁-FAPY

Figure 18. DNA sequences used in glycosylase assays. A five-nucleotide mispair was designed to generate a bubble in the middle of a 24 nucleotide duplex using sequences (1) and (3).

DNA Glycosylase assays

Single turnover kinetic experiments were conducted using the AFB₁-FAPY modified duplex or bubble structure DNA substrates to evaluate the glycosylase activity of hNEIL1. The reaction was initiated by the addition of 160 nM active enzyme into a total volume of 70 μ l in the presence of 20 mM Tris-HCl, pH 7.5, 1 mM EDTA, 100 mM NaCl and 100 μ g/ml BSA at 37°C with a final DNA

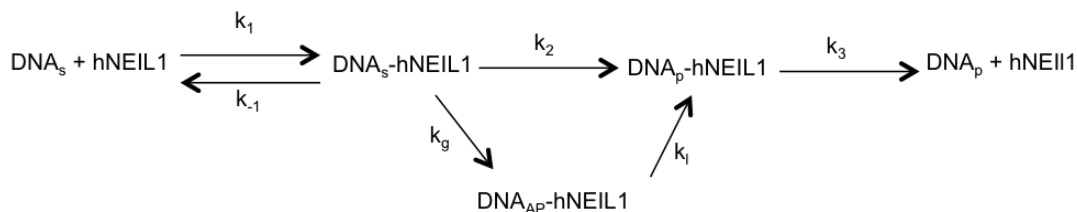
concentration of 20 nM. Five microliter aliquots were removed at 0.25, 0.5, 1, 1.5, 2, 3.5, 5, 8, 10, 15, 30 and 60 min, and quenched by addition of equal volume of 0.5 N NaOH at 90°C for 5 min, followed by addition of 10 µl of DNA denaturing loading buffer (95% formamide, 20 mM EDTA, 0.02% xylene cyanol, and 0.02% bromophenol blue) at 90°C for 2 min. Controls without enzyme were performed at 37°C for 60 min and quenched as described above. The reaction products were separated by electrophoresis in a 15% denaturing polyacrylamide gel containing 8 M urea in Tris-borate-EDTA buffer. Gels were exposed to a phosphor screen and autoradiography was performed by an Amersham Biosciences Storm 820 instrument. Quantification of the image was conducted using ImageQuant software. The background cleavage in the controls without enzyme was subtracted and the data were fitted to a single exponential equation (Equation 1) to determine the first-order rate constant (k_{obs}) as previously described²²⁴ using GraphPad Prism software.

$$\text{Product} = A_0 \{1 - \exp(-k_{\text{obs}} t)\} \quad (\text{eq. 1})$$

Results

General considerations of glycosylase assays

The schematic of the kinetic steps for hNEIL1 is shown in Scheme 1. As a bifunctional glycosylase, hNEIL1 can remove damaged bases and carry out strand scission via its glycosylase and lyase activities, which are tightly coupled steps²²⁴.



Scheme 1. Minimal kinetic scheme used for the analysis of the glycosylase/lyase activity of hNEIL1.

Like other DNA glycosylases, the release of hNEIL1 from its products is the rate-limiting factor, as evidenced by an observed biphasic time course of product formation²²⁴⁻²²⁶. The initial burst phase represents the product generated at the active site of the enzyme during the first cycle of reaction, followed by a linear steady-state phase due to slow enzyme turnover. To gain insight into the chemical process occurring at the active site, a single turnover kinetic approach is commonly utilized to measure the reaction in the burst phase catalyzed by these DNA glycosylases^{224,225}. Under these conditions, enzymes are in excess relative to substrates ($[DNA] \ll [hNEIL1]$) so that all of the substrate DNAs can be processed by enzymes in their first catalytic cycling. The reaction follows first-order kinetics and the product formation curve can be fitted and analyzed by eq 1, where A_0 represents the amplitude of the exponential phase and $k_{obs} = k_2$ (Scheme 1) is the observed rate constant associated with that process. Since hNEIL1 has been shown to repair oxidized DNA bases from both duplex and bubble-containing DNAs^{120,222}, the ability of hNEIL1 to process AFB₁-FAPY adducts was assessed using two 24-bp duplexes containing a centrally located

AFB₁-FAPY, one with complete complementarity and the other with a five-nucleotide bubble structure.

Removal of AFB₁-FAPY from DNA duplex and bubble substrates by hNEIL1

As shown in Figure 19, under single turnover conditions, product formation followed a single exponential time course, and underwent complete cleavage at the damaged base in eight minutes for the complementary duplex DNAs. In marked contrast, the reaction with bubble structure containing AFB₁-FAPY lesions reached a plateau at approximately 30% in three and half minutes (Figure 20). The observed excision rate constants were 0.23 and 0.47 min⁻¹ for the complementary duplex and bubble-structured substrates, respectively (Table 3). The rate was two-fold faster for the bubble DNAs compared to the complementary duplex, indicating a higher intrinsic reactivity for the FAPY adducts in bubble structure. Taken together, these results suggest that the BER pathway may be the alternative mechanism for repair of AFB₁-FAPY adducts, initiated through the glycosylase and lyase activities of NEIL1.

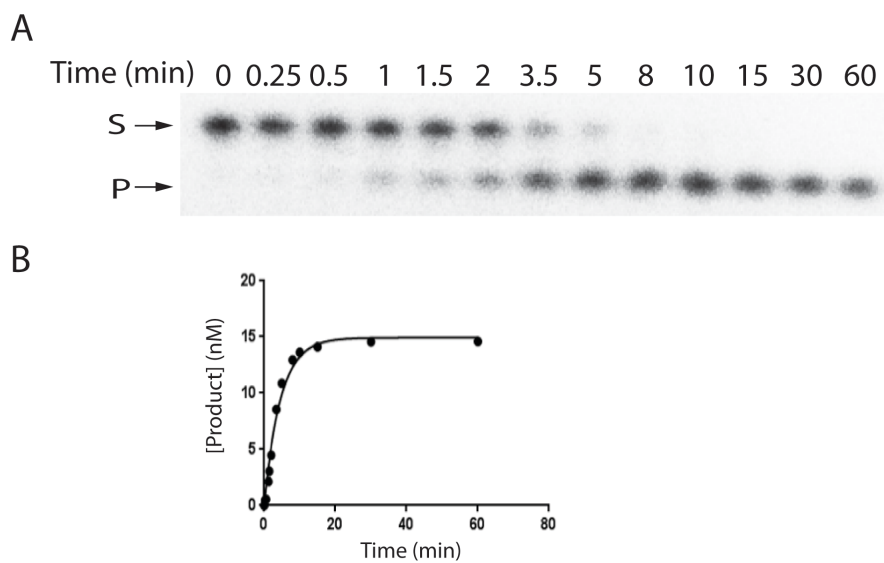


Figure 19. Single turnover analysis to measure AFB₁-FAPY removal in duplex DNA by hNEIL1. hNEIL1 (160 nM) was incubated with 20 nM complementary duplex DNAs containing AFB₁-FAPY at 37°C and product formation was followed for 60 min as described in the text. A. Representative denaturing polyacrylamide gel image showed the separation of substrate (S) and product (P) over the period of 60 min. B. Representative plot of product formation as a function of time. The data were fitted to eq 1 as described in the text.

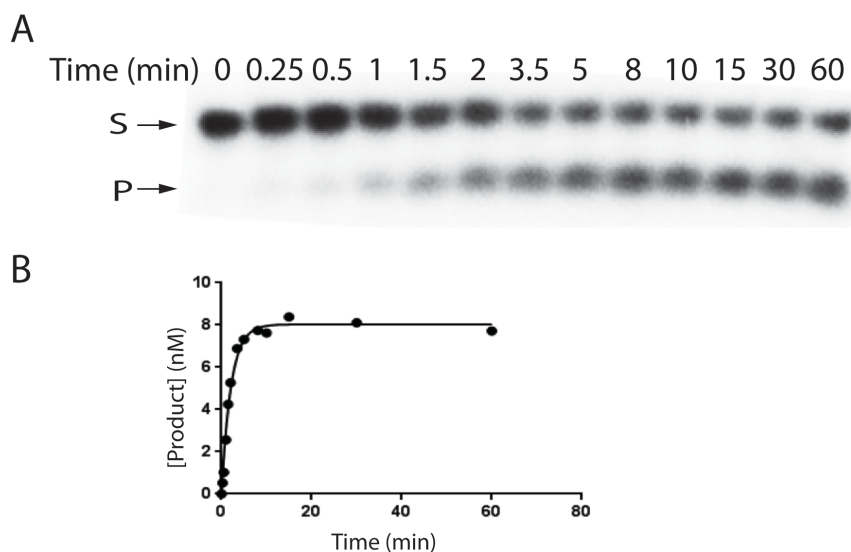


Figure 20. Single turnover analysis for removal of AFB₁-FAPY in bubble-structured DNA by hNEI1. hNEI1 (160 nM) was incubated with 20 nM substrate DNAs containing AFB₁-FAPY adduct in a five nucleotide bubble structure at 37°C and product formation was followed for 60 min as described in the text. A. Representative denaturing polyacrylamide gel image showed the separation of substrate (S) and product (P) over the period of 60 min. B. Representative plot of product formation as a function of time. The data were fitted to eq 1 as described in the text.

	Duplex	Bubble
k_2 (min ⁻¹) ^a	0.233 ± 0.018	0.471 ± 0.057

^a all values represent an average of three independent experiments with SD as error

Table 4. Rate constants determined at 37°C under single turnover conditions for cleavage of AFB₁-FAPY in complementary duplex and bubble DNAs.

Discussion

The current report provides the first evidence for the role of hNEIL1 in repair of AFB₁-FAPY adducts with kinetic parameters, demonstrating a higher catalytic efficiency for lesions located in bubble DNAs. These findings have a number of implications as discussed below.

It has been proposed that NER may not repair AFB₁-FAPY efficiently because of the intercalation of AFB₁-FAPY in the DNA duplex, which leads to an increase in melting temperature of oligodeoxynucleotides⁹⁷, instead of causing distortion in the DNA helix, as is the case for other bulky adducts. On the other hand, the Fpg/Nei family of oxidative DNA glycosylases have three so-called void-filling residues that are inserted into the DNA helix to help flip out the damaged base into the active site of the glycosylase as part of the lesion searching mechanism²²⁷. Thus, it is conceivable that BER may provide an alternative pathway for repairing a specific class of bulky DNA adducts like AFB₁-FAPY lesions through the damage-flipping mechanism utilized by NEIL1 glycosylase. Previously, hNEIL1 has been shown to excise bulky monoadducts induced by photoactivated psoralen²²⁸. Interestingly, AFB₁ and psoralen are structurally similar, both being classified as furocoumarins. Further structural analysis of hNEIL1 complexed with these adducts is needed to reveal the mechanism by which these adducts are recognized and excised.

There are several reports on the single-turnover kinetic analysis of NEIL1 with various oxidized DNA bases. Thymine glycols (Tg) and 5-hydroxyuracil (5-OHU), the oxidation product of thymine and cytosine, are among the most

extensively studied. The rate constant for reactions of hNEIL1 with double-stranded oligodeoxynucleotides containing Tg:A has been reported by two groups: 0.0054 and 1.3 min⁻¹ ^{224,229}. A similar approach was used with mimivirus Nei1, the viral ortholog of hNEIL1, and a rate constant of 0.54 min⁻¹ was reported²³⁰. Moreover, the rate constants of hNEIL1 with double-stranded DNA containing 5-hydroxycytosine (5-OHC):G, 5-OHU:G, dihydrothymine:A and dihydrouracil:G were 0.24, 0.14, 0.0014, and 0.054 min⁻¹, respectively²²⁹. The rate constant of hNEIL1 with 5-OHU in bubble oligodeoxynucleotides was 0.72 min⁻¹ ²³¹. Taken together, our kinetic results indicated that the intrinsic activity of hNEIL1 for AFB₁-FAPY adduct is comparable to that for Tg, 5-OHC and 5-OHU. It is of particular interest to test whether NEIL1 is involved in removal of AFB₁-FAPY adducts *in vivo*, as these adducts may accumulate in NEIL1-deficient cells compared to WT. We noted that the reaction of hNEIL1 with duplex DNAs containing AFB₁-FAPY opposite an A did not undergo completion (data not shown). This observation suggests that hNEIL1 may not remove FAPY lesions after an error-prone replication and consequently a G to T mutation may occur.

The preference of hNEIL1 in removal of AFB₁-FAPY lesions in bubble DNA is consistent with the observation for 5-OHU²²². However, the trend is reversed when using guanidinohydantoin (Gh) and spiroiminodihydantoin (Sp)²³². Sp and Gh are the two secondary oxidation products of guanine that can be first oxidized to 8-oxo-7,8-dihydroguanine (8-oxoG). This inconsistency may depend on the types of DNA lesions tested.

It has been shown that the two anomers of AFB₁-FAPY, α and β forms at the deoxyribose, maintain an equilibrium of 2:1 as α to β in ss DNA. In ds DNA, the β form is normally present^{93,166}. Theoretically, the site-specific AFB₁-FAPY adducts in the bubble structure may consist of a mixture of α and β forms, and since only about 30% of the bubbled substrates were cleaved, it is tempting to speculate that hNEIL1 can only excise the β , not α , form of AFB₁-FAPY. It is also conceivable that bubble structures may allow easier access for hNEIL1 to recognize and remove the β form than in duplex DNA. Detailed structural analysis is warranted.

On the basis of the current results, a carcinogenesis study of AFB₁ using a NEIL1-KO mouse model is under active investigation in our laboratory.

6. Summary and Conclusion

The introduction chapter of this dissertation serves as a literature review of our current knowledge of the global public health issue regarding HCC, with a focus on a particular etiological factor: aflatoxin B₁. The importance of understanding how AFB₁ exerts genotoxic and mutagenic effects as the initial steps of hepatocarcinogenesis was highlighted. The need for detailed studies on mechanisms that contribute and modulate the AFB₁ mutagenicity was also emphasized.

Two types of DNA adducts are formed after exposure to AFB₁: AFB₁-N7-Gua and AFB₁-FAPY. Although it is known that these two adducts can give rise to the commonly observed AFB₁-induced G to T transversions in *E. coli*, the mutation frequency was low. Investigations into the mutagenic potential of these AFB₁-DNA adducts in primate cells using a site-specific mutagenesis assay was described in Chapter 2 and Chapter 3. We discovered that both lesions were considerably more mutagenic in primate cells, with values about 3-10 fold higher than in *E. coli*. In accordance with the observations in *E. coli*, AFB₁-FAPY lesions appear to be more potent than AFB₁-N7-Gua for mutagenesis. To elucidate how these adducts can induce such high mutation frequencies, studies examining the ability of eukaryotic TLS polymerases to replicate past these lesions were discussed. Based on our biochemical characterization, yeast pol ζ was suggested to be the primary candidate to synthesize across AFB₁-FAPY adducts to induce the G to T transversions. In drastic contrast, our studies suggested that

yeast pol ζ may replicate past AFB₁-N7-Gua in an error-free manner compared to other TLS polymerases tested.

To gain insight into the role of pol ζ in TLS for AFB₁-DNA adducts *in vivo*, the response of MEFs with complete KO of *Rev3L* to AFB₁ treatment was discussed in Chapter 4. Our initial studies revealed that *Rev3L*-KO MEFs were sensitive to AFB₁ compared to control cells, and this phenotype was specifically caused by the loss of *Rev3L*. Further supporting a TLS role for pol ζ , failure of replication bypass of AFB₁-induced DNA damage in *Rev3L*-deleted cells elicited checkpoint responses to disrupt cell cycle progression. No cell cycle perturbation was noted in control or human *Rev3L* rescued cells. Overall, these results provide evidence for the biological role of pol ζ in tolerating the genotoxicity of AFB₁.

Since AFB₁-FAPY adduct is a long-lived DNA lesion that exhibits a high mutagenic potential in mammals, repair of this adduct is of particular importance. An investigation of hNEIL1-initiated BER for AFB₁-FAPY was described in Chapter 5. Our biochemical studies indicate that DNA glycosylase hNEIL1 can cleave AFB₁-FAPY adduct from DNA duplexes that were completely complementary or within a bubble-structure. The kinetic parameters indicated that hNEIL1 can excise AFB₁-FAPY adducts in bubble DNAs twice as fast as those in complementary duplexes, although only the reaction for duplex DNAs proceeded to completion. Our discoveries provide the first evidence that human BER could be involved in processing a bulky-DNA adduct as large as that

modified by AFB₁, and this further expands the repertoire of DNA damage that can be repaired by hNEIL1.

7. Future Directions

Pol ζ -KO MEFs were found to be sensitive to AFB₁ with a disruption in cell cycle transition compared to control cells. However, the mechanism of this phenotype is currently unknown. I hypothesize that without a pol ζ -mediated damage tolerance pathway for AFB₁-DNA adducts during replication, the replication fork may collapse. Alternatively, gaps may form due to re-initiation of replication downstream or emergence of adjacent replication forks. Such gaps may induce cell cycle arrest in S phase, or cells may process them in G2 phase through a gap-filling TLS mechanism that again requires pol ζ activity. Un-filled gaps are susceptible to formation of DSBs. Such DNA damage may activate a checkpoint response, leading to G2/M arrest and eventual apoptosis if cells cannot recover from the DNA damage. To test this model, I propose to treat the same set of MEF cell lines with and without *Rev3L* with AFB₁ in the presence of an activating system for the following series of experiments. To examine whether cell death is responsible for the sensitivity observed previously, I propose to carry out an apoptosis assay using Annexin-V and PI-staining with flow cytometry. Additionally, time-course cell cycle studies will be performed to determine S and G2/M cell cycle arrest. Activation of DNA damage response and checkpoint effectors such as ATM, ATR, Chk1 and Chk2 will be examined. Secondary DNA damage, namely single strand breaks (SSBs) and DSBs, will be measured by comet assay or alkaline DNA unwinding method. Immunofluorescent assays for co-localization of 53BP1 and γ -H2AX foci will be assessed as a validation of DSB formation.

Although excision of AFB₁-FAPY adducts by hNEIL1 in complementary and bubble DNAs was demonstrated, the molecular mechanisms of recognition and removal remain unclear. To gain some insights in this aspect, I propose to carry out structural examinations of the hNEIL1-AFB₁-FAPY complex, in which the adduct is situated in complementary and bubble-structured DNA substrates, using X-ray crystallography and NMR spectroscopy through collaborations with Drs. Martin Egli and Michael Stone, respectively, at Vanderbilt University. This will allow elucidation of the effects of DNA structures on the lesion conformations with regard to substrate recognition by hNEIL1.

On the basis of our kinetic data, investigations of the biological role of NEIL1 in modulating AFB₁-induced genotoxicity and mutagenesis are of particular interest. I hypothesize that NEIL1-deficient cells will have more accumulation of AFB₁-FAPY adducts and higher mutation frequency compared to WT cells following AFB₁ exposure. Therefore, I propose to carry out time-course measurements of the FAPY lesions in genomic DNA from AFB₁-treated WT and *Neil1*-KO MEFs and neonatal mouse livers. The detection of AFB₁-FAPY adducts will be performed using liquid chromatography-tandem mass spectrometry through collaboration with Dr. Robert Turesky at University of Minnesota.

The utility of vectors containing a site-specific AFB₁-FAPY adduct for repair assays in WT and NEIL1-deficient cells will be examined so that the repair function of NEIL1 in suppression of AFB₁-induced mutagenesis will be revealed. Once this methodology is established, the *in vivo* effect of DNA structures on NEIL1-mediated repair can be tested as well. Additionally, I propose to conduct

genome sequencing of neonatal WT and *Neil1*-KO mice livers following AFB₁ exposure to determine mutation frequency and spectra. In this study, genome-wide genetic changes induced by AFB₁ in mammalian cells can be identified, specifically mutations in tumor suppressor genes and oncogenes. Information regarding the specificity of NEIL1 repair for the genotoxicity induced by AFB₁ can be surveyed at a genomic level as well.

Overall, my dissertation work provided evidence for the involvement of mammalian TLS pol ζ and hNEIL1 in modulating AFB₁-induced mutagenesis and DNA damage, respectively. This knowledge raises more questions and opens new avenues of research as discussed below. One important question is whether there are any polymorphic variants in *Rev3L* and *NEIL1* genes that may increase people's susceptibility for early onset of HCC associated with chronic HBV infection and dietary exposure to AFB₁. The high mortality rate of HCC is partly due to the low frequency of early detection; advanced disease often occurs at the time of diagnosis. By implementing effective screening and surveillance programs for high-risk population, early detection of HCC may be achievable. Identification of genetic variants as susceptibility biomarkers is integral to recognize people who are at high risk. Along this line, generation of conditional *Rev3L*-KO mouse strain with reduced or abolished pol ζ activity in liver for AFB₁-induced carcinogenesis assay may prove to be valuable. Alternatively, *Rev3L* and *NEIL1* genes may be altered through genetic or/and epigenetic mechanisms that affect their gene expression levels and protein functions during hepatocarcinogenesis. These changes may serve as prognostic and therapeutic

biomarkers for patient stratification. It has been shown that polymorphic variants and promoter hypermethylation in *NEIL1* gene are associated with gastric cancer and head and neck squamous cell carcinoma, respectively^{233,234}. A polymorphic variant in the 3'-terminal untranslated region of *Rev3L* gene was recently observed to enhance lung cancer susceptibility²³⁵.

In addition to dietary exposure to AFB₁, HBV is another major risk factor in regions of high HCC incidence worldwide. The effect of HBV infection on the functions of pol ζ and NEIL1 in response to AFB₁ exposure is of particular importance to understand how concomitant exposure to both risk factors may contribute to early onset of HCC.

There are at least five mammalian DNA polymerases extensively studied for their TLS function (pol η, ι, κ, ζ, Rev1) in the literature, however, it remains unclear how they are recruited and regulated at various types of lesion during DNA synthesis and/or post-replication gap-filling processes. Further investigations of the regulatory networks of pol ζ for replication bypass of AFB₁-DNA adducts may shed some lights into how cells control TLS function for the purpose of DNA damage tolerance and maintenance of genome stability.

REFERENCES

1. *GLOBOCAN 2012: Estimated Cancer Incidence, Mortality and Prevalence Worldwide in 2012*. (International Agency for Research on Cancer, World Health Organization). at http://globocan.iarc.fr/Pages/fact_sheets_population.aspx
2. Serag, El, H. B. & Rudolph, K. L. Hepatocellular Carcinoma: Epidemiology and Molecular Carcinogenesis. *Gastroenterology* **132**, 2557–2576 (2007).
3. McGlynn, K. A. & London, W. T. The global epidemiology of hepatocellular carcinoma: present and future. *Clin Liver Dis* **15**, 223–43–vii–x (2011).
4. Davila, J. A., Morgan, R. O., Shaib, Y., McGlynn, K. A. & Serag, El, H. B. Hepatitis C infection and the increasing incidence of hepatocellular carcinoma: a population-based study. *Gastroenterology* **127**, 1372–1380 (2004).
5. Altekruse, S. F., McGlynn, K. A. & Reichman, M. E. Hepatocellular carcinoma incidence, mortality, and survival trends in the United States from 1975 to 2005. *J. Clin. Oncol.* **27**, 1485–1491 (2009).
6. Blonski, W., Kotlyar, D. S. & Forde, K. A. Non-viral causes of hepatocellular carcinoma. *World Journal of Gastroenterology* **16**, 3603–3615 (2010).
7. *Hepatitis B*. (World Health Organization). at <http://www.who.int/mediacentre/factsheets/fs204/en/>
8. Strosnider, H. *et al.* Workgroup report: public health strategies for reducing aflatoxin exposure in developing countries. *Environ Health Perspect* **114**, 1898–1903 (2006).
9. Kensler, T. W., Roebuck, B. D., Wogan, G. N. & Groopman, J. D. Aflatoxin: a 50-year odyssey of mechanistic and translational toxicology. *Toxicol Sci* **120 Suppl 1**, S28–48 (2011).
10. Gross-Steinmeyer, K. & Eaton, D. L. Dietary modulation of the biotransformation and genotoxicity of aflatoxin B(1). *Toxicology* **299**, 69–79 (2012).
11. Zhu, J. Q. *et al.* Correlation of dietary aflatoxin B1 levels with excretion of aflatoxin M1 in human urine. *Cancer Research* **47**, 1848–1852 (1987).
12. Groopman, J. D. *et al.* Molecular dosimetry of urinary aflatoxin-DNA adducts in people living in Guangxi Autonomous Region, People's Republic of China. *Cancer Research* **52**, 45–52 (1992).
13. Azziz-Baumgartner, E. *et al.* Case-control study of an acute aflatoxicosis outbreak, Kenya, 2004. *Environ Health Perspect* **113**, 1779–1783 (2005).
14. Liu, Y. & Wu, F. Global burden of aflatoxin-induced hepatocellular carcinoma: a risk assessment. *Environ Health Perspect* **118**, 818–824 (2010).
15. Liu, Y., Chang, C.-C. H., Marsh, G. M. & Wu, F. Population attributable

- risk of aflatoxin-related liver cancer: systematic review and meta-analysis. *Eur. J. Cancer* **48**, 2125–2136 (2012).
16. Wu, H.-C. & Santella, R. The role of aflatoxins in hepatocellular carcinoma. *Hepatitis Monthly* **12**, e7238 (2012).
 17. Kensler, T. W., Qian, G.-S., Chen, J. G. & Groopman, J. D. Translational strategies for cancer prevention in liver. *Nat. Rev. Cancer* **3**, 321–329 (2003).
 18. Newberne, P. M. & Butler, W. H. Acute and chronic effects of aflatoxin on the liver of domestic and laboratory animals: a review. *Cancer Research* **29**, 236–250 (1969).
 19. Wogan, G. N., Edwards, G. S. & Newberne, P. M. Structure-activity relationships in toxicity and carcinogenicity of aflatoxins and analogs. *Cancer Research* **31**, 1936–1942 (1971).
 20. Ayres, J. L., Lee, D. J., Wales, J. H. & Sinnhuber, R. O. Aflatoxin structure and hepatocarcinogenicity in rainbow trout (*Salmo gairdneri*). *J. Natl. Cancer Inst.* **46**, 561–564 (1971).
 21. Carnaghan, R. B. Hepatic tumours in ducks fed a low level of toxic groundnut meal. *Nature* **208**, 308 (1965).
 22. Wogan, G. N., Paglialunga, S. & Newberne, P. M. Carcinogenic effects of low dietary levels of aflatoxin B₁ in rats. *Food Cosmet Toxicol* **12**, 681–685 (1974).
 23. Sinnhuber, R. O., Hendricks, J. D., Wales, J. H. & Putnam, G. B. Neoplasms in rainbow trout, a sensitive animal model for environmental carcinogenesis*. *Annals of the New York Academy of Sciences* **298**, 389–408 (1977).
 24. Vesselinovitch, S. D., Mihailovich, N., Wogan, G. N., Lombard, L. S. & Rao, K. Aflatoxin B₁, a hepatocarcinogen in the infant mouse. *Cancer Research* **32**, 2289–2291 (1972).
 25. Gopalan, C., Tulpule, P. G. & Krishnamurthi, D. Induction of hepatic carcinoma with aflatoxin in the rhesus monkey. *Food Cosmet Toxicol* **10**, 519–521 (1972).
 26. Adamson, R. H., Correa, P., Sieber, S. M., McIntire, K. R. & Dalgard, D. W. Carcinogenicity of aflatoxin B₁ in rhesus monkeys: two additional cases of primary liver cancer. *J. Natl. Cancer Inst.* **57**, 67–78 (1976).
 27. Sieber, S. M., Correa, P., Dalgard, D. W. & Adamson, R. H. Induction of osteogenic sarcomas and tumors of the hepatobiliary system in nonhuman primates with aflatoxin B₁. *Cancer Research* **39**, 4545–4554 (1979).
 28. Thorgeirsson, U. P., Dalgard, D. W., Reeves, J. & Adamson, R. H. Tumor incidence in a chemical carcinogenesis study of nonhuman primates. *Regul Toxicol Pharmacol* **19**, 130–151 (1994).
 29. Kujawa, M. Some Naturally Occurring Substances: Food Items and Constituents, Heterocyclic Aromatic Amines and Mycotoxins. IARC Monographs on the Evaluation of Carcinogenic Risks to Humans. *Food/Nahrung* (1994).
 30. Miller, E. C. & Garner, J. A. Liver microsomal metabolism of aflatoxin B₁

- to a reactive derivative toxic to *Salmonella typhimurium* TA 1530. *Cancer Research* **32**, 2058–2066 (1972).
31. Garner, R. C. Microsome-dependent binding of aflatoxin B₁ to DNA, RNA, polyribonucleotides and protein *in vitro*. *Chemico-Biological Interactions* **6**, 125–129 (1973).
 32. Eaton, D. and Gallagher, E. P. Mechanisms of aflatoxin carcinogenesis. *Annu. Rev. Pharmacol. Toxicol.* **34**, 135-172 (1994).
 33. Dohnal, V., Wu, Q. & Kuca, K. Metabolism of aflatoxins: key enzymes and interindividual as well as interspecies differences. *Arch Toxicol* 1–10 (2014). doi:10.1007/s00204-014-1312-9
 34. Sinnhuber, R. O., Lee, D. J., Wales, J. H., Landers, M. K. & Keyl, A. C. Hepatic carcinogenesis of aflatoxin M₁ in rainbow trout (*Salmo gairdneri*) and its enhancement by cyclopropene fatty acids. *J. Natl. Cancer Inst.* **53**, 1285–1288 (1974).
 35. Hsieh, D. P., Cullen, J. M. & Ruebner, B. H. Comparative hepatocarcinogenicity of aflatoxins B₁ and M₁ in the rat. *Food Chem. Toxicol.* **22**, 1027–1028 (1984).
 36. Baertschi, S. W., Raney, K. D., Stone, M. P. & Harris, T. M. Preparation of the 8,9-epoxide of the mycotoxin aflatoxin B₁: the ultimate carcinogenic species. *J Am Chem Soc* **110**, 7929–7931 (1988).
 37. Sabbioni, G., Skipper, P. L., Büchi, G. & Tannenbaum, S. R. Isolation and characterization of the major serum albumin adduct formed by aflatoxin B₁ *in vivo* in rats. *Carcinogenesis* **8**, 819–824 (1987).
 38. Gan, L.-S. *et al.* Serum albumin adducts in the molecular epidemiology of aflatoxin carcinogenesis: correlation with aflatoxin B₁ intake and urinary excretion of aflatoxin M 1. *Carcinogenesis* **9**, 1323–1325 (1988).
 39. Lin, Y.-C. *et al.* Molecular basis of aflatoxin-induced mutagenesis-role of the aflatoxin B₁-formamidopyrimidine adduct. *Carcinogenesis* **35**, 1461–1468 (2014).
 40. Ramsdell, H. S. & Eaton, D. L. Species susceptibility to aflatoxin B₁ carcinogenesis: comparative kinetics of microsomal biotransformation. *Cancer Research* **50**, 615–620 (1990).
 41. Forrester, L. M., Neal, G. E., Judah, D. J., Glancey, M. J. & Wolf, C. R. Evidence for involvement of multiple forms of cytochrome P-450 in aflatoxin B₁ metabolism in human liver. *Proc Natl Acad Sci USA* **87**, 8306–8310 (1990).
 42. Shimada, T. & Guengerich, F. P. Evidence for cytochrome P-450NF, the nifedipine oxidase, being the principal enzyme involved in the bioactivation of aflatoxins in human liver. *Proc Natl Acad Sci USA* **86**, 462–465 (1989).
 43. Ueng, Y.-F., Shimada, T., Yamazaki, H. & Guengerich, F. P. Oxidation of aflatoxin B₁ by bacterial recombinant human cytochrome P450 enzymes. *Chem. Res. Toxicol.* **8**, 218–225 (1995).
 44. Guengerich, F. P. *et al.* Activation and detoxication of aflatoxin B₁. *Mutat Res* **402**, 121–128 (1998).
 45. Ramsdell, H. S., Parkinson, A., Eddy, A. C. & Eaton, D. L. Bioactivation of

- aflatoxin B₁ by human liver microsomes: Role of cytochrome P450 IIIA enzymes. *Toxicology and Applied Pharmacology* **108**, 436–447 (1991).
46. Gallagher, E. P., Wienkers, L. C., Stapleton, P. L., Kunze, K. L. & Eaton, D. L. Role of Human Microsomal and Human Complementary DNA-expressed Cytochromes P450 1A2 and P450 3A4 in the Bioactivation of Aflatoxin B₁. *Cancer Research* (1994).
 47. Gallagher, E. P., Kunze, K. L., Stapleton, P. L. & Eaton, D. L. The kinetics of aflatoxin B₁ oxidation by human cDNA-expressed and human liver microsomal cytochromes P450 1A2 and 3A4. *Toxicology and Applied Pharmacology* **141**, 595–606 (1996).
 48. Hengstler, J. G., Van der Burg, B., Steinberg, P. & Oesch, F. Interspecies differences in cancer susceptibility and toxicity. *Drug Metab. Rev.* **31**, 917–970 (1999).
 49. Degen, G. H. & Neumann, H.-G. The major metabolite of aflatoxin B₁ in the rat is a glutathione conjugate. *Chemico-Biological Interactions* **22**, 239–255 (1978).
 50. O'Brien, K., Moss, E., Judah, D. & Neal, G. Metabolic basis of the species difference to aflatoxin B₁ induced hepatotoxicity. *Biochemical and Biophysical Research Communications* **114**, 813–821 (1983).
 51. Lotlikar, P. D., Jhee, E. C., Insetta, S. M. & Clearfield, M. S. Modulation of microsome-mediated aflatoxin B₁ binding to exogenous and endogenous DNA by cytosolic glutathione S-transferases in rat and hamster livers. *Carcinogenesis* **5**, 269–276 (1984).
 52. Monroe, D. H. & Eaton, D. L. Comparative effects of butylated hydroxyanisole on hepatic *in vivo* DNA binding and *in vitro* biotransformation of aflatoxin B₁ in the rat and mouse. *Toxicology and Applied Pharmacology* **90**, 401–409 (1987).
 53. Garner, R. C. & Wright, C. M. Binding of [¹⁴C]aflatoxin B₁ to cellular macromolecules in the rat and hamster. *Chemico-Biological Interactions* **11**, 121–131 (1975).
 54. Moore, M. R., Pitot, H. C., Miller, E. C. & Miller, J. A. Cholangiocellular carcinomas induced in Syrian golden hamsters administered aflatoxin B₁ in large doses. *J. Natl. Cancer Inst.* **68**, 271–278 (1982).
 55. Lin, J.-K., Kennan, K. A., Miller, E. C. & Miller, J. A. Reduced nicotinamide adenine dinucleotide phosphate-dependent formation of 2,3-dihydro-2,3-dihydroxyaflatoxin B₁ from aflatoxin B₁ by hepatic microsomes. *Cancer Research* (1978).
 56. Raj, H. G., Clearfield, M. S. & Lotlikar, P. D. Comparative kinetic studies on aflatoxin B₁-DNA binding and aflatoxin B₁-glutathione conjugation with rat and hamster livers *in vitro*. *Carcinogenesis* **5**, 879–884 (1984).
 57. Degen, G. H. & Neumann, H.-G. Differences in aflatoxin B₁-susceptibility of rat and mouse are correlated with the capability *in vitro* to inactivate aflatoxin B₁-epoxide. *Carcinogenesis* **2**, 299–306 (1981).
 58. Quinn, B. A. *et al.* Protective activity of different hepatic cytosolic glutathione S-transferases against DNA-binding metabolites of aflatoxin B₁. *Toxicology and Applied Pharmacology* **105**, 351–363 (1990).

59. Ramsdell, H. S. & Eaton, D. L. Mouse liver glutathione S-transferase isoenzyme activity toward aflatoxin B₁-8, 9-epoxide and benzo [a] pyrene-7, 8-dihydrodiol-9, 10-epoxide. *Toxicology and Applied Pharmacology* **105**, 216–225 (1990).
60. Hayes, J. D., Judah, D. J., Neal, G. E. & Nguyen, T. Molecular cloning and heterologous expression of a cDNA encoding a mouse glutathione S-transferase Yc subunit possessing high catalytic activity for aflatoxin B₁-8,9-epoxide. *Biochem. J.* **285 (Pt 1)**, 173–180 (1992).
61. Mandel, H. G. *et al.* Metabolic basis for the protective effect of the antioxidant ethoxyquin on aflatoxin B₁ hepatocarcinogenesis in the rat. *Cancer Research* **47**, 5218–5223 (1987).
62. Hayes, J. D. *et al.* Ethoxyquin-induced resistance to aflatoxin B₁ in the rat is associated with the expression of a novel alpha-class glutathione S-transferase subunit, Yc2, which possesses high catalytic activity for aflatoxin B₁-8,9-epoxide. *Biochem. J.* **279 (Pt 2)**, 385–398 (1991).
63. Johnson, W. W. *et al.* Conjugation of highly reactive aflatoxin B₁ exo-8,9-epoxide catalyzed by rat and human glutathione transferases: estimation of kinetic parameters. *Biochemistry* **36**, 3056–3060 (1997).
64. Raney, K. D., Meyer, D. J., Ketterer, B., Harris, T. M. & Guengerich, F. P. Glutathione conjugation of aflatoxin B₁ exo-and endo-epoxides by rat and human glutathione S-transferases. *Chem. Res. Toxicol.* **5**, 470–478 (1992).
65. Boar, P. *et al.* Genetic heterogeneity of the human glutathione transferases: A complex of gene families. *Pharmacology & Therapeutics* **48**, 357–369 (1990).
66. Brockmöller, J., Kerb, R., Drakoulis, N., Nitz, M. & Roots, I. Genotype and phenotype of glutathione S-transferase class mu isoenzymes mu and psi in lung cancer patients and controls. *Cancer Research* **53**, 1004–1011 (1993).
67. Liu, Y. H., Taylor, J., Linko, P., Lucier, G. W. & Thompson, C. L. Glutathione S-transferase mu in human lymphocyte and liver: role in modulating formation of carcinogen-derived DNA adducts. *Carcinogenesis* **12**, 2269–2275 (1991).
68. McGlynn, K. A. *et al.* Susceptibility to hepatocellular carcinoma is associated with genetic variation in the enzymatic detoxification of aflatoxin B₁. *Proc Natl Acad Sci USA* **92**, 2384–7 (1995).
69. Chen, C. J. *et al.* Chronic hepatitis B carriers with null genotypes of glutathione S-transferase M1 and T1 polymorphisms who are exposed to aflatoxin are at increased risk of hepatocellular carcinoma. *Am. J. Hum. Genet.* **59**, 128–134 (1996).
70. Yu, M. W. *et al.* Effect of aflatoxin metabolism and DNA adduct formation on hepatocellular carcinoma among chronic hepatitis B carriers in Taiwan. *J. Hepatol.* **27**, 320–330 (1997).
71. Kirk, G. D. *et al.* Hepatocellular carcinoma and polymorphisms in carcinogen-metabolizing and DNA repair enzymes in a population with aflatoxin exposure and hepatitis B virus endemicity. *Cancer Epidemiol.*

- Biomarkers Prev.* **14**, 373–379 (2005).
72. Ahsan, H., Wang, L. Y., Chen, C. J., Tsai, W. Y. & Santella, R. M. Variability in aflatoxin-albumin adduct levels and effects of hepatitis B and C virus infection and glutathione S-transferase M1 and T1 genotype. *Environ Health Perspect* **109**, 833–837 (2001).
73. Sun, C. A. *et al.* Genetic polymorphisms of glutathione S-transferases M1 and T1 associated with susceptibility to aflatoxin-related hepatocarcinogenesis among chronic hepatitis B carriers: a nested case-control study in Taiwan. *Carcinogenesis* **22**, 1289–1294 (2001).
74. McGlynn, K. A. *et al.* Susceptibility to aflatoxin B₁-related primary hepatocellular carcinoma in mice and humans. *Cancer Research* **63**, 4594–4601 (2003).
75. Deng, Z.-L., Wei, Y.-P. & Ma, Y. Polymorphism of glutathione S-transferase mu 1 and theta 1 genes and hepatocellular carcinoma in southern Guangxi, China. *World J. Gastroenterol.* **11**, 272–274 (2005).
76. Liu, K. *et al.* Association of GST genetic polymorphisms with the susceptibility to hepatocellular carcinoma (HCC) in Chinese population evaluated by an updated systematic meta-analysis. *PLoS ONE* **8**, e57043 (2013).
77. Shen, Y.-H. *et al.* Quantitative assessment of the effect of glutathione S-transferase genes GSTM1 and GSTT1 on hepatocellular carcinoma risk. *Tumour biology : the journal of the International Society for Oncodevelopmental Biology and Medicine* **35**, 4007–15 (2014).
78. Martin, C. N. & Garner, R. C. Aflatoxin B-oxide generated by chemical or enzymic oxidation of aflatoxin B₁ causes guanine substitution in nucleic acids. *Nature* **267**, 863–865 (1977).
79. Essigmann, J. M. *et al.* Structural identification of the major DNA adduct formed by aflatoxin B₁ in vitro. *Proc Natl Acad Sci USA* **74**, 1870–1874 (1977).
80. Lin, J. K., Miller, J. A. & Miller, E. C. 2, 3-Dihydro-2-(guan-7-yl)-3-hydroxy-aflatoxin B₁, a major acid hydrolysis product of aflatoxin B₁-DNA or-ribosomal RNA adducts formed in hepatic microsome-mediated reactions and in rat liver in vivo. *Cancer Research* **37**, 4430–4438 (1977).
81. Croy, R. G., Essigmann, J. M., Reinhold, V. N. & Wogan, G. N. Identification of the principal aflatoxin B₁-DNA adduct formed *in vivo* in rat liver. *Proc Natl Acad Sci USA* **75**, 1745–1749 (1978).
82. Groopman, J. D., Croy, R. G. & Wogan, G. N. *In vitro* reactions of aflatoxin B₁-adducted DNA. *Proc Natl Acad Sci USA* **78**, 5445–5449 (1981).
83. Groopman, J. D., Donahue, P. R., Zhu, J. Q., Chen, J. S. & Wogan, G. N. Aflatoxin metabolism in humans: detection of metabolites and nucleic acid adducts in urine by affinity chromatography. *Proc Natl Acad Sci USA* **82**, 6492–6496 (1985).
84. Buss, P., Caviezel, M. & Lutz, W. K. Linear dose-response relationship for DNA adducts in rat liver from chronic exposure to aflatoxin B₁. *Carcinogenesis* **11**, 2133–2135 (1990).

85. Dashwood, R. H., Arbogast, D. N., Fong, A. T., Hendricks, J. D. & Bailey, G. S. Mechanisms of anti-carcinogenesis by indole-3-carbinol: detailed in vivo DNA binding dose-response studies after dietary administration with aflatoxin B₁. *Carcinogenesis* **9**, 427–432 (1988).
86. Dashwood, R. H. *et al.* Quantitative inter-relationships between aflatoxin B₁ carcinogen dose, indole-3-carbinol anti-carcinogen dose, target organ DNA adduction and final tumor response. *Carcinogenesis* **10**, 175–181 (1989).
87. Groopman, J. D. *et al.* Molecular dosimetry of aflatoxin-N7-guanine in human urine obtained in The Gambia, West Africa. *Cancer Epidemiol. Biomarkers Prev.* **1**, 221–227 (1992).
88. Bechtel, D. H. Molecular dosimetry of hepatic aflatoxin B₁-DNA adducts: Linear correlation with hepatic cancer risk. *Regulatory Toxicology and Pharmacology* **10**, 74–81 (1989).
89. Ross, R. K. *et al.* Urinary aflatoxin biomarkers and risk of hepatocellular carcinoma. *Lancet* **339**, 943–946 (1992).
90. Qian, G. S. *et al.* A follow-up study of urinary markers of aflatoxin exposure and liver cancer risk in Shanghai, People's Republic of China. *Cancer Epidemiol. Biomarkers Prev.* **3**, 3–10 (1994).
91. Hertzog, P. J., Lindsay Smith, J. R. & Garner, R. C. A high pressure liquid chromatography study on the removal of DNA-bound aflatoxin B₁ in rat liver and in vitro. *Carcinogenesis* **1**, 787–793 (1980).
92. Hertzog, P. J., Smith, J. R. L. & Garner, R. C. Characterisation of the imidazole ring-opened forms of trans-8,9-di-hydro-8-(7-guanyl)9-hydroxy aflatoxin B₁. *Carcinogenesis* **3**, 723–725 (1982).
93. Brown, K. L. *et al.* Unraveling the aflatoxin-FAPY conundrum: structural basis for differential replicative processing of isomeric forms of the formamidopyrimidine-type DNA adduct of aflatoxin B₁. *J Am Chem Soc* **128**, 15188–15199 (2006).
94. Croy, R. G. & Wogan, G. N. Temporal patterns of covalent DNA adducts in rat liver after single and multiple doses of aflatoxin B₁. *Cancer Research* **41**, 197–203 (1981).
95. Gopalakrishnan, S., Harris, T. M. & Stone, M. P. Intercalation of aflatoxin B₁ in two oligodeoxynucleotide adducts: comparative ¹H NMR analysis of d(ATC^{AFB}GAT).d(ATCGAT) and d(AT^{AFB}GAT)₂. *Biochemistry* **29**, 10438–10448 (1990).
96. Jones, W. R., Johnston, D. S. & Stone, M. P. Refined Structure of the Doubly Intercalated d(TAT AFBGCATA)₂ Aflatoxin B₁ Adduct. *Chem. Res. Toxicol.* **11**, 873–881 (1998).
97. Mao, H., Deng, Z., Wang, F., Harris, T. M. & Stone, M. P. An intercalated and thermally stable FAPY adduct of aflatoxin B₁ in a DNA duplex: structural refinement from ¹H NMR. *Biochemistry* **37**, 4374–4387 (1998).
98. Giri, I., Jenkins, M. D., Schnetz-Boutaud, N. C. & Stone, M. P. Structural Refinement of the 8,9-Dihydro-8-(N7-guanyl)-9-hydroxy-aflatoxin B₁ adduct in a 5'-Cp AFBG-3' Sequence. *Chem. Res. Toxicol.* **15**, 638–647 (2002).

99. Giri, I. & Stone, M. P. Thermal stabilization of the DNA duplex by adducts of aflatoxin B₁. *Biopolymers* **65**, 190–201 (2002).
100. Gillet, L. C. J. & Schärer, O. D. Molecular mechanisms of mammalian global genome nucleotide excision repair. *Chem. Rev.* **106**, 253–276 (2006).
101. Lehmann, A. R., McGibbon, D. & Stefanini, M. Xeroderma pigmentosum. *Orphanet J Rare Dis* **6**, 70 (2011).
102. Miki, Y. *et al.* A strong candidate for the breast and ovarian cancer susceptibility gene BRCA1. *Science* **266**, 66–71 (1994).
103. Li, M. L. & Greenberg, R. A. Links between genome integrity and BRCA1 tumor suppression. *Trends Biochem. Sci.* **37**, 418–424 (2012).
104. Takahashi, Y. *et al.* Enhanced spontaneous and aflatoxin-induced liver tumorigenesis in xeroderma pigmentosum group A gene-deficient mice. *Carcinogenesis* **23**, 627–633 (2002).
105. Alekseyev, Y. O., Hamm, M. L. & Essigmann, J. M. Aflatoxin B₁ formamidopyrimidine adducts are preferentially repaired by the nucleotide excision repair pathway *in vivo*. *Carcinogenesis* **25**, 1045–1051 (2004).
106. Michel, B. After 30 years of study, the bacterial SOS response still surprises us. *PLoS Biol.* **3**, e255 (2005).
107. Oleykowski, C. A. *et al.* Repair of aflatoxin B₁ DNA adducts by the UvrABC endonuclease of *Escherichia coli*. *J Biol Chem* **268**, 7990–8002 (1993).
108. Leadon, S. A., Tyrrell, R. M. & Cerutti, P. A. Excision repair of aflatoxin B₁-DNA adducts in human fibroblasts. *Cancer Research* **41**, 5125–5129 (1981).
109. Bedard, L. L., Alessi, M., Davey, S. & Massey, T. E. Susceptibility to aflatoxin B₁-induced carcinogenesis correlates with tissue-specific differences in DNA repair activity in mouse and in rat. *Cancer Research* **65**, 1265–1270 (2005).
110. Mulder, J. E., Bondy, G. S., Mehta, R. & Massey, T. E. Up-regulation of nucleotide excision repair in mouse lung and liver following chronic exposure to aflatoxin B₁ and its dependence on p53 genotype. *Toxicology and Applied Pharmacology* **275**, 96–103 (2014).
111. Long, X.-D. *et al.* XPD codon 312 and 751 polymorphisms, and AFB₁ exposure, and hepatocellular carcinoma risk. *BMC Cancer* **9**, 400 (2009).
112. Long, X.-D., Ma, Y., Zhou, Y.-F., Ma, A.-M. & Fu, G.-H. Polymorphism in xeroderma pigmentosum complementation group C codon 939 and aflatoxin B₁-related hepatocellular carcinoma in the Guangxi population. *Hepatology* **52**, 1301–1309 (2010).
113. Kim, Y.-J. & Wilson, D. M. Overview of base excision repair biochemistry. *Curr Mol Pharmacol* **5**, 3–13 (2012).
114. Iyama, T. & Wilson, D. M. DNA repair mechanisms in dividing and non-dividing cells. *DNA Repair (Amst)* **12**, 620–636 (2013).
115. Lunn, R. M., Langlois, R. G., Hsieh, L. L., Thompson, C. L. & Bell, D. A. XRCC1 polymorphisms: effects on aflatoxin B₁-DNA adducts and glycophorin A variant frequency. *Cancer Research* **59**, 2557–2561 (1999).

116. Long, X.-D. *et al.* Polymorphism of XRCC1 and the frequency of mutation in codon 249 of the p53 gene in hepatocellular carcinoma among Guangxi population, China. *Mol. Carcinog.* **47**, 295–300 (2008).
117. Long, X.-D., Ma, Y., Wei, Y.-P. & Deng, Z. L. The polymorphisms of GSTM1, GSTT1, HYL1*2, and XRCC1, and aflatoxin B₁-related hepatocellular carcinoma in Guangxi population, China. *Hepatology Research* **36**, 48–55
118. Chetsanga, C. J. & Frenette, G. P. Excision of aflatoxin B₁-imidazole ring opened guanine adducts from DNA by formamidopyrimidine-DNA glycosylase. *Carcinogenesis* **4**, 997–1000 (1983).
119. Prakash, A., Doubli, S. & Wallace, S. S. *The Fpg/Nei Family of DNA Glycosylases: Substrates, Structures, and Search for Damage. Mechanisms of DNA Repair* **110**, 71–91 (2012).
120. Hazra, T. K. *et al.* Identification and characterization of a human DNA glycosylase for repair of modified bases in oxidatively damaged DNA. *Proc Natl Acad Sci USA* **99**, 3523–3528 (2002).
121. Morland, I. *et al.* Human DNA glycosylases of the bacterial Fpg/MutM superfamily: an alternative pathway for the repair of 8-oxoguanine and other oxidation products in DNA. *Nucleic Acids Research* **30**, 4926–4936 (2002).
122. Wallace, S. S., Bandaru, V., Kathe, S. D. & Bond, J. P. The enigma of endonuclease VIII. *DNA Repair (Amst)* **2**, 441–453 (2003).
123. Foster, P. L., Eisenstadt, E. & Miller, J. H. Base substitution mutations induced by metabolically activated aflatoxin B₁. *Proc Natl Acad Sci USA* **80**, 2695–2698 (1983).
124. Trottier, Y., Waithe, W. I. & Anderson, A. Kinds of mutations induced by aflatoxin B₁ in a shuttle vector replicating in human cells transiently expressing cytochrome P4501A2 cDNA. *Mol. Carcinog.* **6**, 140–147 (1992).
125. Chen, T., Heflich, R. H., Moore, M. M. & Mei, N. Differential mutagenicity of aflatoxin B₁ in the liver of neonatal and adult mice. *Environ. Mol. Mutagen.* **51**, 156–163 (2010).
126. Woo, L. L. *et al.* Aflatoxin B₁-DNA Adduct Formation and Mutagenicity in Livers of Neonatal Male and Female B6C3F1 Mice. *Toxicol Sci* **122**, 38–44 (2011).
127. Wattanawaraporn, R. *et al.* A single neonatal exposure to aflatoxin b₁ induces prolonged genetic damage in two loci of mouse liver. *Toxicol Sci* **128**, 326–333 (2012).
128. Levy, D. D., Groopman, J. D., Lim, S. E., Seidman, M. M. & Kraemer, K. H. Sequence specificity of aflatoxin B₁-induced mutations in a plasmid replicated in xeroderma pigmentosum and DNA repair proficient human cells. *Cancer Research* **52**, 5668–5673 (1992).
129. Dyaico, M. J. *et al.* Species-specific differences in hepatic mutant frequency and mutational spectrum among lambda/lacl transgenic rats and mice following exposure to aflatoxin B₁. *Carcinogenesis* **17**, 2347–2356 (1996).

130. Hsu, I. C. *et al.* Mutational hotspot in the p53 gene in human hepatocellular carcinomas. *Nature* **350**, 427–428 (1991).
131. Bressac, B., Kew, M., Wands, J. & Ozturk, M. Selective G to T mutations of p53 gene in hepatocellular carcinoma from southern Africa. *Nature* **350**, 429–431 (1991).
132. Scorsone, K. A., Zhou, Y. Z., Butel, J. S. & Slagle, B. L. p53 mutations cluster at codon 249 in hepatitis B virus-positive hepatocellular carcinomas from China. *Cancer Research* **52**, 1635–1638 (1992).
133. Ozturk, M. p53 mutation in hepatocellular carcinoma after aflatoxin exposure. *Lancet* **338**, 1356–1359 (1991).
134. Kress, S., Jahn, U.-R., Buchmann, A., Bannasch, P. & Schwarz, M. p53 Mutations in Human Hepatocellular Carcinomas from Germany. *Cancer Research* (1992).
135. Oda, T., Tsuda, H., Scarpa, A., Sakamoto, M. & Hirohashi, S. p53 Gene Mutation Spectrum in Hepatocellular Carcinoma. *Cancer Research* (1992).
136. Fujimoto, Y. *et al.* Alterations of tumor suppressor genes and allelic losses in human hepatocellular carcinomas in China. *Cancer Research* **54**, 281–285 (1994).
137. Hainaut, P. *et al.* IARC Database of p53 gene mutations in human tumors and cell lines: updated compilation, revised formats and new visualisation tools. *Nucleic Acids Research* **26**, 205–213 (1998).
138. Aguilar, F., Harris, C. C., Sun, T., Hollstein, M. & Cerutti, P. Geographic variation of p53 mutational profile in nonmalignant human liver. *Science* **264**, 1317–1319 (1994).
139. Puisieux, A., Lim, S., Groopman, J. & Ozturk, M. Selective targeting of p53 gene mutational hotspots in human cancers by etiologically defined carcinogens. *Cancer Research* **51**, 6185–6189 (1991).
140. Denissenko, M. F. *et al.* The p53 codon 249 mutational hotspot in hepatocellular carcinoma is not related to selective formation or persistence of aflatoxin B₁ adducts. *Oncogene* **17**, 3007–3014 (1998).
141. Aguilar, F., Hussain, S. P. & Cerutti, P. Aflatoxin B₁ induces the transversion of G→T in codon 249 of the p53 tumor suppressor gene in human hepatocytes. *Proc Natl Acad Sci USA* **90**, 8586–8590 (1993).
142. Macé, K. *et al.* Aflatoxin B₁-induced DNA adduct formation and p53 mutations in CYP450-expressing human liver cell lines. *Carcinogenesis* **18**, 1291–1297 (1997).
143. Besaratinia, A., Kim, S.-I., Hainaut, P. & Pfeifer, G. P. *In vitro* recapitulating of TP53 mutagenesis in hepatocellular carcinoma associated with dietary aflatoxin B₁ exposure. *Gastroenterology* **137**, 1127–1137 (2009).
144. Kunkel, T. A. Evolving views of DNA replication (in) fidelity. *Cold Spring Harb Symp Quant Biol.* **74**, 91–101 (2009).
145. Lange, S. S., Takata, K.-I. & Wood, R. D. DNA polymerases and cancer. *Nat. Rev. Cancer* **11**, 96–110 (2011).
146. Freed-Pastor, W. A. & Prives, C. Mutant p53: one name, many proteins.

- Genes & Development* **26**, 1268–1286 (2012).
147. Muller, P. A. J. & Vousden, K. H. p53 mutations in cancer. *Nature Cell Biology* **15**, 2–8 (2013).
 148. Crook, T., Marston, N. J., Sara, E. A. & Vousden, K. H. Transcriptional activation by p53 correlates with suppression of growth but not transformation. *Cell* **79**, 817–827 (1994).
 149. Suad, O. *et al.* Structural basis of restoring sequence-specific DNA binding and transactivation to mutant p53 by suppressor mutations. *J Mol Biol* **385**, 249–265 (2009).
 150. Gouas, D. A. *et al.* Effects of the TP53 p.R249S mutant on proliferation and clonogenic properties in human hepatocellular carcinoma cell lines: interaction with hepatitis B virus X protein. *Carcinogenesis* **31**, 1475–1482 (2010).
 151. Cao, Y., Gao, Q., Wazer, D. E. & Band, V. Abrogation of wild-type p53-mediated transactivation is insufficient for mutant p53-induced immortalization of normal human mammary epithelial cells. *Cancer Research* **57**, 5584–5589 (1997).
 152. Junk, D. J. *et al.* Different mutant/wild-type p53 combinations cause a spectrum of increased invasive potential in nonmalignant immortalized human mammary epithelial cells. *Neoplasia (New York, N.Y.)* **10**, 450–461 (2008).
 153. Gaiddon, C., Lokshin, M., Ahn, J., Zhang, T. & Prives, C. A subset of tumor-derived mutant forms of p53 down-regulate p63 and p73 through a direct interaction with the p53 core domain. *Mol Cell Biol* **21**, 1874–1887 (2001).
 154. Noll, J. E. *et al.* Mutant p53 drives multinucleation and invasion through a process that is suppressed by ANKRD11. *Oncogene* **31**, 2836–2848 (2012).
 155. Xu, J. *et al.* Gain of function of mutant p53 by coaggregation with multiple tumor suppressors. *Nat. Chem. Biol.* **7**, 285–295 (2011).
 156. Bisio, A., Ciribilli, Y., Fronza, G., Inga, A. & Monti, P. TP53 Mutants in the Tower of Babel of Cancer Progression. *Human mutation* **35**, 689–701 (2014).
 157. Dumenco, L., Oguey, D., Wu, J., Messier, N. & Fausto, N. Introduction of a murine p53 mutation corresponding to human codon 249 into a murine hepatocyte cell line results in growth advantage, but not in transformation. *Hepatology* **22**, 1279–1288 (1995).
 158. Lee, M. K. & Sabapathy, K. The R246S hot-spot p53 mutant exerts dominant-negative effects in embryonic stem cells *in vitro* and *in vivo*. *J Cell Sci* **121**, 1899–1906 (2008).
 159. Lee, M. K. *et al.* Cell-type, dose, and mutation-type specificity dictate mutant p53 functions *in vivo*. *Cancer Cell* **22**, 751–764 (2012).
 160. Cho, Y., Gorina, S., Jeffrey, P. D. & Pavletich, N. P. Crystal structure of a p53 tumor suppressor-DNA complex: understanding tumorigenic mutations. *Science* **265**, 346–355 (1994).
 161. Wong, K. B. *et al.* Hot-spot mutants of p53 core domain evince

- characteristic local structural changes. *Proc Natl Acad Sci USA* **96**, 8438–8442 (1999).
162. Friedler, A., DeDecker, B. S., Freund, S. & Blair, C. Structural Distortion of p53 by the Mutation R249S and its Rescue by a Designed Peptide: Implications for 'Mutant Conformation'. *J. Mol. Biol.* **336**, 187-196 (2004).
 163. Bullock, A. N., Henckel, J. & Fersht, A. R. Quantitative analysis of residual folding and DNA binding in mutant p53 core domain: definition of mutant states for rescue in cancer therapy. *Oncogene* **19**, 1245–1256 (2000).
 164. Friedler, A., Veprintsev, D. B., Hansson, L. O. & Fersht, A. R. Kinetic instability of p53 core domain mutants: implications for rescue by small molecules. *J Biol Chem* **278**, 24108–24112 (2003).
 165. Bailey, E. A., Iyer, R. S., Stone, M. P., Harris, T. M. & Essigmann, J. M. Mutational properties of the primary aflatoxin B₁-DNA adduct. *Proc Natl Acad Sci USA* **93**, 1535–1539 (1996).
 166. Smela, M. E. *et al.* The aflatoxin B₁ formamidopyrimidine adduct plays a major role in causing the types of mutations observed in human hepatocellular carcinoma. *Proc Natl Acad Sci USA* **99**, 6655–6660 (2002).
 167. Ferlay, J. *et al.* Estimates of worldwide burden of cancer in 2008: GLOBOCAN 2008. *Int. J. Cancer* **127**, 2893–2917 (2010).
 168. Chang, Y. J. *et al.* Analysis of ras gene mutations in rainbow trout liver tumors initiated by aflatoxin B₁. *Mol. Carcinog.* **4**, 112–119 (1991).
 169. Autrup, H., Jørgensen, E. C. & Jensen, O. Aflatoxin B₁ induced lacI mutation in liver and kidney of transgenic mice C57BL/6N: effect of phorone. *Mutagenesis* **11**, 69–73 (1996).
 170. Smela, M. E., Currier, S. S., Bailey, E. A. & Essigmann, J. M. The chemistry and biology of aflatoxin B₁: from mutational spectrometry to carcinogenesis. *Carcinogenesis* **22**, 535–545 (2001).
 171. Waters, L. S. *et al.* Eukaryotic translesion polymerases and their roles and regulation in DNA damage tolerance. *Microbiol. Mol. Biol. Rev.* **73**, 134–154 (2009).
 172. Knobel, P. A. & Marti, T. M. Translesion DNA synthesis in the context of cancer research. *Cancer Cell Int.* **11**, 39 (2011).
 173. Sale, J. E., Lehmann, A. R. & Woodgate, R. Y-family DNA polymerases and their role in tolerance of cellular DNA damage. *Nat Rev Mol Cell Biol* **13**, 141–152 (2012).
 174. Yamanaka, K. & Lloyd, R. S. in *DNA Repair and Cancer: From Bench to clinic* (Madhusudan, S. & Wilson, D. M., III) 325–371 (CRC press, 2013).
 175. Prakash, S. Translesion DNA synthesis in eukaryotes: A one- or two-polymerase affair. *Genes & Development* **16**, 1872–1883 (2002).
 176. Livneh, Z., Ziv, O. & Shachar, S. Multiple two-polymerase mechanisms in mammalian translesion DNA synthesis. *Cell Cycle* **9**, 729–735 (2010).
 177. Johnson, R. E., Prakash, S. & Prakash, L. Efficient bypass of a thymine-thymine dimer by yeast DNA polymerase, pol eta. *Science* **283**, 1001–1004 (1999).
 178. Johnson, R. E. Fidelity of human DNA polymerase eta. *J Biol Chem* **275**,

- 7447–7450 (2000).
179. Wang, Y. *et al.* Evidence that in xeroderma pigmentosum variant cells, which lack DNA polymerase eta, DNA polymerase iota causes the very high frequency and unique spectrum of UV-induced mutations. *Cancer Research* **67**, 3018–3026 (2007).
 180. Ziv, O., Geacintov, N., Nakajima, S., Yasui, A. & Livneh, Z. DNA polymerase zeta cooperates with polymerases kappa and iota in translesion DNA synthesis across pyrimidine photodimers in cells from XPV patients. *Proc Natl Acad Sci USA* **106**, 11552–11557 (2009).
 181. Banerjee, S., Brown, K. L., Egli, M. & Stone, M. P. Bypass of aflatoxin B₁ adducts by the *Sulfolobus solfataricus* DNA polymerase IV. *J Am Chem Soc* **133**, 12556–12568 (2011).
 182. Jin, Y. H. *et al.* The multiple biological roles of the 3'→5' exonuclease of *Saccharomyces cerevisiae* DNA polymerase delta require switching between the polymerase and exonuclease domains. *Mol Cell Biol* **25**, 461–471 (2005).
 183. Moriya, M. Single-stranded shuttle phagemid for mutagenesis studies in mammalian cells: 8-oxoguanine in DNA induces targeted G.C→T.A transversions in simian kidney cells. *Proc Natl Acad Sci USA* **90**, 1122–1126 (1993).
 184. Kanuri, M. *et al.* Error prone translesion synthesis past gamma-hydroxypropano deoxyguanosine, the primary acrolein-derived adduct in mammalian cells. *J Biol Chem* **277**, 18257–18265 (2002).
 185. Minko, I. G. *et al.* Mutagenic potential of DNA-peptide crosslinks mediated by acrolein-derived DNA adducts. *Mutat Res* **637**, 161–172 (2008).
 186. Fernandes, P. H., Hackfeld, L. C., Kozekov, I. D., Hodge, R. P. & Lloyd, R. S. Synthesis and mutagenesis of the butadiene-derived N3 2'-deoxyuridine adducts. *Chem. Res. Toxicol.* **19**, 968–976 (2006).
 187. Minko, I. G. *et al.* Role for DNA polymerase kappa in the processing of N2-N2-guanine interstrand cross-links. *J Biol Chem* **283**, 17075–17082 (2008).
 188. Riley, J. *In vitro* activation of the human Harvey-ras proto-oncogene by aflatoxin B₁. *Carcinogenesis* **18**, 905–910 (1997).
 189. Guo, Y., Breeden, L. L., Zarbl, H., Preston, B. D. & Eaton, D. L. Expression of a human cytochrome p450 in yeast permits analysis of pathways for response to and repair of aflatoxin-induced DNA damage. *Mol Cell Biol* **25**, 5823–5833 (2005).
 190. Brown, K. L. *et al.* Structural perturbations induced by the alpha-anomer of the aflatoxin B₁ formamidopyrimidine adduct in duplex and single-strand DNA. *J Am Chem Soc* **131**, 16096–16107 (2009).
 191. Roze, L. V., Hong, S.-Y. & Linz, J. E. Aflatoxin biosynthesis: current frontiers. *Annu Rev Food Sci Technol* **4**, 293–311 (2013).
 192. Johnston, D. S. & Stone, M. P. Replication of a site-specific trans-8,9-dihydro-8-(N7-guanyl)-9-hydroxyaflatoxin B₁ adduct by the exonuclease deficient Klenow fragment of DNA polymerase I. *Chem. Res. Toxicol.* **13**,

- 1158–1164 (2000).
193. Maddukuri, L. *et al.* Enhancement of human DNA polymerase η activity and fidelity is dependent upon a bipartite interaction with the Werner syndrome protein. *J Biol Chem* **287**, 42312–42323 (2012).
 194. Makarova, A. V., Stodola, J. L. & Burgers, P. M. A four-subunit DNA polymerase ζ complex containing Pol δ accessory subunits is essential for PCNA-mediated mutagenesis. *Nucleic Acids Research* **40**, 11618–11626 (2012).
 195. Gopalakrishnan, S., Stone, M. P. & Harris, T. M. Preparation and characterization of an aflatoxin B₁ adduct with the oligodeoxynucleotide d(ATCGAT)₂. *J Am Chem Soc* **111**, 7232–7239 (1989).
 196. Yamanaka, K., Minko, I. G., Finkel, S. E., Goodman, M. F. & Lloyd, R. S. Role of High-Fidelity Escherichia coli DNA Polymerase I in Replication Bypass of a Deoxyadenosine DNA-Peptide Cross-Link. *Journal of Bacteriology* **193**, 3815–3821 (2011).
 197. Fernandes, P. H. & Lloyd, R. S. Mutagenic bypass of the butadiene-derived 2'-deoxyuridine adducts by polymerases eta and zeta. *Mutat Res* **625**, 40–49 (2007).
 198. Lin, Y.-C. *et al.* Error-prone replication bypass of the primary aflatoxin B1 DNA adduct, AFB1-N7-Gua. *J Biol Chem* **289**, 18497–18506 (2014).
 199. Sharma, S., Helchowski, C. M. & Canman, C. E. The roles of DNA polymerase ζ and the Y family DNA polymerases in promoting or preventing genome instability. *Mutat Res* (2012). doi:10.1016/j.mrfmmm.2012.11.002
 200. Johnson, R. E., Prakash, L. & Prakash, S. Pol31 and Pol32 subunits of yeast DNA polymerase δ are also essential subunits of DNA polymerase ζ . *Proc Natl Acad Sci USA* **109**, 12455–12460 (2012).
 201. Baranovskiy, A. G. *et al.* DNA polymerase delta and zeta switch by sharing accessory subunits of DNA polymerase. *J Biol Chem* **287**, 17281–17287 (2012).
 202. Lee, Y.-S., Gregory, M. T. & Yang, W. Human Pol ζ purified with accessory subunits is active in translesion DNA synthesis and complements Pol η in cisplatin bypass. *Proc Natl Acad Sci USA* **111**, 2954–2959 (2014).
 203. Johnson, R. E., Washington, M. T., Haracska, L., Prakash, S. & Prakash, L. Eukaryotic polymerases iota and zeta act sequentially to bypass DNA lesions. *Nature* **406**, 1015–1019 (2000).
 204. Gueranger, Q. *et al.* Role of DNA polymerases eta, iota and zeta in UV resistance and UV-induced mutagenesis in a human cell line. *DNA Repair (Amst)* **7**, 1551–1562 (2008).
 205. Shachar, S. *et al.* Two-polymerase mechanisms dictate error-free and error-prone translesion DNA synthesis in mammals. *EMBO J.* **28**, 383–393 (2009).
 206. Gan, G. N., Wittschieben, J. P., Wittschieben, B. Ø. & Wood, R. D. DNA polymerase zeta (pol zeta) in higher eukaryotes. *Cell Res.* **18**, 174–183 (2008).

207. Zander, L. & Bemark, M. Immortalized mouse cell lines that lack a functional Rev3 gene are hypersensitive to UV irradiation and cisplatin treatment. *DNA Repair (Amst)* **3**, 743–752 (2004).
208. Wittschieben, J. P., Reshmi, S. C., Gollin, S. M. & Wood, R. D. Loss of DNA polymerase zeta causes chromosomal instability in mammalian cells. *Cancer Research* **66**, 134–142 (2006).
209. Lange, S. S., Wittschieben, J. P. & Wood, R. D. DNA polymerase zeta is required for proliferation of normal mammalian cells. *Nucleic Acids Research* **40**, 4473–4482 (2012).
210. Sharma, S. *et al.* REV1 and polymerase facilitate homologous recombination repair. *Nucleic Acids Research* **40**, 682–691 (2012).
211. Wu, F., Lin, X., Okuda, T. & Howell, S. B. DNA polymerase zeta regulates cisplatin cytotoxicity, mutagenicity, and the rate of development of cisplatin resistance. *Cancer Research* **64**, 8029–8035 (2004).
212. Shen, X. *et al.* REV3 and REV1 play major roles in recombination-independent repair of DNA interstrand cross-links mediated by monoubiquitinated proliferating cell nuclear antigen (PCNA). *J Biol Chem* **281**, 13869–13872 (2006).
213. Wittschieben, J. P. *et al.* Loss of DNA polymerase zeta enhances spontaneous tumorigenesis. *Cancer Research* **70**, 2770–2778 (2010).
214. Ahuja, D., Sáenz-Robles, M. T. & Pipas, J. M. SV40 large T antigen targets multiple cellular pathways to elicit cellular transformation. *Oncogene* **24**, 7729–7745 (2005).
215. Casciano, J. C., Bagga, S., Yang, B. & Bouchard, M. J. *Modulation of Cell Proliferation Pathways by the Hepatitis B Virus X Protein: A Potential Contributor to the Development of Hepatocellular Carcinoma.* (InTech, 2012).
216. Guo, Y. *et al.* Analysis of cellular responses to aflatoxin B(1) in yeast expressing human cytochrome P450 1A2 using cDNA microarrays. *Mutat Res* **593**, 121–142 (2006).
217. Fasullo, M., Chen, Y., Bortcosh, W., Sun, M. & Egner, P. A. Aflatoxin B(1)-Associated DNA Adducts Stall S Phase and Stimulate Rad51 foci in *Saccharomyces cerevisiae*. *Journal of Nucleic Acids* **2010**, 456487 (2010).
218. Ricordy, R., Gensabella, G., Cacci, E. & Augusti-Tocco, G. Impairment of cell cycle progression by aflatoxin B1 in human cell lines. *Mutagenesis* **17**, 241–249 (2002).
219. Gursoy-Yuzugullu, O., Yuzugullu, H., Yilmaz, M. & Ozturk, M. Aflatoxin genotoxicity is associated with a defective DNA damage response bypassing p53 activation. *Liver International* **31**, 561–571 (2011).
220. Philip A Knobel, I. N. K. E. F.-B. R. A. S. T. M. M. Inhibition of REV3 Expression Induces Persistent DNA Damage and Growth Arrest in Cancer Cells. *Neoplasia (New York, N.Y.)* **13**, 961 (2011).
221. Bandaru, V., Sunkara, S., Wallace, S. S. & Bond, J. P. A novel human DNA glycosylase that removes oxidative DNA damage and is homologous to *Escherichia coli* endonuclease VIII. *DNA Repair (Amst)* **1**,

- 517–529 (2002).
222. Dou, H., Mitra, S. & Hazra, T. K. Repair of oxidized bases in DNA bubble structures by human DNA glycosylases NEIL1 and NEIL2. *J Biol Chem* **278**, 49679–49684 (2003).
223. Roy, L. M. *et al.* Human polymorphic variants of the NEIL1 DNA glycosylase. *J Biol Chem* **282**, 15790–15798 (2007).
224. Krishnamurthy, N., Zhao, X., Burrows, C. J. & David, S. S. Superior removal of hydantoin lesions relative to other oxidized bases by the human DNA glycosylase hNEIL1. *Biochemistry* **47**, 7137–7146 (2008).
225. Porello, S. L., Leyes, A. E. & David, S. S. Single-turnover and pre-steady-state kinetics of the reaction of the adenine glycosylase MutY with mismatch-containing DNA substrates. *Biochemistry* **37**, 14756–14764 (1998).
226. Sassa, A., Beard, W. A., Shock, D. D. & Wilson, S. H. Steady-state, pre-steady-state, and single-turnover kinetic measurement for DNA glycosylase activity. *J Vis Exp* e50695 (2013). doi:10.3791/50695
227. Wallace, S. S. DNA glycosylases search for and remove oxidized DNA bases. *Environ. Mol. Mutagen.* **54**, 691–704 (2013).
228. Couve-Privat, S., Mace, G., Rosselli, F. & Saporbaev, M. K. Psoralen-induced DNA adducts are substrates for the base excision repair pathway in human cells. *Nucleic Acids Research* **35**, 5672–5682 (2007).
229. Vik, E. S. *et al.* Biochemical mapping of human NEIL1 DNA glycosylase and AP lyase activities. *DNA Repair (Amst)* **11**, 766–773 (2012).
230. Imamura, K., Averill, A., Wallace, S. S. & Doublie, S. Structural Characterization of Viral Ortholog of Human DNA Glycosylase NEIL1 Bound to Thymine Glycol or 5-Hydroxyuracil-containing DNA. *J Biol Chem* **287**, 4288–4298 (2012).
231. Dou, H. *et al.* Interaction of the human DNA glycosylase NEIL1 with proliferating cell nuclear antigen. The potential for replication-associated repair of oxidized bases in mammalian genomes. *J Biol Chem* **283**, 3130–3140 (2008).
232. Zhao, X., Krishnamurthy, N., Burrows, C. J. & David, S. S. Mutation versus repair: NEIL1 removal of hydantoin lesions in single-stranded, bulge, bubble, and duplex DNA contexts. *Biochemistry* **49**, 1658–1666 (2010).
233. Shinmura, K. *et al.* Inactivating mutations of the human base excision repair gene NEIL1 in gastric cancer. *Carcinogenesis* **25**, 2311–2317 (2004).
234. Chaisaingmongkol, J. *et al.* Epigenetic screen of human DNA repair genes identifies aberrant promoter methylation of NEIL1 in head and neck squamous cell carcinoma. *Oncogene* **31**, 5108–5116 (2012).
235. Zhang, S. *et al.* REV3L 3'UTR 460 T>C polymorphism in microRNA target sites contributes to lung cancer susceptibility. *Oncogene* **32**, 242–250 (2013).